INFORMATION-DRIVEN DATA GATHERING IN WIRELESS SENSOR NETWORKS

by

JING WANG

Presented to the Faculty of the Graduate School of
The University of Texas at Arlington in Partial Fulfillment
of the Requirements
for the Degree of

DOCTOR OF PHILOSOPHY

THE UNIVERSITY OF TEXAS AT ARLINGTON

August 2010

ACKNOWLEDGEMENTS

I would like to thank my supervising professors, Prof. Sajal K. Das and Prof. Yonghe Liu, for providing me the opportunity to work on the fantastic topic and guiding me throughout my Ph. D. study with great patience. I am also grateful to the committee members, Prof. Mohan Kumar, Prof. Bob Weems and Prof. Nan Zhang, for their valuable comments and suggestions on my work.

I would also like to thank my colleges at CReWMaN laboratory for kindly sharing the experience on their study and work.

The last but not the least, I would like to thank my family for the unselfishness support for the many years of my study. The dissertation would not happen without their understanding and sacrifice.

MAY 10, 2010

ABSTRACT

INFORMATION-DRIVEN DATA GATHERING IN WIRELESS SENSOR NETWORKS

Jing Wang, Ph.D.

The University of Texas at Arlington, 2010

Supervising Professor: Sajal K. Das, Yonghe Liu

Since the advance of wireless technology enables the mass production of low-cost, small-sized sensor nodes, sensor nodes can be densely deployed in an area for high tolerance to node failure or to achieve better coverage statistically. The redundancy of sensor nodes results in the temporal and spatial correlation of sensory data, which motivates the information-driven data gathering approaches for wireless sensor networks (WSNs).

Since existing approaches target at the sensory data that are already highly correlated with each other, little attention has been paid to the idea of changing the sampling schedules of the sensor nodes to reduce the correlation among sensory data. In this dissertation, sampling strategies and the relevant medium access control (MAC) protocol are presented to demonstrate how the correlation can be reduced through adjusting the sampling time shifts of sensor nodes.

The asynchronous lossless data gathering strategy aims at extending the sampling cycle of individual node while guaranteeing the original signal to be fully recovered by the sink. Based on the correlation signal model, details of the collaborative

reconstruction of the original signal are presented. An exponential temporal-spatial correlation model is introduced for presenting lossy data gathering strategies. It is justified by real data collected from wireless sensor networks. Regarding lossy data gathering applications, the sensor nodes take samples asynchronously to obtain more informative samples. Furthermore, the entropy of the joint Gaussian random variables is adopted to quantify the improvement on the quality of information obtained from the asynchronous samples. Oppeinhem's inequality is applied to prove the entropy is increased by introducing a non-zero temporal correlation parameter. A recursive algorithm is designed to solve the optimal asynchronous sampling problem with a set of sub-optimal sampling time shifts. Bounds on the performance of the three asynchronous sampling strategies are derived respectively.

Motivated by the benefit of asynchronous sampling strategies, an information-driven MAC protocol is proposed to avoid the severe collisions of event reports in the event detection applications. Other than choosing a subset of nodes to report to the sink, the proposed protocol assigns sampling shifts to nodes in order to change the bursty traffic into a streamlined traffic. Consequently, the MAC performance is improved by essentially replacing the collision prone traffic with the streamlined one. An optimal probability model is adopted for selecting nodes' transmission slots that minimize collisions and in turn reduce the correlation among event reports. Through theoretical analysis and simulations, it is shown that the protocol relates the MAC performance with the information quality of event reports, which is quantified by the Cramer-Rao lower bound (CRLB) of parameter estimation. In addition to the benefit of reduced collision probability, the CRLB is lowered by the proposed MAC protocol after the nodes' s sampling time moments are shifted from each other.

TABLE OF CONTENTS

LIST OF FIGURES

LIST OF TABLES

CHAPTER 1

INTRODUCTION

With the advance of integrated circuit technology, sensor nodes, composed of micro-processor, wireless radio and small sensors, are capable of sensing, processing and communicating [1, 2]. A network formed by low-cost, small-sized sensor nodes attracts extensive attentions in recent years, because it enables a vast number of applications to collect information within a certain area and supply the information to remote computers. However, the implementation of wireless sensor networks suffers from resource constraints such as battery capacity, memory size, communication range, bandwidth. Various solutions have been proposed in the literature to relief the network from these constraints. Among them, information-driven strategies are motivated by the observation on data correlations in dense wireless sensor networks. To avoid the energy consumption on unnecessary data transmissions, it is favorable to send only data containing useful information to the sink. Aiming at the tradeoff between energy consumption and the quality of information, a set of information-driven data gathering strategies is proposed in this dissertation. It is able to reduce the correlation of sensory data through carefully scheduling the sampling time instances of sensor nodes. The resulted asynchronous sampling strategies can effectively reduce the correlation without requiring additional resources to process sensory data by individual node. Furthermore, an information-driven medium access control (MAC) protocol is introduced to apply asynchronous sampling to streamline the collision prone traffic in event detection and reporting scenario.

A brief overview of wireless sensor networks (WSNs) is presented first in this chapter. After that, the challenges for widespread deployment of WSNs are discussed along with existing solutions extending the lifetime of network. Specifically, approaches in the literature that exploit data correlations are presented before a brief description of the information-driven data gathering strategies is provided. The contributions of this dissertation are summarized too. Finally, the organization of the dissertation is introduced.

1.1 Background

Wireless sensor networks (WSNs) have been envisioned to revolutionize the interaction between humans and the physical world. As shown in Fig. 1.1, a vast number of sensor nodes can be deployed to collect the sensory data about the physical world. With the help of wireless links between each other, they are able to relay the sensory data or the aggregated data from one node to another until the data reach their destination. Usually, the sink, a node that bridges the network to the remote computer or other networks, is the destination of the data packets from sensor nodes and consumes the data according to instructions from humans. Furthermore, decisions can be made according to the collected data about the physical world. Typical applications of WSNs include smart environment, machine monitoring, environment and habitat monitoring, health care applications and intelligent transportation.

From the application's point of view, the applications of WSNs can be grouped into three categories: data gathering, information gathering, query-based data gathering. Data gathering applications require that sensor nodes transmit the collected sensory data to the sink for further processing. Examples of data gathering applications include habitat monitoring, environmental monitoring etc [3, 4, 5]. Information gathering applications require that the sensor nodes apply on-board data processing

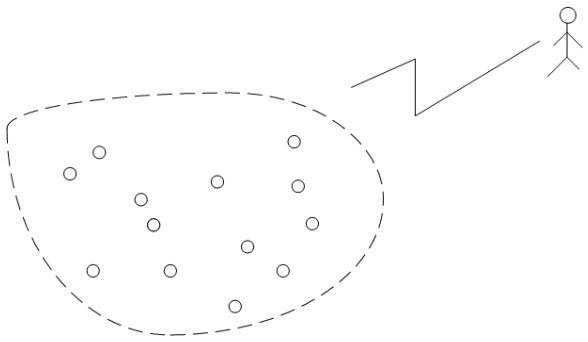

Figure 1.1: Overview of wireless sensor networks

and report the result to the sink. Target tracking is a typical information gathering application that keeps localizing the mobile nodes and sends the observed trajectory to the sink [6, 7]. Query-based data gathering does not demand constant transmissions of sensory data or the processed result. The sink or remote computer actively queries the sensor node about particular sensory data or specific processed result instead of passively retrieving all available data from sensor nodes [8, 9]. In this dissertation, data gathering application is the focus.

Besides, density of the sensor nodes plays an important role in the design and operation of WSNs [10, 11]. For sparse WSNs, the key is to maintain coverage and connectivity in order to provide the desired service to users [12, 13, 14]. While for dense WSNs, the critical issues are collisions and redundancy of nodes [15, 16]. In this dissertation, dense WSNs with data correlation is the focus.

The implementation of WSNs is still restricted to experimental practices rather than what had been anticipated at the emergence of the idea. Although more and more implementations of WSNs are reported, the lifetime of the WSNs usually lasts to the end date of the academic project due to the lack of maintenance. The value of these implementations mostly lies in verifying the research approaches and bench marking the proposed protocols or design methods.

The reasons for the above situation are the follows.

(1) Lifetime: The lifetime of the WSNs depends on the capacity of the battery equipped on the sensor nodes. Given the current power level of sensor nodes, the lifetime of the WSNs is usually several months without recharging the batteries. For the applications of WSNs, especially for those deployed in the remote area, it is difficult to recharge the batteries every several months.

(2) Cost: Since WSNs has not been widely deployed, the manufacture cost of sensor nodes is still high due to the small scale of production. Implementations of WSNs are subject to at most hundreds of nodes, which is far less than the assumptions of thousands of nodes in the simulations of WSNs [17]. The cost issue of WSNs will be resolved after the lifetime problem is tackled.

1.2 Existing Solutions

Since the major bottleneck for widely deploying WSNs is the battery lifetime. Solutions to this problem fall into two categories: to extend the battery lifetime through constantly charging it; and to reduce the energy consumption of operating the WSN. The first category greatly relies on the advance of battery technology and energy harvesting techniques [18]. Although the last few decades have seen exponential development advances in semiconductor industry that lead to the widespread usage of smart devices, the progress on battery technology lags far behind. For instance, the camera sensor that is able to capture images or even videos is getting considerably smaller and cheaper due to the changes of ICs integrated in it. Consequently, camera sensors are integrated into many electronic devices, such as mobile phones and laptops. Noticeably, the energy consumption of the camera sensor still requires it to either share the power supply of the devices that can be recharged frequently or get the power supply through USB connections. Although studies on

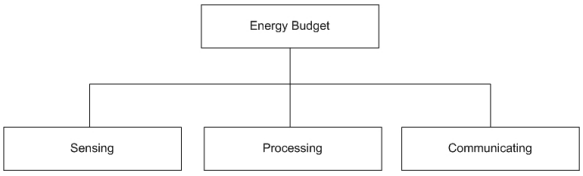

Figure 1.2: Energy budget of a sensor node

visual sensor network reveal its potential in providing more vivid observation on the environment, the energy consumption issue remains to be a great challenge [19]. Solar energy technology provides WSNs a way to extend the lifetime of outdoor applications with abundant sunlight. With the help of the solar panel and the rechargeable batteries, the lifetime of the WSN can be extended from several months to years [20]. However, the solar energy solution is not applicable in the area with little sunshine. Other energy harvesting techniques have been proposed in recent years [21]. Unless the advance of battery technology and the energy harvesting techniques are able to provide abundant energy to the sensor nodes with small-form factor and low-cost, energy consumption will remain to be the key issue for the widespread deployment of WSNs.

The second category of solutions sprawls into a range of aspects of the energy consumption problem, as demonstrated in Fig. 1.2. Depending on different sensing goals, sensors themselves could hold a significant share of the energy budget of the whole node. For instance, the soil moisture sensor consumes 15mW power while it is working [22]. Given the energy-hungry sensors, reducing the number of samples taken by the sensor nodes becomes the goal of a series of energy efficient protocols for WSNs [23, 24]. However, the number of samples also affects the decision-making process based on the sensory data. The tradeoff between the energy consumption and the performance of the application is at the center of the approaches leveraging on the number of samples.

Table 1.1: Power breakdown for processor integrated with radio

	processor	radio	flash	USB
power save	0.5μA	200μA	1μA	100μA
active state	5$\sim$12mA	15mA	4mA	100mA

For sensors with little energy consumption or even no energy consumption at all, the number of samples still plays an important role in designing energy efficient communication protocols for WSNs. The reason is that there are two other major energy-consuming tasks: on-board processing of sensory data and communicating between pairs of sensor nodes. Table 1.2 shows a detailed breakdown of energy budget for a node when its wireless radio is integrated with its processor [25, 26]. It is worth noticing that processing sensory data consumes much less energy than relaying them to another sensor node. Inspired by this, data aggregation has been proposed to reduce the amount of data traffic in the network through relaying the aggregation result to the other sensor nodes rather than the raw sensory data [27, 28, 29]. Although in-network aggregation is able to significantly reduce the communication costs, it is subject to the loss of useful information if not applied with additional care on the application's requirement on estimation or regression performance.

Since the sensor node consumes little energy during the idle state, duty-cycle scheduling methods have been proposed to let sensor nodes go to sleep whenever it is possible. Ideally, sensor nodes' working states should exactly follow traffic pattern of the network in order to avoid unnecessary energy spending on idle listening. Fig. 1.3 illustrates the ideas of scheduling the radio or the entire node respectively. The schedule of wireless radios leads to energy efficient MAC protocol of WSNS [30], while the schedule of the sensor node faces the problem of maintaining connectivity and coverage with a subset of the deployed sensor nodes [31]. The drawbacks of introducing the scheduling protocols include the reduced band-width, end-to-end delay and the

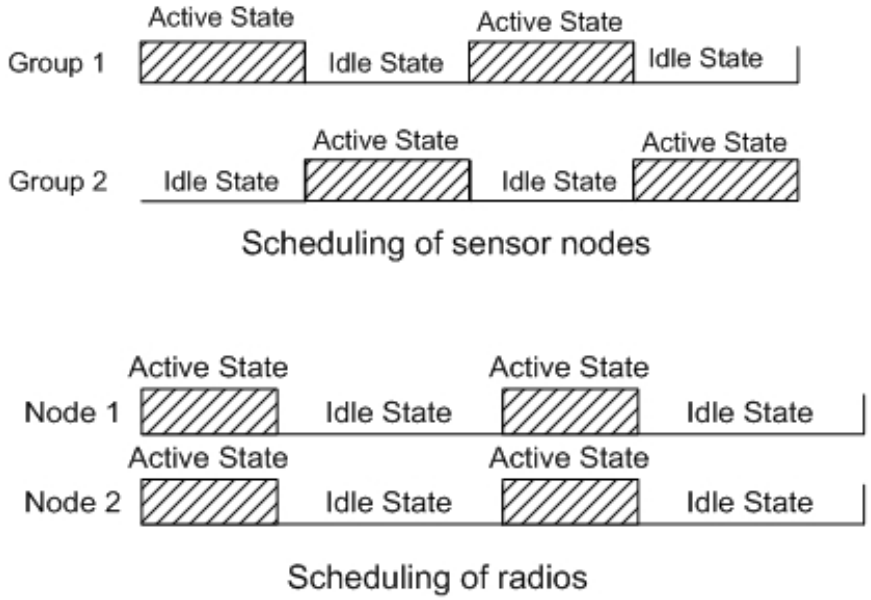

Figure 1.3: Scheduling of sensor nodes and radios

additional costs to maintain highly synchronized clocks of the neighboring nodes in order to schedule the radio [32, 33]. In addition, the changes in the connectivity and coverage of the network need to be addressed in the routing protocols for WSNs with duty-cycled sensor nodes [34, 35, 36].

Mobility-based approaches tackle the energy consumption problem through introducing a number of mobile elements to assist the operations of the network. Since mobile elements are exempt from resource constraints, scalability and cost issues, they traverse the area where the static sensors are deployed to perform data collection, localization etc in order to save energy consumption of the static sensors [37, 38, 39]. However, mobility-enabled nodes require complex method to control and manage their own operations and are limited to the applications whose deployment area is accessible to mobile nodes.

1.3 Exploiting Data Correlation

Recognizing that the amount of traffic in the network affects both lifetime of WSNs and the application's performance, researchers investigated the problem of determining the amount of traffic needed to accomplish tasks and to extend lifetime of the network. Aiming at reducing the amount of data to be transmitted by sensor nodes, distributed compressive sensing [40, 41, 42] has been attracting extensive attentions recently. It provides a promising approach to reduce the amount of traffic while preserving the necessary amount of information in the transmitted data required by application tasks. It is motivated by the observation that sensory data are spatially correlated when nodes are closely located to each other [43]. The idea is to use a subset of the samples to restore all the samples when the samples are from correlated sources. It has been proved that the sensor data can be reconstructed with high probability from a reduced number of samples projected to a linear basis.

Compressive sensing is attractive to the applications of WSNs because it does not require complicated computation at the nodes' side. The total amount of traffic can be reduced greatly while the amount of information at the sink's side is guaranteed. A recent study on compressive sensing demonstrated that the capacity of the network can be increased by adopting the compressive sensing technique [44]. It is necessary to consider routing path of the samples from the nodes to the sink when implement distributed compressive sensing. Therefore, joint design of routing scheme and compressive sensing is critical to the success of compressive sensing.

Beside, correlation in sensory data leaves space for squeezing the number of bits needed to represent the data given the other correlated sources [45, 46]. A typical compression-based approach consists of two processes: compression process, reconstruction process. It was shown that sensory data can be fully reconstructed at the sink when properly compressed. The key of compression-based sensing is to

determine the compression rate, which is directly related to the amount of traffic flow in the network. However, compression algorithm may overload the resource constrained sensor nodes due to its complexity.

Given the correlation between each pair of neighboring sensor nodes, a dominating correlated minimum set was proposed to select a subset of sensor nodes to perform sensing and transmitting to the sink [47]. The difference between the node selection method and compressive sensing is that the dominating correlated minimum set is subject to be updated constantly throughout the lifetime of the network to balance energy level of the nodes. Consequently, additional costs are introduced each time the set is updated.

Being able to reduce energy consumption of WSNs, distributed source encoding was widely adopted in multimedia communication applications [48]. According to the Slepian-Wolf theorem [49, 50], correlated data sources can be encoded separately and the compressed data from the sources can be jointly decoded by the sink. The attracting feature of distributed source encoding is that sensor nodes are able to encode sensory data without communicating with the other correlated sources. However, the theorem claims the achievable compression rate without hints on deriving specific codecs. Therefore, researches on distributed source encoding has been focused on finding the right codecs that can approximate the theoretically achievable compression rate [64, 51].

The proposed information-driven data gathering approach consists of two parts. One is the set of asynchronous sampling strategies, the other is the information-driven medium access control (MAC) protocol. The asynchronous sampling strategies focus at the sampling process taken place at the individual sensor nodes and the signal recover or regression process at the sink respectively. Whereas, the information-driven

MAC protocol aims at reducing the collisions between nodes' attempts to access the medium and improving lower bound of the estimation accuracy.

Recall the discussions on correlation motivated approaches to extend the lifetime of WSNs, advantages of the existing approaches are summarized in the following:

1. The amount of traffic is reduced through various techniques managing to reduce the communication cost of data transmissions from nodes to the sink.
2. It is preferable for sensor nodes to perform necessary computations independently with each other in order to avoid the additional communication costs on facilitating compression or encoding process.
3. Computation load of the resource constrained sensor nodes is restricted to avoid excessive energy consumption on computation.

The information-driven approach presented in this dissertation manages to extend WSNs' lifetime and preserve sufficient amount of information for accomplishing application tasks. It also shares advantages of the existing approaches exploiting correlations of sensory data in WSNs. In addition to spatial correlations, the proposed approach takes temporal correlations into consideration to further reduce energy consumption. The correlation of sensory data is reduced through explicitly introducing shifts of the sampling time moments among sensor nodes. The asynchronous sampling strategies are proposed for two scenarios: lossless data gathering; lossy data gathering. For lossless data gathering, the asynchronous sampling strategy is able to reduce the number of samples needed to fully recover the original signal through collaborative reconstruction. For lossy data gathering, the asynchronous sampling strategy is able to improve the regression performance through increasing the entropy of sensory data. Furthermore, the information-driven MAC protocol proposes to schedule the sampling time moments of sensor nodes at the MAC layer. Consequently, the colli-

sion prone traffic generated by sensor nodes can be streamlined, while less correlated event reports leads to a better lower bound of the estimation accuracy.

1.4 Summary of Contributions

Information-driven data gathering strategies proposed in this dissertation introduces the scheduling of sampling time instances. As a result, the tradeoff between energy consumption and quality of information is improved. Specifically, the contributions can be summarized as follows:

1. The proposed asynchronous sampling strategy for lossless data gathering in WSNs is able to reduce the number of samples needed by the sink to fully recover the original signal observed by correlated sensor nodes. Therefore, energy consumption of transmitting the samples from sensor nodes to the sink is reduced significantly. The theoretical analysis is verified through simulations conducted on both synthetic and real sensory data.
2. A set of asynchronous sampling strategies is proposed to improve quality of information for lossy data gathering in WSNs. Through quantifying the quality of information contained in sensory data, it is proved that the amount of information contained in the asynchronous samples from correlated sources is greater than that in the synchronous samples at the same sampling rate from the same sources. Consequently, the regression performance in terms of regression distortion is improved through introducing sampling time shifts for sensor nodes. The results of applying asynchronous sampling strategies are validated through simulations on both real and synthetic sensory data.
3. The ID-MAC protocol is proposed to reduce collisions between nodes' attempts to send their event reports about the same event in event detection and reporting applications and to improve the quality of event reports through reducing the

correlation. Since the protocol is based on slotted CSMA/CA MAC model, the optimal probability for each sensor node to select the slots is derived. Quality of event report is quantified by the Cramer-Rao lower bound (CRLB) of estimation accuracy. It is shown that the CRLB can be reduced as the result of the ID-MAC protocol as well as collisions at the MAC layer.

1.5 Dissertation Organization

The rest of the dissertation consists of seven chapters. Chapter 2 discusses the related work that exploits the correlation among sensory data. The comparison between the proposed data gathering strategies and the existing strategies is also provided at the end of Chapter 2. Before proceeding with the details of the proposed strategies, the preliminaries, including motivating scenarios, signal model, correlation models, event detection model and the adopted slotted CSMA/CA MAC protocol model, are introduced in Chapter 3.

Based on the deterministic signal model and the relevant correlation model, Chapter 4 presents the asynchronous lossless data gathering strategy, which focuses on gathering asynchronous samples for fully recovering of the original signal. It is presented with detailed description of the strategy and discussions on solving an optimization problem for scheduling the sampling time moments of sensor nodes. Based on a different correlation model, the asynchronous lossy data gathering strategy is proposed in Chapter 5. It demonstrates the benefits of the strategy in terms of the increased entropy of sensory data through quantifying the amount of information with the entropy model. An optimization problem maximizing the entropy of sensory data is formulated and solved accordingly. Consequently, a suboptimal strategy along with two other candidate strategies are described.

After that, Chapter 6 describes the ID-MAC protocol, which apply the idea of asynchronous sampling the MAC layer. The sampling shifts of sensor nodes are determined by the MAC layer when the traffic is collision prone in the event detection and reporting scenario. Analysis on the impact of the ID-MAC protocol shows that the tradeoff between the collision probability and the lower bound of the estimation accuracy can be improved. In order to verify the theoretical analysis in the previous chapters and to demonstrate benefits of the proposed strategies and protocol, simulation study has been conducted on both synthetic and real data set. Simulation results on reduced energy consumption, increased entropy, event reconstruction and lower bound of estimation accuracy are presented in Chapter 7. Finally, Chapter 8 concludes the dissertation and discusses future work can be further explored.

CHAPTER 2

RELATED WORK

As energy efficiency is the bottleneck for widespread implementation of wireless sensor networks, it has become the prevailing goal of approaches designed for different levels of the protocol stack. Aiming at correlations of sensor nodes, information-driven data gathering strategies manage to extend lifetime of WSNs through avoiding unnecessary energy consumption on sending highly correlated sensory data to the sink. In order to incur less communication cost, existing approaches either process the raw sensory data for less amount of packet transmissions or reduce the number of samples to be sent to the sink. The challenges facing these approaches include the difficulty in fully recovering the original samples at the sink from the processed data and the request to guarantee the application level performance given a limited number of samples. This chapter describes the existing approaches in addressing these challenges. More importantly, a comparative analysis on the energy consumption of different approaches is provided to show the differences among them. Finally, a taxonomy of the information-driven strategies is proposed to summarize their common features and differences.

2.1 Overview

Various energy efficient approaches have been proposed for data gathering in wireless sensor networks. Among them, a group of approaches focus on the quality of information obtained by the sink. Since the application's goal is to retrieve the information about certain physical process from sensory data, the amount of sensory

data to be transmitted and the quality of the information can be retrieved from the sensory data are at the center of the investigation on achieving energy efficiency. The amount of sensory data usually depends on the number of samples that has been taken by individual sensor node, if no compression or little preprocessing of the sensory data is performed. The information-driven approaches aim at maximizing the quality information while reducing the communication costs. In order to reduce the amount of data to be transmitted, the approaches either reduce the number of samples to be taken or compress the raw sensory data.

Regarding data gathering applications, the efforts of achieving energy efficiency reside in different processes of collecting the sensory data and sending them to the sink. Compression and coding based approaches propose to exploit the sparsity of the sensory data, while the sampling based approaches aim at reduce the sparsity of the sensory data through selecting node placements and sampling time instances. Aside from the sparsity of sensory data, correlations among sensory data from closely located sensor nodes motivate the research on distributed compressive sensing, distributed source coding and optimal sampling. Given the prior knowledge of the spatial correlations of sensory data, the raw sensory data can be further compressed to reduce communication cost.

When prior knowledge of spatial correlations is not available or time variant, adaptive sampling approach determines the time instance to take samples according to the feedbacks from the regression or estimation process. The goal of adaptive sampling is to take the least number of samples while guaranteeing the regression performance. It is capable of capturing the changes of the correlations while the other approaches can not without additional efforts.

2.2 Distributed Compressive Sensing

Distributed compressive sensing [52, 53, 54] is proposed to exploit spatial correlations among sensory data from closely located sensor nodes in addition to the sparsity of sensory data from individual sensor node. Since the spatial correlation model is the basis of the distributed compressive sensing, it is presented before the detailed discuss on compression ratio. At the end this section, implementation issues of distributed compressive sensing are discussed.

2.2.1 Models

In order to further compress the sensory data, the strategy assumes that spatial correlations among sensory data exist when the sensor nodes are deployed densely in an area [55, 56]. Distributed compressive sensing terms the joint sparsity as the sparsity of the entire sensory data in comparison to the sparsity of the sensory data from one individual sensor node. It addresses not only the intra-signal sparsity but also the inter-signal sparsity. The joint sparsity is usually smaller than the simple addition of the sparsities of the sensory data from individual nodes [57]. An example of the correlation model is shown in Eq. (2.1).

$$S_i = X_c + X_i \tag{2.1}$$

where S_i is the sensory data from the ith sensor node, X_c is the common part signal that is shared by all the sensor nodes, and X_i is the innovation part signal that is specific to the ith sensor node. Either the common part signal, the innovation part signals or both can be sparse. For a signal represented by a weighted sum of N

basis vectors, being sparse means that K out of the N coefficients are non-zero. The sparsity of the signal can be formulated in Eq. (2.2).

$$x = \sum_{n=1}^{N} \delta_n \varphi_n = \sum_{k=1}^{K} \delta_{n_k} \varphi_{n_k} \tag{2.2}$$

Consequently, a K sparse signal can be recovered given the non-zero (or significant) coefficients and their locations (the corresponding series number n_k). However, compressive sensing goes beyond that by only requesting the non-zero coefficients. It projects the sensory data to a second set of M functions. Only the M ($M < N$) coefficients are requested for recovering the original K-sparse sensory data, when the sparse basis and the projection vectors are incoherence. The compressive sensing outperforms the conventional compression based approaches because it eliminates the communication costs on sending the locations of the non-zero (or significant) coefficients.

It has been proved that $K + 1$ coefficients are sufficient for the recovering of the K-sparsity sensory data with known sparse basis. To recover the original sensory data from the linear projection to ϕ, an optimization problem, shown in Eq. (2.3), needs to be solved.

$$Minimize \text{ U} \quad \text{st. } \chi = \phi\psi\delta \tag{2.3}$$

where U is the number of non-zero entries in δ, χ is the linear projection of the sensory data $x = \psi\delta$, and δ is the coefficient vector of the sparse sensory data.

The incoherence of the basis ψ and the projection vector ϕ guarantees that the coefficient vector δ is the unique solution to the optimization problem. With the knowledge of basis ψ and the coefficient vector δ, the original sensory data can be recovered accordingly.

In solving the optimization problem, the search for the coefficient vector δ that has the least number of non-zero entries is NP-hard. In order to obtain computation tractability, the objective is changed to minimizes the sum of the coefficients. Although the new optimization problem can be solved with linear programming techniques, it requires $M \geq cK$ number of projected coefficients, where $c > 1$.

Regarding the correlation model given in Eq. (2.1), the typical scenarios for applying distributed compressive sensing include: (i) the common part signal, X_c, is K_c sparse, and the innovation part signal of the ith sensor node, X_i, is K_i sparse; (ii) the common part signal is zero, and the innovation part signal of the ith sensor node is K sparse; (iii) the common part signal is not sparse, and the innovation part signal of the ith sensor nodes is K_i sparse. The corresponding joint sparsity D is given in the following:

$$D = \begin{cases} K_c + \sum_{i=1}^{V} K_i & \text{(i)} \\ V \times K & \text{(ii)} \\ N + \sum_{i=1}^{V} K_i & \text{(iii)} \end{cases} \tag{2.4}$$

where K_c is the sparsity of the common part signal, K_i is the sparsity of the innovation part signal of the ith sensor node, V is the number of sensor nodes, K is the sparsity of the sensory data.

2.2.2 Compression Ratio

Given the correlation models, distributed compressive sensing can be applied to a set of spatially correlation sensor nodes to reduce the sensing cost of the common part signal while taking advantage of the sparsity of the sensory data. For the correlation model with sparse common part signal and sparse innovation part signal, the total number of projected coefficients needed to recover the sensory data is the

sum of the number of projected coefficients obtained from each sensor node, M_i. The distributed compressive sensing requires that:

$$\sum_{i=1}^{V} M_i \geq K_c + \sum_{i=1}^{V} K_i + V - K_r \tag{2.5}$$

where K_r is represents the number of coefficients that are shared by the common part signal and the innovation part signal.

Therefore, the sensing cost of the common part signal can be greatly reduced from $V \times (K_c + 1)$ to $K_c + V$.

Apparently, the distributed compressive sensing can not reduce the sensing cost when the common part signal is zero in the second scenario of the correlation model. Although the common part signal is no longer sparse in the third scenario of the correlation model, the distributed compressive sensing is still able to take advantage of the correlated sensory data to amortize the sensing cost of the common part signal among all the sensor nodes. The total number of projected coefficients requires that:

$$\sum_{i=1}^{V} M_i \geq N + \sum_{i=1}^{V} K_i + V - K_r \tag{2.6}$$

where N is the number of samples required to recover the non-sparse common part signal.

2.2.3 Implementation Issues

There are two main issues in implementing distributed compressive sensing: computation load and communication cost. Benefits of applying distributed compressive sensing also come from these two aspects. The strategy leverages prior knowledge of the sparsity of sensory data to reduce the communication cost and shift the com-

putation load to the sink. The joint sparsity of sensory data enables sensor nodes to cooperate with each other on sharing the sensing cost of the common part signal. However, computation load of the sink is increased because of the additional efforts needed to solve the optimization problem seeking the original sensory data from a smaller set of projected coefficients sent by sensor nodes.

Computation Load As the sink usually has more power supply and better hardware support in terms of computation speed and memory usage, the computation load tends to be shifted from the sensor node to the sink in the strategies for wireless sensor networks. Less computation load at the sensor node is always favorable because the energy consumption of computation will not increase significantly. Although distributed compressive sensing follows the same trend with the conventional compression based strategies to trade the computation load on the sensor node for the saving on the communication cost, it replaces the computation intensive compression algorithm with the multiplication between the data sample and a random number, which consumes far less energy and takes little process time. While at the sink's side, an optimization problem needs to be solved in order to recover the original sensory data, which can be NP-hard. Requiring a greater number of projected coefficients, another optimization problem can be solved with traditional linear programming techniques trading the saving on computation for the reduced communication cost.

Communication Cost The communication cost of the distributed compressive sensing strategy includes two main part: the cost to propagate the random seed to the sensor nodes, and the cost to send the projected coefficients from the sensor nodes to the sink. The cost for broadcasting the random seed from the sink to the sensor nodes is a one-time cost and depends on the cost of the broadcasting protocol. The cost of sending the projected coefficients is determined by the number of the coefficients and the routing paths to the sink. Distributed compressive sensing strategy

successfully reduces the communication cost of the sensor nodes by decreasing the number of coefficients transferring from the nodes to the sink.

2.3 Distributed Source Coding

Distributed source coding consists of a set of strategies that exploits the correlation among sensor nodes [58, 59, 60], including the distributed compressive sensing strategy. It is based on Slepian-Wolf coding theorem [49] and Wyner-Ziv coding theorem [50]. The fundamental assumption of distributed source coding is the correlated data sources. Slepian-Wolf coding theorem provides a lower bound on encoding rate for lossless compression, while Wyner-Ziv coding theorem corresponds to a lower bound on encoding rate for the compression with losses.

2.3.1 Overview

The idea of distributed source coding can be demonstrated with an example of two correlated sources X and Y. Apparently, the coding rate $R \geq H(X|Y)$ is sufficient for describing X when the side information is available to both the encoder and decoder of X. Whereas, Slepian-Wolf theorem says that the coding rate $R \geq H(X|Y)$ is still sufficient for describing X when the side information is available to the decoder but the encoder.

In detail, X and Y are composed of binary words of length 3. They are correlated in the sense that the hamming distance between two words from X and Y is 1. Then it suffices to send 2 bits for X and to decode X without loss given side information Y. The reason is that as the hamming distance between X and Y is no more than 1, then binary words 000 and 111, having a hamming distance of 3, could be encoded using same code given the fact that its impossible to find a binary word in Y having hamming distance of 1 with both 000 and 111. 100,011, 110, 001, 101,

010 are the other pairs of binary words in X that share one code. As a result, the 4 pairs of binary words require only 2 bits to be encoded. In this example, the prior knowledge of the correlation is embodied by the known hamming distance between the two words.

Similarly, Wyner-Ziv theorem states a generalization of Slepian-Wolf theorem considering encode distortion. It says that coding rate $R(d) \geq R_{X|Y}(d)$ suffices, where $R(d)$ is the coding rate with distortion d when the side information is available to the decoder but the encoder and $R_{X|Y}(d)$ is the coding rate with distortion d when side information is available to both the decoder and the encoder.

Encoding the correlated sources without knowledge of side information is of great importance to wireless sensor networks, because it is no longer necessary for the correlated sensor nodes to talk to each other in order to encode their data at the sufficient rate. Remarkable saving on communication is achieved by applying Slepian-Wolf or Wyner-Ziv coding schemes.

As Slepian-Wolf coding and Wyner-Ziv coding only provide theoretical limits on the coding rate, the implementation of encoding schemes requires the knowledge of correlation, the source coding algorithm, the channel coding algorithm and the estimation algorithm, all of which demand a careful design in order to approach the theoretical coding rate limits.

2.3.2 Typical Applications

As wireless multimedia sensor networks exhibit strong inter-sensor correlation and intra-sensor correlation [61], distributed source coding strategies find wireless multimedia sensor networks promising to achieve energy efficiency through encoding the heavily correlated images.

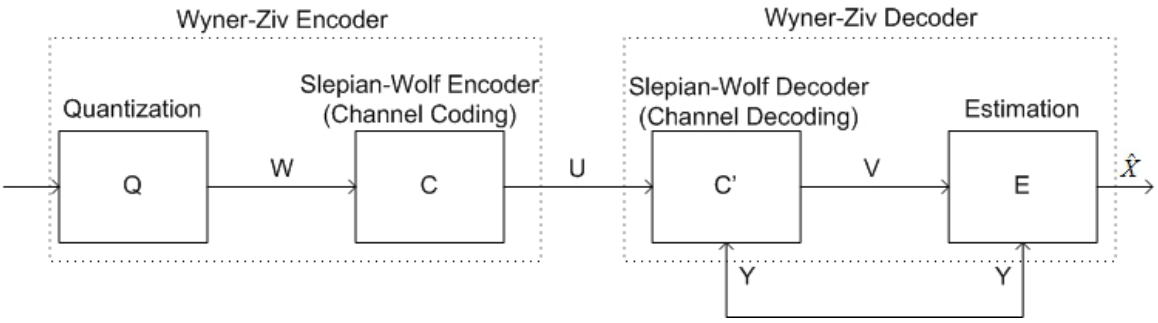

Figure 2.1: DISCUS: A Framework of Applying Distributed Source Coding

A framework of applying distributed source coding, namely DISCUS, was proposed [62]. As shown in Fig. 2.1, it is composed of an encoder and a decoder. The encoder not only quantizes the source with certain fidelity, but also constructs coset containing the code words of the source X. The decoder firstly looks up the code words in the coset with the help of the side information, Y, which is correlated to X. Then the decoder estimates X using the resulted code words and the side information.

The source coding algorithm is able to encode the source at the rate R_s by dividing the source space into $2LR_s$ number of index set, where L is the length of the code words corresponding to the quantized source. Because the correlation between X and Y implies the correlation between W and Y, it is assumed that there exists a fictitious channel between the input W and the output Y. The channel coding algorithm achieves the rate of R_c given the correlation model of the source X and the side information Y. Consequently, the final encoding rate of the encoder in the framework is $R = R_s - R_c$.

Design of the source coding algorithm aims at minimizing R_s, while design of the channel coding algorithm targets at maximizing R_c. An approach using trellis-coded scalar-quantization (TCSQ) [63] and the construction of the corresponding coset is reported to obtain the performance 2-5 dB from the Wyner-Ziv bound when the

correlated sources are identically distributed Gaussian sources with side information in the form of a noisy source.

A similar approach of applying Wyner-Ziv coding schemes was presented [64]. A nested lattice quantizer is proposed to take the place of TCSQ in the preceding framework. Turbo and low-density parity check (LDPC) code [65] is discussed as the promising channel coding method to approach the Slepian-Wolf limits. Regarding the practical deployment of distributed source coding, the issue of modeling the correlation of sensor nodes is emphasized since the performance of Slepian-Wolf coding greatly relies on the correlation model.

Besides, approaches for constructing low-complexity video encoding based on Wyner-Ziv coding was summarized in [66]. In contrast to the conventional inter-frame coding, the proposed scheme encodes individual frames independently and decodes them jointly. It benefits the video compression process carried out on the encoder in terms of low cost because the independent encoding of frames only involves intra-frame process with low complexity. The complexity of inter-frame processing is shifted to the decoder in order to achieve performances that are comparable to the conventional inter-frame coding.

There are two types of approaches introduced respectively: the pixel-domain encoding and the transform-domain encoding. As shown in Fig. 2.2, the pixel-domain encoding compresses the frames through independently applying Wyner-Ziv coding on a set of frames and performing conventional intra-frame compression scheme on the other frames, which are the key frames regularly spaced in the frame sequence. The Wyner-Ziv frames are decoded with the knowledge of the side information provided by the decoded key frames and the other available decoded Wyner-Ziv frames. A Rate-Compatible Punctured Turbo (RCPT) code [67] is applied in the Slepian-Wolf encoder. Its flexible coding rate enables the decoder to require more encoded bits in

the effort to adapt to the varying correlation between the encoded frames and the key frames. Through the repeated process of acquiring more encoded bits, the decoder is able to provide stream bits that are good enough for reconstruction of the Wyner-Ziv frames. Side informations involvement in the reconstruction process is the key of compressing the video frames, because only k bits are requested from the encoder to estimate the 2^M quantization bins, where $k \geq M$. However, the feedback of the request bits is not favorable in wireless multimedia sensor networks. The benefit of compressing the video frames transmitted from the encoder to the decoder could be easily wiped off due to the extra communication cost by the feedback mechanism from the decoder to the encoder.

The transform-domain encoding has a similar structure with the pixel-domain one. But it applies Slepian-Wolf coding on the independently quantized transform coefficients of the source vectors. The side information is generated through applying the same blockwise DCT [68] on the previously available frames. Source vectors are reconstructed from the outputs of the Slepian-Wolf decoders and their corresponding side information using a band of turbo decoders. In the simulation conducted in the paper, at most 2 dB gain of the PSNR is obtained because of the higher complexity of the encoder compared to that of the pixel-domain encoding system. Nevertheless, the transform-domain coding is able to obtain a performance comparable to the inter-frame process at a cost comparable to the intra-frame process.

Based on the preceding discussions, the following conclusions on the distributed source coding can be obtained.

- Distributed source coding based on Slepian-Wolf theorem and Wyner-Ziv theorem takes advantage of the correlation of distributed sources in order to reduce the communication cost.

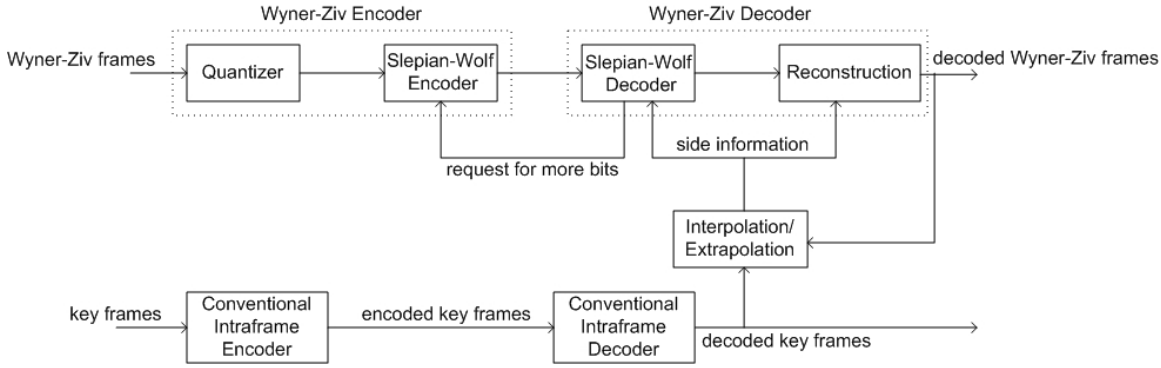

Figure 2.2: Pixel-domain Wyner-Ziv Coding Scheme

- Slepian-Wolf theorem and Wyner-Ziv theorem only provide the theoretical limits on coding rate. Practical solutions involve modeling the correlation; designing the source-coding algorithm, the channel coding algorithm and the reconstruction algorithm. The goal of practical solutions of wireless multimedia sensor networks is to approach the theoretical limits with reasonable encoder complexity.
- There are two types of solutions for wireless multimedia sensor networks to apply distributed entropy coding. One targets on the correlation of sensory data from the spatially correlated sensor nodes. The other focuses on the correlation among the video frames from one individual video sensor. Both of them are capable of reducing the communication cost to transmit the encoded data from the encoders to the decoders implemented in nodes equipped with comparatively abundant resources.
- Solutions based on either Slepian-Wolf theorem or Wyner-Ziv theorem vary from each other in that they deal with different correlations. The approaches discussed in this section fall into two categories: correlation of sensory data within one sensor; correlation of sensory data from multiple sensors. Future work in wireless multimedia sensor networks is expected to explore the corre-

lation of video frames within one sensor in conjunction with the correlation of video streams from multiple sensors.

2.4 Optimal Sampling

Other than compressing or encoding the original sensory data for less communication costs, optimal sampling strategies achieve energy efficiency through selecting the most informative samples and sending them to the application. In other words, optimal sampling strategies attempt to avoid wasting bandwidth and energy on unnecessary samples while performing applications' tasks. The criteria of selecting samples is based on metrics of the amount of information or the accuracy of parameters estimation. Optimal sampling strategies focus on a better tradeoff between sensing cost and application performance without introducing additional computation load to sensor nodes with limited resources. However, they assume that prior knowledge of either the sensory data correlation or the estimator for processing sensory data.

2.4.1 Optimal Node Placements

The optimal node placements approach [69] embodies the idea of optimal sampling at the individual node's level. It assumes that the sensor network is dense thus sensor nodes are spatially correlated with each other. Intuitively, the idea of selecting a subset of less correlated sensor nodes helps to reduce the communication cost without affecting the application performance. The tradeoff between communication cost and the amount of information inspires two optimization problems: minimizing communication cost while guaranteeing the quality of mutual information; and maximizing mutual information while restraining communication cost below a certain threshold.

In order to formulate the optimization problems, communication cost is quantified through a simplified transmission model with unit transmission cost. Consequently, the optimization problems can be interpreted as finding the most informative placements of at most V sensor nodes and finding the placements of sensor nodes providing a certain amount of mutual information. The amount of mutual information is the conditional entropy $H(X_s|X_A)$, where X_s is the data source and X_A is the data to be estimated. As the data sources are modeled as Gaussian Process [70], the mutual information is given:

$$H(X_s|X_A) = \frac{1}{2}log((2\pi e)^n detK_{s|A}) \tag{2.7}$$

where $K_{s|A}$ is the estimation covariance matrix representing the covariance between the sensory data and the estimated data.

To solve the NP-hard optimization problem of finding the most informative placements of sensor nodes, an approximation algorithm based on the submodularity and monotonicity of the mutual information function is presented. The key of the approximation algorithm is to generate a modular approximation graph and solve two optimization problems respectively.

The approach actually involves three steps:

- Collect data from the initial dense deployment of sensor nodes.
- Establish the probabilistic models of sensing quality and wireless link quality.
- Approximately solve the optimization problems based on the probabilistic models.

It is worth noticing that the solutions are based on the learning process that extracts the probabilistic models from the initial deployment. The approach implicitly assumes that the statistical characteristic of the measured physical signal is time invariant.

2.4.2 Optimal Adaptive Sampling

In contrast to the optimal node placements approach, the optimal adaptive sampling approach [71] aims at selecting the informative samples from regression's perspective or estimation's perspective. The uniqueness of the approach lies in its iterative nature. The sink performs multi-output Gaussian Process formulation based on the sensory data it collects. A probabilistic model based on Gaussian Process enables the sink to decide the time instance of the next sample and the location of the sensor node to take the next sample. Therefore, energy savings are obtained through avoiding unnecessary samples to be taken. The correlation of sensor nodes is addressed in the covariance function model. Since the correlation of the sensor nodes leads to unnecessary samples, the optimal adaptive sampling approach skipped the samples to save sensing cost.

Due to the approach's adaptive nature, the actual selection of sampling time instances and sensor nodes depends on the correlation of sensory data. When the correlation of sensory data is time-variant, for instance, sensor nodes are mobile, the approach is able to adjust to the changes along time. Furthermore, the approach does not assume regular samples, which indicates that the selection of sampling time instances may not follow the regular sampling pattern due to the nature of the sensory data. Interestingly, as shown in the experimental results, the spatial correlation of the sensory data leads to the result that samples are taken at different sensor nodes at different time instances.

The adaptive nature comes with the price of additional computation load, communication costs of assigning the sampling time instances to sensor nodes. It is shown in Fig. 2.3 that the selection of sampling time instances is determined by the sink after it evaluates the utility function. The utility function is a function of the prediction uncertainty. It assures that the sink selects a shorter time to wait before taking

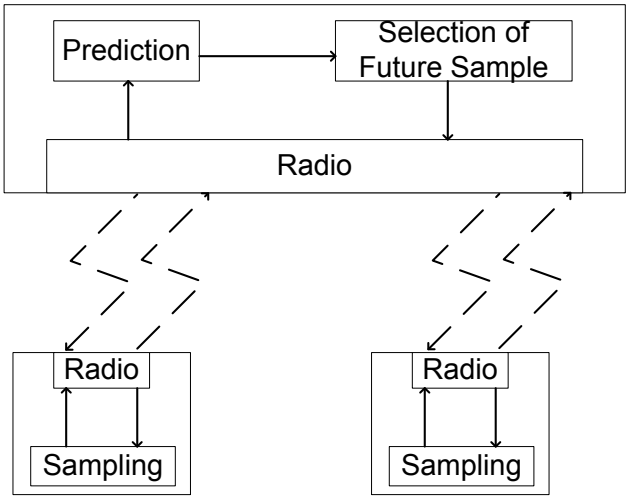

Figure 2.3: The optimal adaptive sampling approach

the next sample when the prediction uncertainty tends to increase, and vice versa. The goal is to keep the prediction uncertainty below a certain threshold. Therefore, the resulted sampling time instances could be regular, irregular or a concatenation of regular samples and irregular samples. Although the additional computation load is not a burden to the sink with abundant resources, the communication costs becomes an unnecessary overhead when the resulted samples follow a regular pattern, which can be predefined during the initial deployment.

2.5 Summary

Although information-driven strategies focus on the tradeoff between quality of information and energy consumption, they vary from each other in defining the correlations, quantifying the quality of information, sampling patterns, algorithmic aspects etc. The comparative study of information-driven strategies leads to a set of taxonomy to category them and to compare them under the taxonomy.

2.5.1 Taxonomy

Correlation: There are two types of correlations considered in information-driven strategies. One is the temporal correlation, which is the autocorrelation of sensory data from an individual sensor node, and the other is the spatial correlation, which is the correlation among sensory data from different sensor nodes. Therefore, temporal correlation is also called intra-node correlation, while spatial correlation is called inter-node correlation. Especially, compressive sensing strategies consider the sparsity of sensory data. Temporal correlation is thus called sparsity, while spatial correlation is called joint sparsity. When sensor nodes are located closely to each other, spatial correlation is significant. For mobile sensor networks, spatial correlation can be time-variant, since the it is related to the distance between a pair of sensor nodes. Despite the different names, information-driven strategies target the same phenomenon to achieve the same goal of reducing energy consumption.

Quality of information: In order to quantify the quality of information to be extracted by the sink from the received data, several metrics have been proposed depending on the application's tasks. For lossless data gathering task, the application expects to recover the original sensory data with a high probability. For lossy data gathering task, the application expects to have the most informative sensory data, which implies that the parameter estimation or prediction can be accomplished with high accuracy. Specifically, the metrics include reconstruction probability, entropy, conditional entropy, estimation accuracy, and prediction uncertainty.

Sampling: As information-driven strategies deal with sensory data taken by sensor nodes, data samples and the way the they are taken play an important role in the process of compression, encoding or selection of samples etc. Sensor nodes can synchronize the sampling time instances or not, take samples regularly or irregularly,

and take samples synchronously or asynchronously. The choice of sampling pattern also depends on the hardware capabilities of sensor nodes.

Algorithmic aspects: The algorithmic aspects of information-driven strategies lay in the centralized process at the sink and the distributed process performed by individual node to extract useful information from sensory data. In addition, an iterative or one-time process is necessary for the strategies to adjust to different degrees of correlations. The centralized process at the sink can afford computation intensive tasks, while the distributed process at the individual sensor node favors light-weight calculations that demand less energy and memory usage. The one-time process is sufficient for time invariant correlations, while the iterative process is necessary for time variant correlations.

Protocol layers: The key of information-driven strategies is the tradeoff between energy consumption and application performance. Therefore, they mostly reside at the application layer. However, efforts to introduce the information-driven concept into the MAC layer have shown promising results.

2.5.2 Comparative Analysis

The comparison of information-driven strategies is shown in Table 2.1. Since distributed compressive sensing is originated from distributed source coding, it has identical entries with the distributed source coding in the table. However, the difference between these approaches lies in the technique processing the original sensory data. Distributed compressive sensing focuses on the linear projection of sensory data, while distributed source coding usually applies encoding schemes. Although the asynchronous sampling strategy shares the similar set of characteristic with distributed compressive sensing, it does not require processing sensory data at individual

sensor node. Thus, the asynchronous sampling strategy is ideal for applications with extremely strict budget on the computation power of sensor nodes.

Table 2.1: Comparison of Information-driven Strategies

Strategy	Correlations	Quality of Information	Sampling	Algorithmic Characteristic	Protocol Layer
Compressive Sensing	temporal	recover probability	regular	one-time	application
Distributed Compressive Sensing	temporal and spatial	recover probability	regular	one-time	application
Distributed Source Coding	temporal and spatial	recover probability	regular	one-time	application
Optimal Node Placements	temporal and spatial	conditional entropy	regular	one-time	application
Optimal Adaptive Sampling	spatial	prediction uncertainty	irregular	iterative	application
Asynchronous Sampling	temporal and spatial	recover probability entropy	asynchronous regular	one-time	application
Information-driven MAC protocol	temporal and spatial	estimation accuracy	asynchronous regular	one-time	MAC and application

In order to demonstrate different performances of information-driven strategies, an energy model is established for a specific data gathering application. The data gathering scenario is described in the following:

- There is one sink in the network to collect sensory data from sensor nodes, which take samples of the physical phenomena regularly.
- The network of sensors is organized in a hierarchical architecture, in which a node with abundant resources serves as the cluster head of a number of neighboring sensor nodes. The cluster head collects sensory data and forward them to the sink.
- Sensor node is equipped with sufficient resources to process sensory data before transmitting the processed result to the cluster head.

The above specifications are also applicable for the event reporting application, since the requirement on data gathering is same.

Accordingly, the energy model is given:

$$P = (E_s + b_s \times e_c + b_t \times e_t + m \times e_m) \times f_s + P_n \tag{2.8}$$

where

P is the power of one sensor node.

E_s is the energy consumed by the sensor to take one sample.

b_s is the number of bits in one data sample.

e_c is the average energy consumed by the node to process one bit of data.

b_t is the number of bits per sample to be transmitted to the cluster head.

e_t is the energy consumed by the wireless radio to transmit one bit of data.

m is the average number of backoffs per sample before the node obtain the channel for transmission.

e_m is the energy consumed by the wireless radio per backoff.

f_s is the sampling frequency, which equals to the average number of samples per second.

P_n is the share of node's power on maintaining the network.

Specifically, b_s is able to quantify how many bits of data are needed to represent one sample; and the average computation cost in terms of the average energy consumed by processing one bit of data is represented by e_c. Therefore, the energy consumed by processing one sample can be calculated by multiplying the number of bits processed and the energy of processing one bit of the samples. Apparently, the number of bits to be processed is actually the total number of bits of the samples.

After processing the samples, sensor node will attempt to access the wireless medium for transmitting the processed result to the cluster head. The total energy

spent on access the medium can be calculated by multiplying the average energy consumed per sample, $m \times e_m$, and the number of samples.

Then, sensor node will transmit the processed result to the cluster head. The total energy for transmitting the data obtained from one sample equals to the multiplication of b_t and e_t.

Given the energy consumed for taking, processing and transmitting one sample, the power of one sensor node can be obtained by multiplying the energy per sample and the sampling frequency. In addition to the sensing and transmitting tasks, the sensor node is also subject to tasks related to maintaining the connectivity and time synchronization etc. Therefore, the power of one sensor nodes is composed of two parts: the power for sensing and transmitting, and the power for network maintenance.

Although parameters in the model can vary with different hardware and software specifications, it is still of interest to the comparison study of information-driven strategies to choose a set of parameters for the data gathering application. Regarding the energy consumed by taking samples, E_s, let take the typical value of a soil moisture sensor [22], which requires $5mW$ for $10ms$ for one sample. Therefore, $E_s = 50\mu J$. However, the typical value for a low power temperature sensor [72] results in $P_s = 0.025\mu J$.

For distributed compressive sensing, the computation cost of linear projection is negligible. However, for distributed source coding, the computation cost can be comparable to the communication cost. Therefore, let $e_c \approx 0$ for distributed compressive sensing strategies, while let $e_c \approx 0.4 \times e_t$ for distributed source coding strategies.

The average transmitting energy per bit, e_t, can be determined by the transmitting power and the average length of time needed to transmit one bit of data.

Take the popular radio CC1100 [73] for example, the transmitting power is $25mW$. According to the transmitting rate of 802.15.4 [74], 20k$bits/S$, $e_t = 1.25\mu J/bit$.

Each attempt of the node to access the channel leads to a certain length of backoff idle time subject to the configuration of the CSMA/CA protocol, The random backoff time of the 802.15.4 protocol vary from 0 to $(2^3 - 1) \times 320\mu s$. For the sake of tractability, let the average backoff time to be $1ms$. Accordingly, $e_m = 20\mu J$.

Since P_n is irrelevant to the parameters of sensing and transmitting, the focus of the comparison among information-driven data gathering strategies will be $P - P_n$.

Regarding synchronous sampling strategies, let the sampling frequency to be $0.01Hz$, which means the node takes one sample every 100 seconds. A typical A/D converter can convert one sample to be 16 bits of data [75]. Ideally, the average number of attempts needed to access the medium for sending one packet is one. Let the average number of attempts per sample to be 0.03. Finally, the total power for the sensor node applying synchronous sampling strategies and IEEE 802.15.4 protocol is $0.76\mu W + P_n$ for the moisture sensor, and $0.26\mu W + P_n$ for the temperature sensor.

If the asynchronous sampling strategy for lossless data gathering is able to reduce the sampling rate by half, while guaranteeing the recover of the original signal, the power of the sensor node without applying the asynchronous sampling strategy is $1.52\mu W + P_n$ and $0.52\mu W + P_n$ respectively.

Regarding the distributed compressive sensing with the same set of parameters, the power of the sensor node is $1.26\mu W + P_n$ for the moisture sensor, and $0.26\mu W + P_n$ for the temperature sensor. Energy consumption of the distributed compressive sensing is greater than the asynchronous sampling strategy when the sampling cost is significant. Furthermore, the computation task at the sensor node may require additional hardware than the asynchronous sampling strategy.

Regarding the distributed source coding with the same set of parameter, the power of the sensor node is $1.34\mu W + P_n$ for the moisture sensor, and $0.34\mu W + P_n$ for the temperature sensor. The energy consumption of the distributed source coding strategy is higher than the others due to the computation cost of encoding the sensory data. However, multimedia applications still depend on distributed source coding to enable streaming of videos or images.

Regarding the optimal adaptive sampling strategies, the energy consumed by feeding back the desired sampling time instances can be comparable to the energy consumed by transmitting the samples to the cluster head. Therefore, the power of the sensor node can be twice of the distributed compressive sensing or the asynchronous sampling strategies.

Regarding the ID-MAC protocol, the energy savings lie in the sampling process and the medium access process. Assume the ID-MAC is able to reduce the average number of attempts needed to access the medium from 0.03 to 0.02, the power of the sensor node can be $0.74\mu W + P_n$ and $0.24\mu W + P_n$ respectively.

After comparing the power of sensor node for different strategies given a particular set of parameters, the following conclusions can be reached:

- Asynchronous sampling strategies save energy through reducing the number of samples needed to recover the original signals.
- Distributed compressive sensing is able to achieve energy efficiency through reducing the number of bits to be transmitted.
- Further energy savings can be achieved by the ID-MAC protocol through reducing the number of attempts to access the medium for transmitting.
- Distributed source coding consumes more energy than the other information-driven strategies due to the computation intensive encoding algorithms.

- Optimal adaptive sampling strategy is less energy efficient than the others due to the iterative process to assign the sampling time instance to the sensor nodes.

CHAPTER 3

PRELIMINARIES

The scenarios motivating the asynchronous sampling and the information-driven MAC protocol are introduced firstly in this chapter. As data correlation is the basis of the study on information-driven approaches, signal model of lossless data gathering, exponential correlation model of lossy data gathering are presented. After that, event detection model and CSMA-based MAC model are introduced to facilitate the discussions on the proposed MAC protocol.

3.1 Motivating Scenarios

Data gathering is one of the most important applications of WSNs. The focus is on continuous data gathering scenarios where sensory data are collected consistently and periodically from the monitored field. As energy consumption of the sensor network is directly determined by the amount of data samples transmitted to the sink, the goals here are either to transmit fewer samples or to gain more knowledge about the monitored physical phenomena. The first goal is pursued in *lossless* data gathering, while the second goal is approached in *lossy* data gathering. In fact, these two goals lead to a better tradeoff between energy consumption and sensing quality from different perspectives. As the monitored signals are to be fully reconstructed in lossless data gathering scenarios, it is desirable to use fewer numbers of samples in the reconstruction, thus saving energy consumption without affecting the sensing quality. In contrast, lossy data gathering would have more informative samples containing increased amount of information due to the proposed asynchronous sampling.

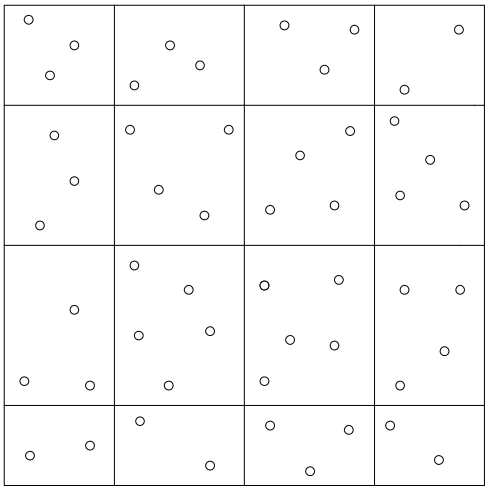

Figure 3.1: Cluster-based correlation model of a WSN.

As a result, the sensing quality is significantly improved without increasing energy consumption in lossy data gathering with asynchronous sampling strategies.

A few assumptions on the targeting scenario are made before proceeding further. Firstly, it considers densely deployed WSNs, where redundancy of the sensor nodes results in spatial correlation among the sensory data. As spatial correlation is usually strong among neighboring nodes, this dissertation aims at cluster-based WSNs in establishing the correlation models. Without loss of generality, discussions on correlation will be limited to only sensors within a cluster. Fig. 3.1 illustrates an example of clustering in sensor networks. Furthermore, it is also assumed that clocks of different sensor nodes within a cluster are synchronized with each other. In order to exploit temporal-spatial correlation of sensory data, it is assumed that the correlation knowledge is available at the sink through, for example, exploration of existing sensory data to derive the correlation coefficients.

Instead of calculating precisely the energy consumed by the network, the number of samples during a particular time period is used to represent energy consumption of the sensor nodes. This allows the work to isolate the performance of the proposed

strategy from those of the other components of the network such as routing and medium access control (MAC) layers. Event detection applications involve two distinct processes: detection and monitoring, as shown in Fig. 3.2. Normally, the event sprawl in a certain space, in which the deployed sensor nodes are able to detect the event by examining the samples of the relevant physical value continuously. In order to reconstruct the event or estimate its parameters, the sink (the laptop shown in Fig. 3.2) requests the reports from the nodes that monitor the event throughout its duration.

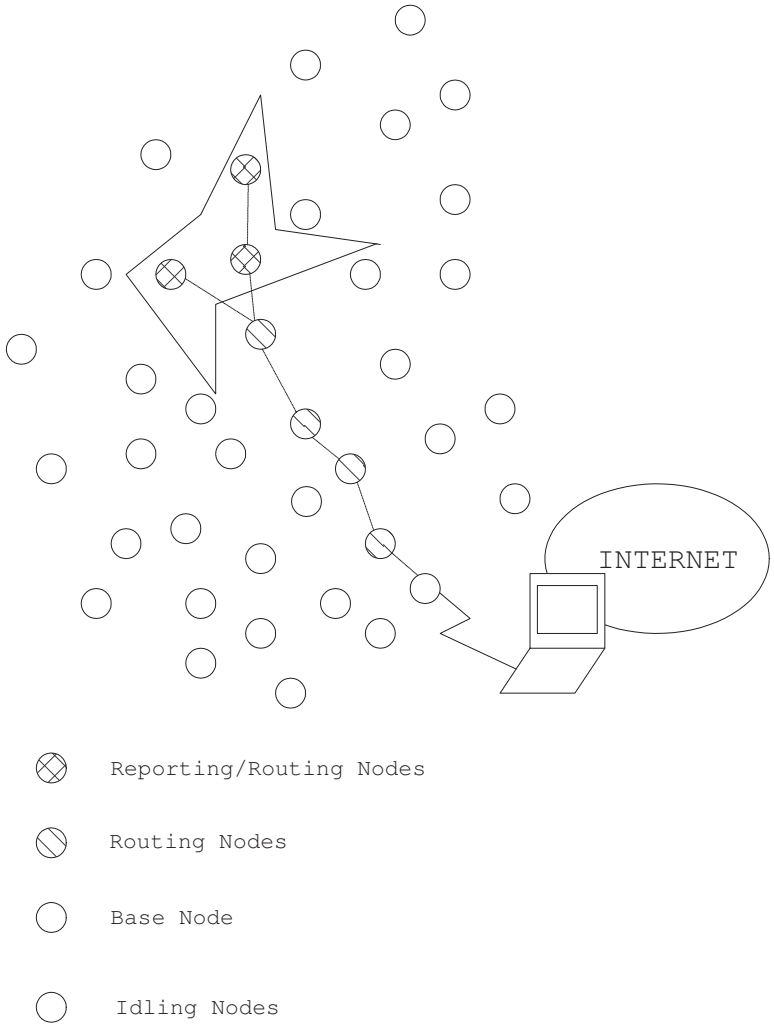

Figure 3.2: Event detection and monitoring with a wireless sensor network

The sensor nodes located within the event area detect the happening of the event through evaluating the predefine triggering criteria. Each sensor node attempts to send the event reports to the sink immediately after the event is detected. The event reports can be a simple binary value, a set of data describing the characteristics of the event observed by an individual sensor node, or a series of samples of a physical value to be processed by the sink. In the dissertation, the last type of event reports is considered.

3.2 Signal Model

Collaboration among spatially correlated sensor nodes has been proposed in [76] as an approach to achieve energy efficiency of WSNs. Previous efforts [77, 46, 78, 79] focused on distributed algorithms for signal processing or aggregating data from different nodes. In this section, the correlation among sensor nodes in WSNs is explored from a novel perspective in the context of lossless data gathering. In the proposed strategy, the sampling time instances of each node are shifted from each other along the time line. Through theoretical analysis and simulation results, it is shown that the original signal can be recovered from the asynchronous samples with a lower sampling rate.

Given a cluster of sensor nodes, let the physical signal monitored by the ith node at time t in the cluster be denoted by $Z_i(t)$, which is time variant and composed of two parts as shown in Eq. (3.1). Let $X_c(t)$ be the common part and $X_i(t)$ the innovation part. The common part refers to global effects on the physical phenomena that can be observed by all the nodes in the cluster, while the innovation part refers to local effects that are observable only to an individual node.

$$Z_i(t) = X_c(t) + X_i(t) \tag{3.1}$$

This correlation model has been adopted to exploit the redundancy of sensor nodes [80]. Clearly, this model fits well into certain monitoring applications such as habitat monitoring in that the common part represents the contribution from the global factors, such as sunlight, while the innovation part is due to the local factors, such as rain falls, affecting the physical phenomena.

Besides, it is worth noticing the frequencies of the signals when considering monitoring the physical phenomena from the viewpoint of signal processing. Let f_c be the frequency of the common part signal and let f_i be that of the innovation part signal. In order to examine the relationship between $X_c(t)$ and $X_i(t)$, the bandwidth of these signals are defined as follows:

$$\begin{aligned} f_{c,l} \leq f_c \leq f_{c,h} \\ f_{i,l} \leq f_i \leq f_{i,h} \end{aligned} \tag{3.2}$$

where $f_{c,l}$ and $f_{c,h}$ are the lowest and highest frequencies of f_c, whereas $f_{i,l}$ and $f_{i,h}$ are the lowest and highest frequencies of f_i. If $f_{i,h} << f_{c,l}$, the following argument will be satisfied.

$$f_{i,l} \leq f_i \leq f_{i,h} << f_{c,l} \leq f_c \leq f_{c,h} \tag{3.3}$$

Another interpretation of the argument is that the global factors vary at a frequency much higher than that of the local factors. For instance, temperature measurements of an outdoor environment show that the global factors, such as daily variation of sunlight, change much faster than the local factors like rain falls. The spectrum of an example signal, $Z_1(t)$, that satisfies the argument is displayed in Fig. 3.3. The bandwidth of the common part signal, $X_c(t)$, is within 15% to 20% of

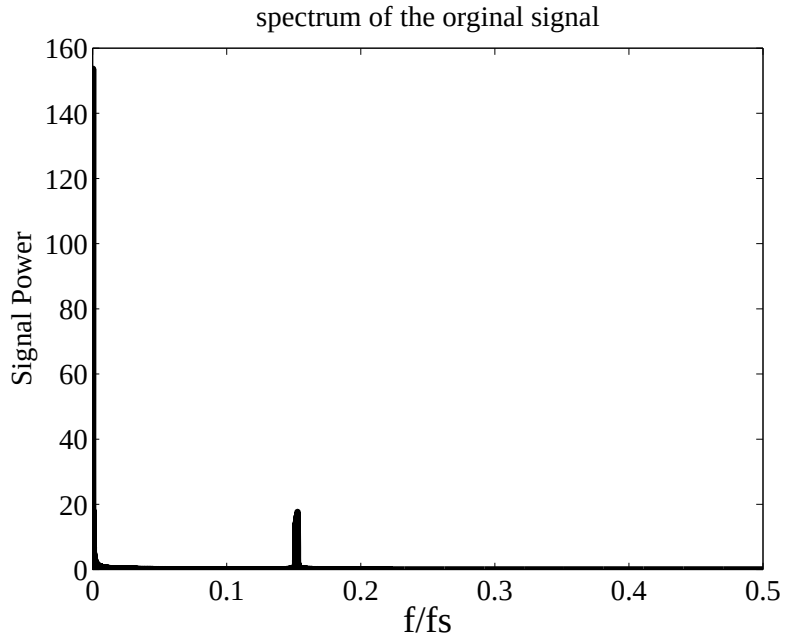

Figure 3.3: Spectrum of $Z_1(t)$ sampled at f_s.

the synchronous sampling frequency, f_s. The innovation part signal, $X_c(t)$, has the bandwidth from 1% to 5% of f_s. Fig. 3.4 shows the spectrum of the signal sampled at a reduced frequency, f_u. Although the spectrum is shifted and suppressed to some extent, the separation between the common part signal and the innovation part signal is preserved.

The argument indicates that the reconstruction of the physical signal requires a sampling rate higher than two times of $f_{c,h}$, although the reconstruction of $X_i(t)$ only requires a sampling rate higher than two times of $f_{i,h}$, which is much lower than that of $Z_i(t)$. In the next section, it will be further demonstrated how to tackle this discrepancy in sampling rates.

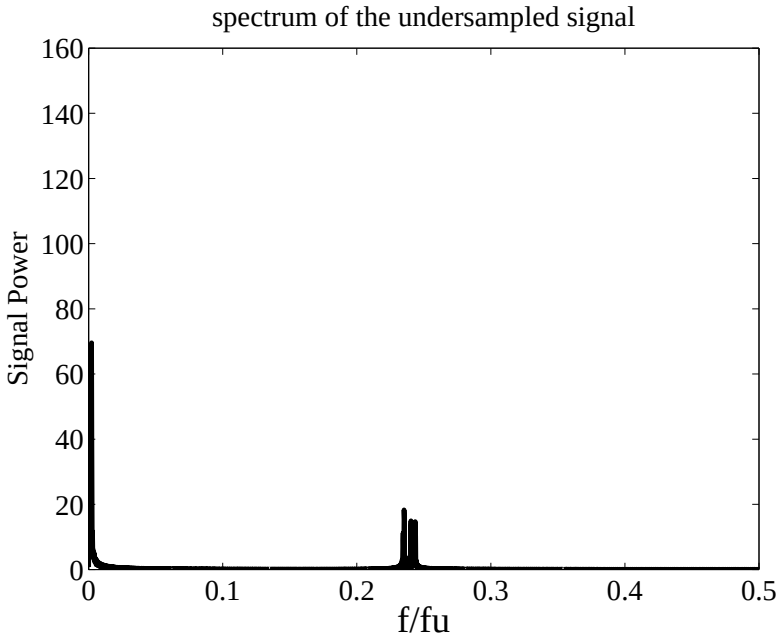

Figure 3.4: Spectrum of $Z_1(t)$ sampled at f_u.

3.3 Exponential Correlation Models

The key benefit of asynchronous sampling is redundancy reduction in the sensory data, which can in turn be exploited to maximize entropy of the information or minimize the energy consumption (through reduction of the sampling rate). Before detailing the asynchronous sampling strategies, discussions on the correlation model considered in this chapter are presented.

3.3.1 Exponential Correlation Model

This dissertation considers a dense WSN monitoring a physical process such as wind speed or temperature field. The data gathered by a sensor node consists of the true measurement value and a noise. Assuming that the location of the sensor node i is denoted by (x_i, y_i, z_i), a sensory sample U_i at time t can be expressed as

$$U_i(t) = M(x_i, y_i, z_i, t) + P(x_i, y_i, z_i, t), \tag{3.4}$$

where M represents the (true) measurement value determined by (x_i, y_i, z_i) and t, and P is the corresponding noise introduced by the environment or the sampling process.

Spatial correlation is due to the spread of the physical process in the space. If sensor nodes sample the physical value in a synchronized pattern, the correlation among sensory data is mainly determined by the locations of the nodes. Specifically, suppose the sensory data given in Eq. (3.4) are Joint Gaussion Random Variables (JGRVs) with zero mean and σ_M^2 variances, and the noise P_i is independent and identically distributed (i.i.d.) Gaussian random variable with zero mean and σ_P^2 variances. Then the spatial correlation between the sensor nodes i and j can be expressed as

$$\rho_s(i,j) = \frac{E[U_i U_j]}{\sigma_M^2 + \sigma_P^2}. \tag{3.5}$$

As a commonly employed model [81], the spatial correlation is assumed to be inversely proportional to the distance $d_{i,j}$ between two nodes i and j:

$$\rho_{i,j}^{spatial} = e^{-\alpha d_{i,j}} = e^{-(\alpha(\sqrt{(x_i-x_j)^2+(y_i-y_j)^2+(z_i-z_j)^2})} \tag{3.6}$$

where $\alpha > 0$ denotes a constant for spatial correlation intensity.

Temporal correlation often denotes the correlation between the data sampled at different time instances. Similarly, for a wide-sense stationary process [82] as a Gaussian random process, the temporal correlation can be expressed as

$$\rho_{i,j}^{temporal} = e^{-\beta \tau_{i,j}} \tag{3.7}$$

where $\tau_{i,j} = |t_j - t_i|$ is the difference between the sampling time of nodes i and j, and β is the constant measuring the temporal correlation intensity.

For synchronous sampling, $\tau_{i,j}$ is close to zero and hence the correlation among the data is often the largest. In the asynchronous sampling strategy, τ will vary according to the network, which intuitively will increase the entropy of the sensory data. Combining both spatial and temporal correlations, the correlation of sensory data between nodes i and j is defined as:

$$\rho_{i,j} = e^{-(\alpha d_{i,j} + \beta \tau_{i,j})} \tag{3.8}$$

Although $\rho_{i,j}$ may vary with time, it is assumed that β is a constant in the further discussions on the asynchronous sampling strategies. As the correlation among the sensory data could vary slowly in comparison with the sampling rates, it can be assumed that β remains to be a constant for a short period of time during which the asynchronous sampling strategy can be applied. Furthermore, for asynchronous sampling strategies that do not require prior knowledge of the correlation among sensory data, the assumption of a constant β can be discarded.

3.3.2 Correlation Example

Two examples are presented to verify the above exponential correlation model. One is a stochastic process whose covariance is an exponential model. The other is the covariance of experimental data from spatially correlated sensor nodes.

Denoting a Brownian motion process as $\{X(t), t \geqslant 0\}$, a stochastic process is given as

$$V(x, y) = e^{-\frac{1}{2}(\alpha x + \beta y)} X(e^{(\alpha x + \beta y)}) \tag{3.9}$$

where $\alpha > 0$, $\beta > 0$.

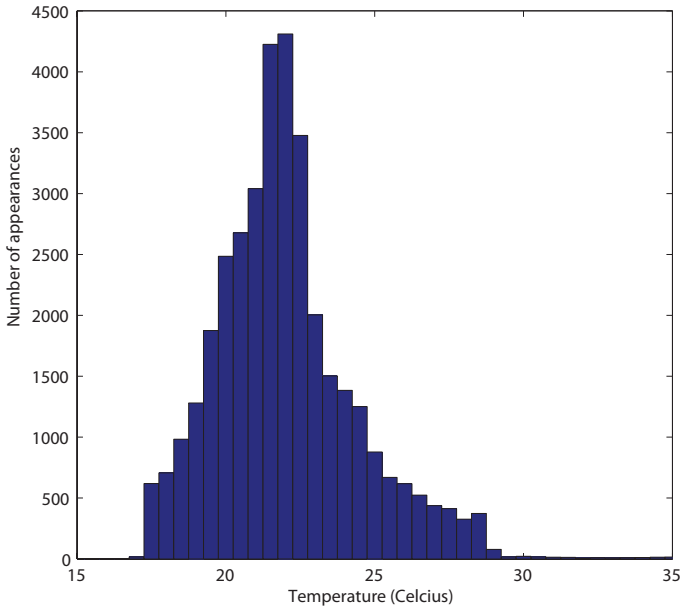

Figure 3.5: Histogram of temperature readings from one node

Then, its expected value and covariance are computed as follows:

$$E[V(x,y)] = 0$$

$$\begin{aligned}
&Cov[V(x,y), V(x+\Delta x, y+\Delta y)] \\
&= e^{-\frac{1}{2}(\alpha x+\beta y)} e^{-\frac{1}{2}(\alpha(x+\Delta x)+\beta(y+\Delta y))} Cov[X(e^{(\alpha x+\beta y)}), X(e^{(\alpha x+\beta y)+(\alpha\Delta x+\beta\Delta y)})] \\
&= e^{-(\alpha x+\beta y)} e^{-\frac{1}{2}(\alpha\Delta x+\beta\Delta y)} e^{(\alpha x+\beta y)} \text{ (by property of Brownian motion process)} \\
&= e^{-\frac{1}{2}(\alpha\Delta x+\beta\Delta y)}
\end{aligned} \tag{3.10}$$

The above derivation shows that the stochastic process given in Eq. (3.9) has exponential covariance that fits the correlation model in Eq. (3.8).

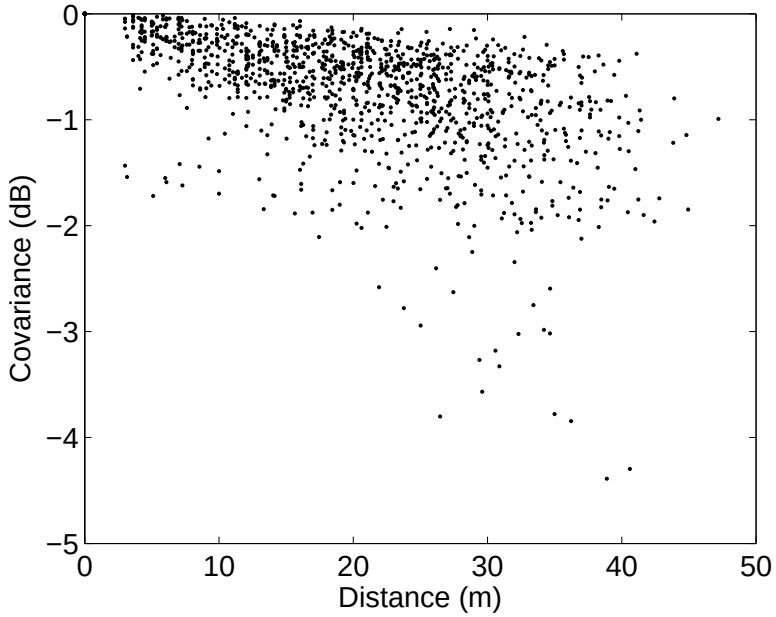

Figure 3.6: Coefficients and distances

A set of experimental data from Intel Berkeley Lab [83] is considered to demonstrate the correlation among data. Temperatures at different locations in the lab space were measured by sensor nodes. Given temperature measurements and locations of sensor nodes, the measurement covariances between any pair of sensor nodes are calculated. In Fig. 3.5, the histogram of the temperature readings from one node resembles a Gaussian distribution, which agrees with the assumption of JGRVs. Fig. 3.6 shows the relationship between the covariance coefficients and the distance between two sensors. It is obvious that the experimental data do not fit the spatial correlation model in Eq. (3.6), although the covariance coefficients decrease with the distance between sensors. The covariance coefficients are calculated using decibel to transform exponential relationship into linear relationship for the sake of simplicity in the plots.

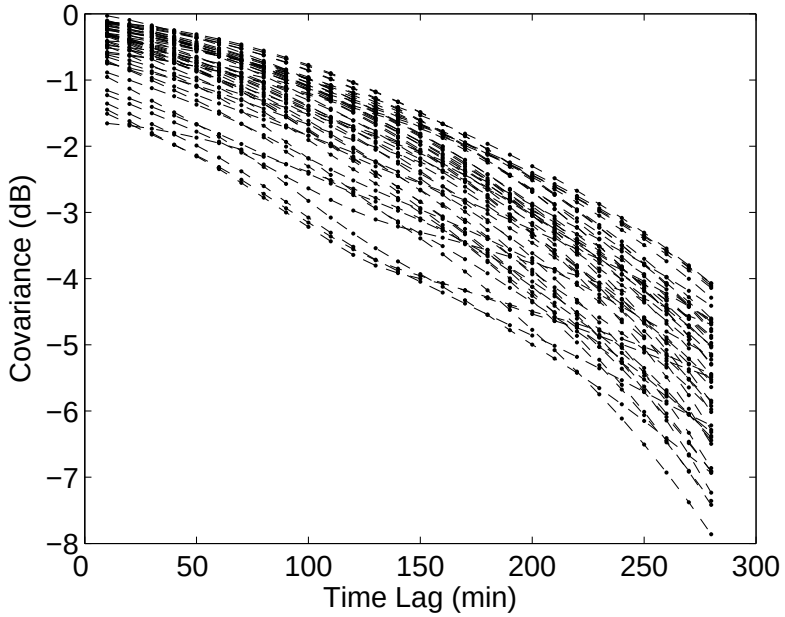

Figure 3.7: Coefficients and time lags

It is observed that the covariance coefficient of temperature measurements from one sensor and those taken after a certain time lag from another sensor exponentially decreases with the time lag as shown in Fig. 3.7. Each dashed line corresponds to a pair of sensor nodes. For each pair, its covariance coefficient in decibel declines approximately linearly with time lag between temperature measurements taken at the two nodes. Therefore, the observed covariances can be approximated through the exponential model described in Eq. (3.8). More generally, the ordered exponential model, given in Eq. (3.11), can be introduced to model the coefficients for a broad range of applications.

$$\rho_{i,j} = e^{-(\alpha d_{i,j} + \beta \tau_{i,j}^{\xi})} \tag{3.11}$$

When the model type constant $\xi = 1$, Eq. (3.11) is the same as the exponential model adopted in the previous discussions. When $\xi = 2$, it leads to the squared

exponential model that is common in the literature of Gaussian processes and usually leads to a close approximation of the covariance coefficients.

Although spatial correlation of the experimental data is irregularly dispersed, its temporal correlation nicely follows the exponential model, which enables the work to apply asynchronous sampling to reduce the correlation among sensory data by adopting the exponential temporal correlation model.

3.4 Event Detection Model

In WSNs performing event detection, each node takes samples frequently and makes its own decision according to the samples. The decision making procedure could be formulated as follows. Assume N sensors within the event area A. The signals being measured by each node, $x_i(t)$ is composed of two parts: the real signal $s_i(t)$ and the noise $v_i(t)$. The event detection decision can be made according to a certain threshold h. Normally, the detection of an event is accomplished at individual nodes. After detecting the event, each node tries to send the sensory data about the event to the sink for further analysis. Let the moment when the event is detected by each node be denoted by Δt_d. It is a small time period, during which nodes residing in the area A detect the event. Thus,

$$x_i(t) = s_i(t) + v_i(t), \text{ for } i = 1, 2, ..., N \tag{3.12}$$

$$F_i = \frac{1}{t_L - t_1} \sum_{j=1}^{L} x_i^2(t_j) > h, i = 1, 2, ..., N, j = 1, 2, ..., L \tag{3.13}$$

and

$$\Delta t_d = Max\{t_i\} - Min\{t_i\}, i = 1, 2, ..., N \tag{3.14}$$

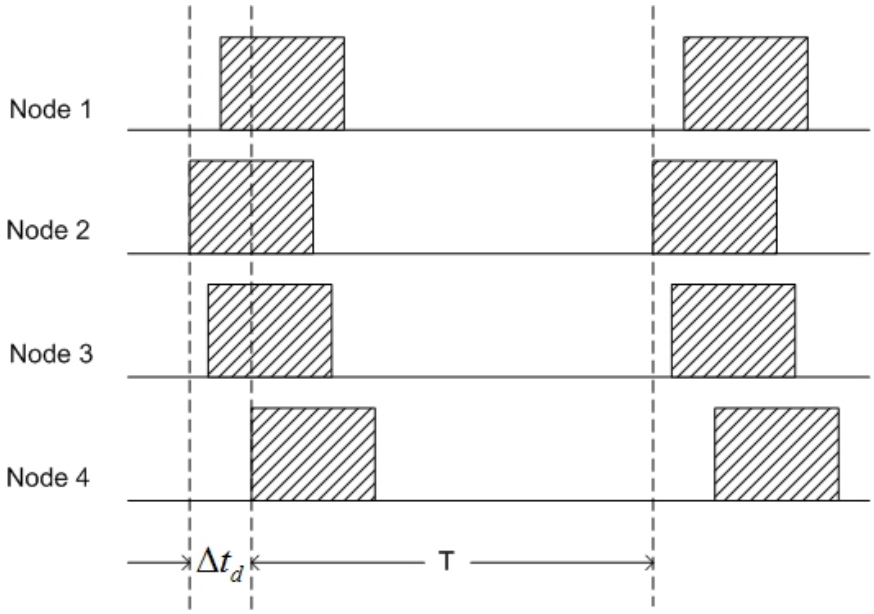

Figure 3.8: Traffic pattern of event reporting

where t_j is the sampling moments at the jth sampling instances, t_i is the sampling moments for the ith node, and F_i is the event detection criteria, which is usually the power of the signal during a time period. Starting from the moment of detection, the data traffic is generated continuously while the nodes take samples at a constant rate $1/T$, where T is the sampling cycle. The duration of the data traffic is equal to the duration of the event Δt_e. When sensor nodes are synchronized with each other, they are supposed to detect the event simultaneously, albeit $\Delta t_d \approx 0$. The traffic pattern is shown in Fig. 3.8. Clearly, the bursty traffic poses a significant challenge to the MAC layer by requiring the shared channel simultaneously.

Given the event detection model, to achieve energy efficiency and fulfill the realtime requirement greatly rely on the event report procedure. WSNs that work for event detection applications consumes little energy when no event is detected. The majority of the energy consumption is thus spent on event reporting. Therefore, the lifetime of the network mainly depends on the event reporting procedure. In

addition to energy efficiency, the sink is expected to make timely decisions based on the collected sensory data to fulfill the realtime requirement in many applications.

3.5 CSMA-based MAC Model

Although TDMA-based MAC protocols outperform CSMA-based protocols, the latter are more popular in real applications due to their simplicity and effectiveness. For CSMA-based protocols, the focus is how to adapt to the traffic and avoid collisions. Considering the traffic pattern discussed in the previous section, collisions are severe due to the bursty traffic. Therefore, to avoid collisions outweighs the goal to adapt to the traffic in the event detection scenario. CSMA/CA protocols apply carrier sensing to find out the availability of the channel. As shown in Fig. 3.9, the result of CSMA/CA protocol is the streamlined transmissions along the timeline. Compared with the original traffic pattern shown in Fig. 3.8, the real transmissions of the data packets in a neighborhood of nodes are finally streamlined along the timeline sharing the same medium. Here, the single channel transmission is taken into account without loss of generality.

Normally, the goal of the CSMA/CA protocols is to avoid collisions and also achieve low latency. When a node senses a busy channel, it waits for the end of the current transmission. Given the slotted CSMA protocol, each node chooses a slot based on a probability distribution. The number of slots is the length of the collision window CW. Let p_j be the probability for a node to choose the jth slot. Assuming uniform distribution, it has

$$p_1 = p_2 = ... = p_M = \frac{1}{M} \tag{3.15}$$

where M is the number of the slots.

The probability of a node to choose a certain slot could be optimized according to different criteria. For instance, minimizing collisions over the slots could be achieved by tuning the probabilities instead of assigning the same probability to each slot as shown in (3.15). Transmission collisions not only increase energy consumption for retransmitting the packets but also lead to longer delay on the arrivals of packets at their destinations. Although packet delay at the MAC layer is inevitable for bursty traffic, it could be an optimization goal for the MAC protocol besides the goal of minimizing collisions.

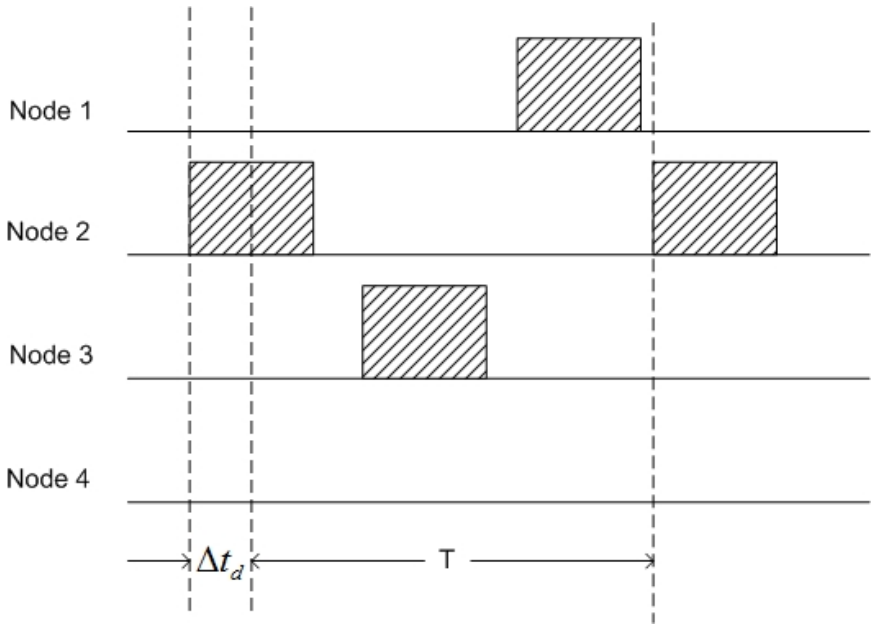

Figure 3.9: Streamlining the transmissions

3.6 Summary

The specific models that are the basis of the proposed approaches are formulated respectively. The correlation model of deterministic signals is based on the addition of two signals, while the correlation model of statistical signals is based on

the covariance that is exponentially proportional to distance, time or both. Besides, the event detection model reveals the inherently bursty traffic from the nodes that detects the event. And the slotted CSMA-based MAC protocol allows the traffic to be streamlined to reduce collisions.

CHAPTER 4

ASYNCHRONOUS LOSSLESS DATA GATHERING

Given the correlation model of the deterministic signals provided in the previous chapter, the asynchronous sampling gathering strategy is presented, which includes the motivation, overview and details of the strategy. In addition, an optimization problem is formulated to address the energy saving of the proposed strategy. It is shown that the optimal sampling schedule can be derived through solving the optimization problem. After that, methods of reconstructing the original signal from asynchronous samples and even the irregular samples.

4.1 Asynchronous Sampling Strategy

Correlation among sensory data makes it possible to maintain a certain level of sensing quality at a reduced sampling rate. It has been explored in the context of scheduling the duty-cycle of sensor nodes. The key to exploiting the correlation among sensor nodes is how to collaboratively process the data collected from different nodes. In this section, it will be described how to meet the goal of energy conservation through asynchronous sampling strategy.

4.1.1 Motivation

Referring to the correlation model presented in the previous section, suppose that a user is not interested in the innovation part signal, $X_i(t)$. Instead, only the common part signal, $X_c(t)$, is critical to the monitoring task of the WSN. Therefore, the nodes within one cluster would be able to sample the same signal $X_c(t)$ containing

noise $X_i(t)$. Since the nodes take samples of the same signal, an immediate solution to achieve energy efficiency is to schedule the nodes' duty-cycle.

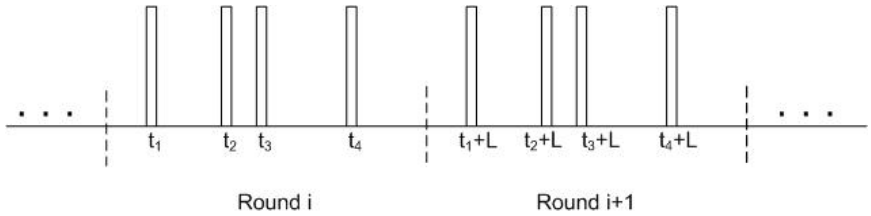

Figure 4.1: Schedule sampling of 4 nodes in one cluster

Before considering the innovation part signal at hand, an alternative sampling schedule of the sensor nodes is shown in Fig. 4.1. Assume in each sampling round, each node takes one sample in turn. The samples are taken at times $t_1, t_1, \cdots, t_N$, where N is the number of nodes in a given cluster. A longer sampling round, L, is always favorable in WSNs due to the reduced amount of data to be reported to the base station, especially for data gathering applications. However, the sampling schedule should also guarantee the reconstruction of $X_c(t)$. The problem of reconstructing band-limited signals from irregular samples has been investigated in [84], in which the proposed reconstruction algorithm requires that the length of the interval between two samples should not exceed the length of the interval corresponding to the Nyquist sampling rate in order to uniquely recover the signal through the irregular samples. Therefore, the maximal length of the sampling round is achieved when the samples are taken regularly along the time line. Specifically for $X_c(t)$, the Nyquist rate is $2f_{c,h}$. Fortunately, the Nyquist rate of each node is $1/L$, which is much lower than $2f_{c,h}$. In fact,

$$L = N(\frac{1}{2f_{c,h}}) \tag{4.1}$$

which implies that the Nyquist rate of each node is reduced from $2f_{c,h}$ to $\frac{2f_{c,h}}{N}$, where N is the number of sensor nodes in the cluster.

By collaboratively sampling and processing the samples, it is shown that the reconstruction of $X_c(t)$ is accomplished even when each node takes samples at a significantly reduced sampling rate. At this point, it almost becomes requisite to explore the possibility of extending this approach to the case of considering both the common part and the innovation part signals.

The main challenge of implementing collaborative signal processing on $Z_i(t)$ lies in dealing with $X_i(t)$, since it no longer represents noises contained in the samples but a meaningful and indispensable interpretation of the monitored physical phenomena.

Recall the assumption on the bandwidths of $X_c(t)$ and $X_i(t)$. The Nyquist rate with respect to $X_i(t)$ is much lower than that of $X_c(t)$, which suggests that if $Z_i(t)$ is sampled by each node at a reduced rate, it is possible to reconstruct $X_i(t)$ except for $X_c(t)$.

Given the samples are taken asynchronously at a reduced rate, a potential solution would be to reconstruct $X_c(t)$ collaboratively from samples of the spatially correlated sensor nodes and to reconstruct $X_i(t)$ independently from samples of the corresponding node. The feasibility of this solution greatly lies in the successful separation of the common part signal and the innovation part signal.

As digital filters are able to suppress particular frequencies in the signal, the assumption that is made in Eq. (3.3) warrants the validity of the digital filters regarding the separation of the common part and the innovation part signals.

Motivated by the above insights, an asynchronous sampling strategy is proposed in the following section that exploits the data correlation.

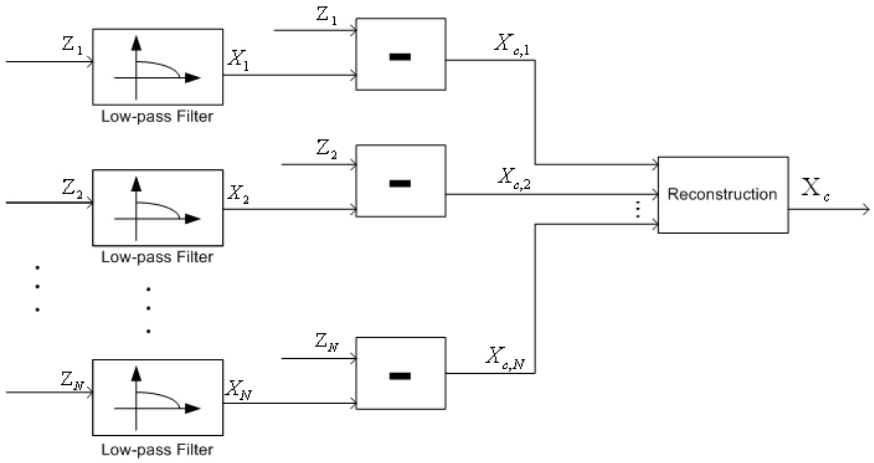

Figure 4.2: Reconstruction of Correlated Signals from Asynchronous Samples

4.1.2 Strategy Overview

Based on the knowledge of correlation structure, the nodes sample the monitored field asynchronously at a reduced sampling rate as compared to the Nyquist rate of the common part signal. The reconstruction process of $X_i(t)$ and $X_c(t)$ is shown in Fig. 4.2. Before reconstructing the desired signal from the asynchronous samples, the common part signal is filtered out of the sample sequences according to its frequency distribution. Then the innovation part signal of each node can be reconstructed through the respective filtered results. After that, the samples of the common part signal are obtained by subtracting the recovered innovation part from the original asynchronous samples. Finally, the common part samples resulting from each node is combined to form a new sequence for its reconstruction.

4.1.3 Strategy Description

Continuing the example in the previous section, an asynchronous sampling and reconstruction of the signal are presented with the previously discussed correlation model. The signals are sampled asynchronously by five sensor nodes. The spectrum

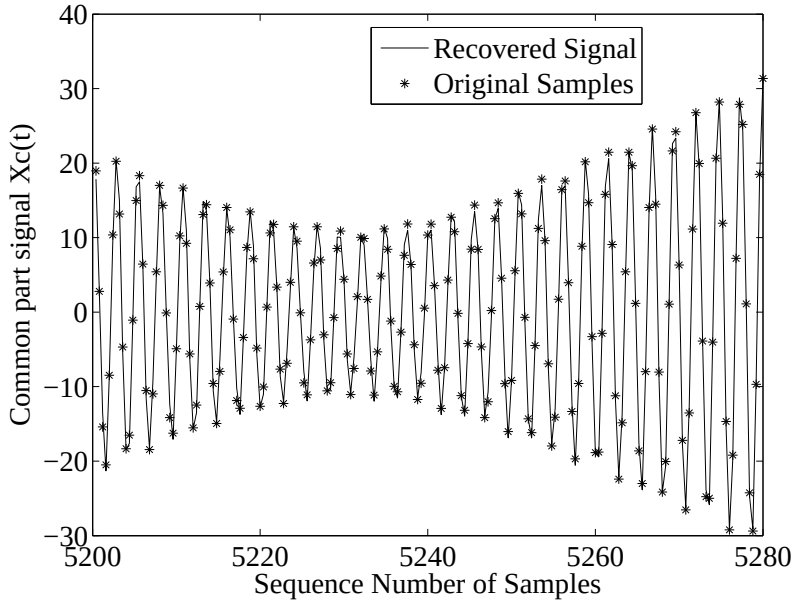

Figure 4.3: Recontruction of $X_c(t)$.

of $Z_1(t)$ sampled asynchronously at f_u, where $f_u < 2f_{c,h} < f_s$, is shown in Fig. 3.4. As shown, the spectrum of the common part signal is shifted and depressed. Due to the space limitation, this section does not include the spectrum analysis of the other signals, $Z_2(t), \cdots, Z_5(t)$, which are similar to that of $Z_1(t)$.

After the asynchronous samples being filtered by an equiripple finite impulse response (FIR) low-pass filter, they are subtracted from the original asynchronous samples. Thus, the common part signal is reconstructed through sequentially combining the subtracted samples from each sensor node. The reconstructed common part signal is shown in Fig. 4.3, while one of the innovation part signals reconstructed from the filtered samples is shown in Fig. 4.4.

As the digital low-pass filter cannot produce ideal results due to its own theoretical limitations, it is worth noticing that the reconstruction of $X_c(t)$ is not ideal too. The spectrum of the original and reconstructed $X_c(t)$ are compared in Figs. 4.5

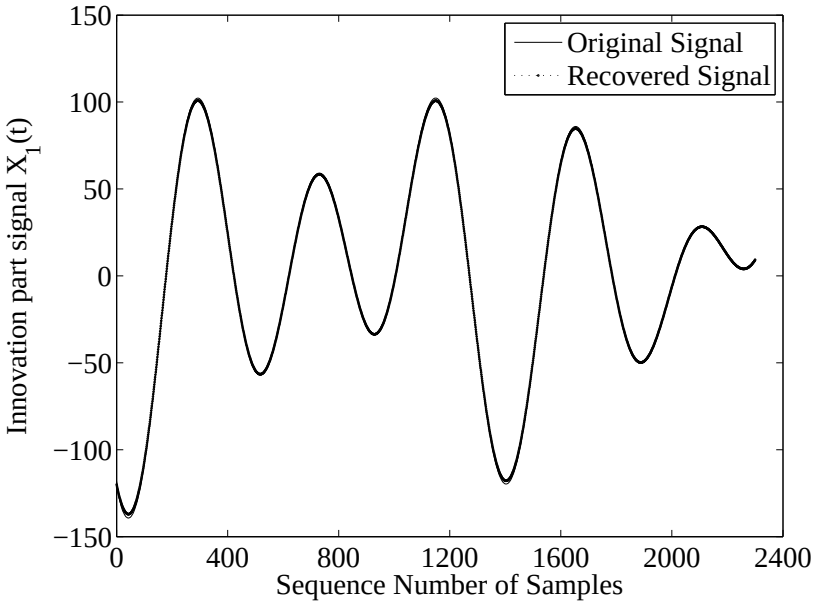

Figure 4.4: Reconstruction of $X_1(t)$.

and 4.6, respectively. In Fig. 4.6, the spectrum includes a few small spikes caused by the imperfection of the digital filter.

In summary, each node's role in the asynchronous strategy is determined by its sampling rate and time shift. Since the reconstruction algorithm provided in [84] requires that the distance between two samples along the time-line should be smaller than Nyquist rate of the signal to be reconstructed. The sampling rates and shifts are subject to the following conditions:

$$\Delta t_l < \frac{1}{2f_{c,h}} \tag{4.2}$$

where

$$\Delta t_l = (\widehat{t_l} - \widehat{t}_{l-1}), \text{ for } l \in \mathbb{N}, \widehat{t}_1 < \widehat{t}_2 < \cdots$$

$$\widehat{t_l} \in \{t_{i,k} = \varphi_i + kT_i, i = 1, 2, \cdots, N, k \in \mathbb{N}\}$$

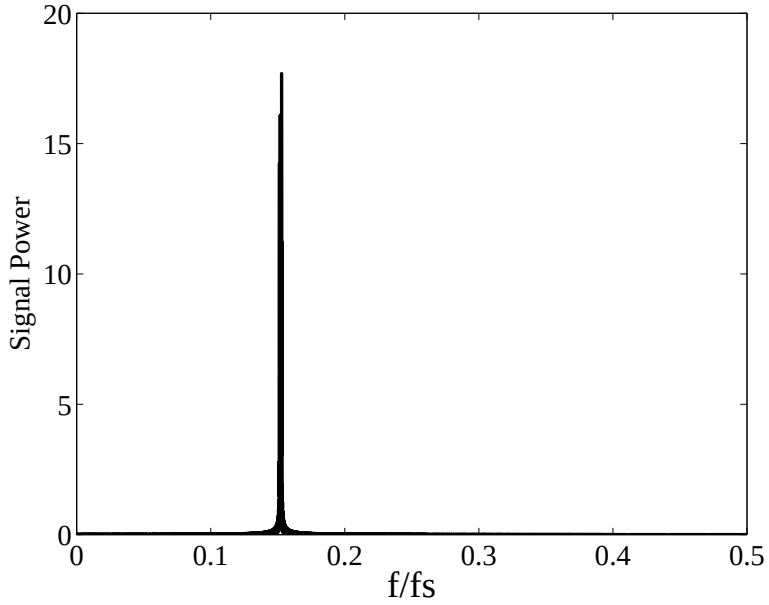

Figure 4.5: Spectrum of the original $X_c(t)$.

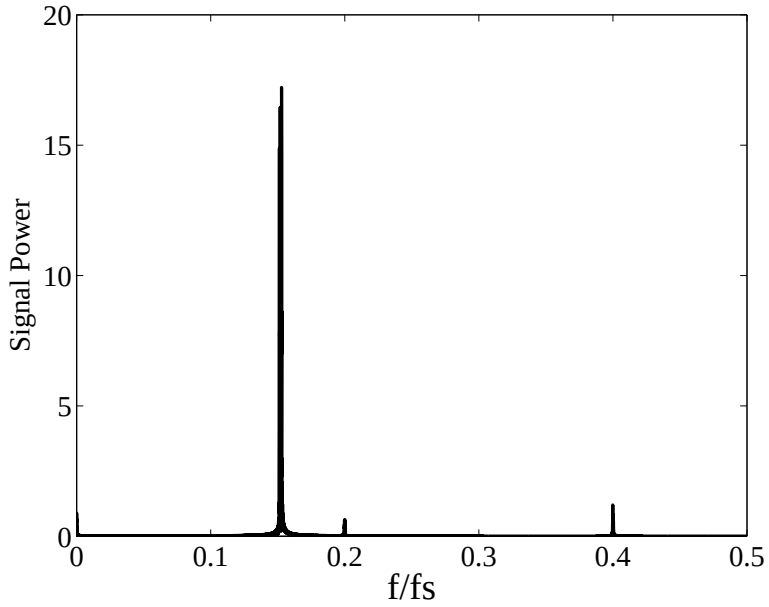

Figure 4.6: Spectrum of the reconstructed $X_c(t)$.

and

$$T_i < \frac{1}{2f_{i,h}}$$

Here φ_i is the sampling shift, while T_i is the sampling rate of the ith node.

4.1.4 Energy Savings

For the sake of simplicity, but without loss of generality, it is assumed that the communication cost of each node is proportional to its sampling rate. Therefore, the energy efficient goal for data gathering can be achieved by taking samples at the lowest possible rates. This section formulates the following optimization problem on asynchronous sampling rates in order to obtain an upper bound on the improvement brought by the asynchronous sampling strategy. Given the set of frequencies of the innovation part signals $\{f_{i,h}, i = 1, 2, \cdots, N\}$ and the frequency of the common part signal $f_{c,h}$, the problem is defined as follows:

$$\begin{aligned} \max \quad & \sum_{T_j \in \Omega} T_j \\ \text{such that} \quad & \Omega \subseteq \{T_i, i = 1, 2, \cdots, N\}. \\ & T_i < \frac{1}{2f_{i,h}}. \\ & T_j < \frac{|\Omega|}{2f_{c,h}}. \end{aligned} \tag{4.3}$$

The sampling rates and shifts that maximize the energy saving are derived from the following algorithm.

Algorithm 1 Deriving sampling rates for spatially correlated sensor nodes

1. sort $f_{i,h}$ so that $f_{1,h} < f_{2,h} < \cdots < f_{n,h}$.
2. for $K = 1$ to N, sort $\frac{f_{i,h}}{i}$ and $f_{c,h}$ so that $\forall i \leqslant K$, $\frac{f_{i,h}}{i} < f_{c,h}$ and $\forall i > K$, $\frac{f_{i,h}}{i} > f_{c,h}$.
3. $\forall i \leqslant K$, $T_i < \frac{1}{2f_{K-1,h}}$, $\varphi_i < \frac{f_{K-1,h}}{K}$; and $\forall i > K$, $T_i < \frac{1}{2f_{i,h}}$, $\varphi_i = 0$.

Note that there are two extreme cases for the above algorithm. In the first case $f_{i,h} < \frac{f_{c,h}}{N}, \forall i \leqslant N$, in which Algorithm 1 results in $T_i < \frac{N}{2f_{c,h}}, \varphi_i < \frac{1}{2f_{c,h}}$. This leads to an upper bound of $\frac{1}{N}$, which indicates the smallest ratio between the asynchronous sampling frequencies and the synchronous sampling frequencies. In contrast, for the second case, $f_{i,h} \geqslant \frac{f_{c,h}}{i}, \forall i \leqslant N$. The result produced by Algorithm 1 will be $T_i < \frac{1}{2f_{i,h}}$, $\varphi_i = 0$, which means the asynchronous sampling strategy degenerates into the synchronous sampling strategy.

4.2 Collaborative Reconstruction

Reconstruction of all the signals sampled by the nodes is a three-stage process. First, the common part signal is filtered out from the asynchronous samples of each node. The filtered results provide enough information to reconstruct the innovation part signal. Secondly, the innovation part of the samples is subtracted from the original samples in order to obtain the common part of each sample sequence. Combining asynchronous samples after subtraction, enough samples are obtained for the reconstruction of the common part signal. Finally, the original signal could be approximated from the previous reconstruction results of the common part and the innovation part signals.

4.2.1 From Asynchronous Samples

The key idea behind collaborative reconstruction of the common part signal is combining the filtered asynchronous samples from sensor nodes. As shown in Eq. (4.4), m asynchronous samples from one node are filtered by a low-pass filter $F(a, b, r)$, where a, b are the filter coefficients, and r is order of the filter.

$$
\begin{aligned}
y(i) &= b(1)x(i) + z_1(i-1) \\
z_1(i) &= b(2)x(i) + z_2(i-1) - a(2)y(i) \\
&\cdots \\
z_{r-2}(i) &= b(r-1)x(i) + z_{r-1}(i-1) - a(r-1)y(i) \\
z_{r-1}(i) &= b(r)x(i) - a(r)y(i)
\end{aligned} \tag{4.4}
$$

The filtered result y contains only the innovation part signal since the common part signal is filtered out by the low-pass filter. State-of-art digital filters are available for various filtering purposes [85]. Therefore, this section does not elaborate on specifications of low-pass filters since the focus of this chapter is to propose the asynchronous sampling strategy.

Next, the common part signal is reconstructed with the help of the following equation:

$$x_c(t) = \sum_{k=1}^{m} D[k] \cdot \frac{sin(\pi(\frac{t-kT}{T}))}{\pi(\frac{t-kT}{T})} \tag{4.5}$$

where $D[i + (j-1)n] = x_i[j] - y_i[j]$.

As the innovation part signal captured by each node can be reconstructed through the filtered result y, the original signal sampled by each node can be obtained accordingly.

4.2.2 From Irregular Samples

This section discusses the impact of the local clock drifts on the reconstruction of the sampled signals. It is necessary to implement the reconstruction method for irregular samples resulting from clock drifts of sensor nodes.

Impact of Local Clocks: Time synchronization plays an important role in wireless sensor networks. Every node has its own local clock. The differences between the local clocks pose significant challenges on the wake-up schedule, communication protocols, and so on. Although the samples of one particular node are taken regularly, the samples from different sensor nodes are taken irregularly because of the different local clocks. When reconstructing the common part of the signal from the correlated data, the irregularity of the sample sequences may corrupt the reconstruction result. Various time synchronization approaches have been proposed in the literature for wireless sensor networks [86]. Specifically, Cluster-based synchronization of WSNs has been proposed in [87]. However, the most energy efficient synchronization method for WSNs may not often guarantee synchronization of local clocks at any time. Therefore, the reconstruction of the common part signal should be able to cope with the irregularity of the samples shown in Eq. (4.6). Fortunately, there exist algorithms to reconstruct the signal from irregular samples.

$$s_i' = s_i + \Delta s_i \tag{4.6}$$

where $\Delta s_i = |tclk_i - t_0|$, and $tclk_i$ is the time indicated by node i's clock, while t_0 is the time indicated by a non-drift clock.

Reconstruction From Irregular Samples: An adaptive weights method based on iterative reconstruction is provided in [84], where the sampling set and the weighted

frame are as in Eq. (6.3) and Eq. (4.8), respectively. The algorithm can be drawn from Eq. (6.4).

$$\mu = \sup_{n \in Z}(x_{n+1} - x_n) < \frac{\pi}{\omega} \tag{4.7}$$

$$(1 - \frac{\mu\omega}{\pi})\|f\|^2 \leqslant \sum_{n \in Z} \frac{x_{n+1} - x_{n-1}}{2}|f(x_n)|^2 \leqslant (1 - \frac{\mu\omega}{\pi})\|f\|^2 \tag{4.8}$$

$$f_0 = Sf = \frac{\pi^2}{\pi^2 + \mu^2\omega^2} \sum_{n \in Z} \frac{x_{n+1} - x_{n-1}}{2} \frac{\omega}{\pi} f(x_n) \sin c(\omega x - x_n) \tag{4.9}$$

$$f_{k+1} = f_k + S(f - f_k), k \geqslant 0$$

where μ is the largest difference between two sampling time instances, ω is 2π times the Nyquist rate of the sampled signal, and S is an operator described in Eq. (6.4).

The reconstruction error of the algorithm is bounded by Eq. (6.5).

$$f = \lim_{k \to \infty} f_k$$

$$\|f - f_k\| \leqslant \lambda^{k+1}\|f\| \tag{4.10}$$

$$\lambda = \frac{2\pi\mu\omega}{\pi^2 + \mu^2\omega^2}$$

The asynchronous sampling rate introduced in Section 4.1.2 should be adjusted to meet the requirement on the sampling set. Given the irregularity of the samples in Eq. (4.6), the sampling rates of nodes need to be modified as follows:

$$T_i' = T_i - \Delta s_i \tag{4.11}$$

From the above adjustments on the sampling rate, it is concluded that the energy saving performance of the asynchronous sampling is impacted by the drift of local clocks.

4.3 Summary

This chapter starts with the motivation of the proposed strategy based on the signal model and the correlation model provided in the previous chapter. Followed by the description of the proposed strategy, the motivation behind the strategy is explained. The frequencies of the correlated signal enables the asynchronous sampling strategy to take less samples and to recover the original signal through collaborative reconstruction. Detailed demonstration on the filtering of the samples, combining the filtered samples and recovering the original signal is shown too. Furthermore, the benefit of applying the strategy is discussed based on solving the optimization problem formulated for maximizing the energy saving. Finally, the reconstruction method dealing with irregular samples is presented to show the feasibility of the strategy even for applications with clock jitters.

CHAPTER 5

ASYNCHRONOUS LOSSY DATA GATHERING

In this chapter, the discussion focuses on how to improve the tradeoff between network lifetime and sensing quality in lossy data gathering applications. Since the sampling rate is subject to certain bandwidth limitation and battery capacity of nodes, the limited number of samples can not guarantee complete knowledge of the monitored physical phenomena in such applications. This dissertation proposes asynchronous sampling to improve the quality of the sensory data in terms of increasing the entropy thereof. The benefit of increased entropy using examples of data regression is showcased. An optimization problem is formulated to achieve maximal entropy with the help of asynchronous sampling. Specifically, two asynchronous sampling strategies are proposed to compliment the computation-expensive optimal strategy.

5.1 Benefits of Asynchronous Sampling

Given temporal-spatial correlation model of the sensory data, it is shown next that the asynchronous sampling strategy, if employed, can indeed increase the entropy of the data and hence reduce the regression distortion as a result of increased entropy.

5.1.1 Asynchronous Sampling Increases Entropy

For tractability, it is assumed that the sensory data are Jointly Gaussian Random Variables (JGRVs). The probability density function for zero-mean JGRVs is given by

$$f_\chi(\chi) = \frac{1}{(2\pi)^{n/2}\sqrt{det\Lambda_\chi}} e^{-\frac{1}{2}\chi^T\Lambda_\chi^{-1}\chi}, \tag{5.1}$$

where Λ_χ is the covariance matrix of χ, whose entry is the covariance of elements in χ and *det* denotes the determinant.

The entropy of the sensory data composed of the samples $U_1, \cdots, U_n$ following JGRVs can then be derived as

$$H = \frac{1}{2}\log(2\pi e)^n det\Lambda_n - \log\Delta. \tag{5.2}$$

Here entry $\kappa_{i,j}$ in the covariance matrix Λ_n corresponding to sensor data samples U_i and U_j from nodes i and j can be expressed as

$$\kappa_{i,j} = \begin{cases} \sigma_i^2 & i = j, \text{ for } i \leqslant n,\ j \leqslant n, \\ \sigma_i\sigma_j\rho_{i,j} & i \neq j, \text{ for } i \leqslant n,\ j \leqslant n, \end{cases}$$

where σ_i and σ_j are the standard deviation of the samples U_i and U_j, respectively, and $\log\Delta$ is a constant due to quantization. For the sake of simplicity, a normalization on the covariance matrix Λ_n is applied in order to get a correlation coefficient matrix A_n, whose entry is:

$$a_{i,j} = \begin{cases} 1 & i = j, \text{ for } i \leqslant n,\ j \leqslant n, \\ \rho_{i,j} & i \neq j, \text{ for } i \leqslant n,\ j \leqslant n, \end{cases} \tag{5.3}$$

Then the determinant of Λ_n can be derived as

$$det\Lambda_n = \prod_{i=1}^{n} \sigma_i^2 det A_n \tag{5.4}$$

According to the properties of $\rho_{i,j}$, the matrix A_n is positive symmetric implying $a_{i,j} = a_{j,i}$. Now the following theorem is derived.

Theorem 5.1.1 *The entropy of sensory data samples $U_1, \cdots, U_n$ increases through asynchronous sampling.*

Proof: From the temporal-spatial correlation model, observe that the redundancy of sensory data can be reduced by asynchronous sampling, which results in a non-zero $\tau_{i,j}$. The goal here is to show that the determinant of Λ_n will be increased if some of its entries are decreased due to asynchronous sampling and consequently the entropy of the sensory data will be increased.

Suppose that A_n is constructed from synchronous sampling. Now if the sampling sequence of the jth sensor node is shifted from t_j to $t_j + \tau$. The correlation $\rho_{i,j}$ between the jth node and the other sensor nodes changes to $\hat{\rho}_{i,j}$, where

$$\hat{\rho}_{i,j} = \rho_{i,j} e^{-\beta \tau_{i,j}} \quad \text{for } i \leqslant n,\ j \leqslant n,$$

Then $\hat{A}_n$ corresponding to asynchronous sampling is given by $\hat{A}_n = A_n \circ B_n$, where B_n is the sampling shift matrix whose entry is defined as follows:

$$b_{i,j} = \begin{cases} 1 & i = j, \text{ for } i \leqslant n,\ j \leqslant n, \\ e^{-\beta \tau_{i,j}} & i \neq j, \text{ for } i \leqslant n,\ j \leqslant n, \end{cases} \tag{5.5}$$

Here $A_n \circ B_n$ is the Hadamard product, the element-wise product of two matrices. Because A and B are correlation matrices, they are positive definite or positive semidefinite. The Hadamard product of two positive definite matrices are also positive definite because of the closure property. According to Oppenheim's Inequality [82], $det(A_n \circ B_n) \geqslant detA_n \prod_{i=1}^{n} b_{i,i} = detA_n$ (the equality holds if and only if A_n is a diagonal matrix), which shows $detA_n < det\hat{A}_n$. Therefore, $det\Lambda_n < det\hat{\Lambda}_n$, which infers that $H < \hat{H} = \frac{1}{2}\log(2\pi e)^n det\hat{\Lambda}_n - \log\Delta$.

Recalling the generalized exponential correlation model, it is apparent that the proof remains to be true with the squared exponential model, in which $\xi = 2$. Specifically, the matrix $\hat{A}_n$ corresponding to the asynchronous sampling strategies is given by $\hat{A}_n = A_n \circ B_n$, where an entry of B_n is defined as:

$$b_{i,j} = \begin{cases} 1 & i = j, \text{ for } i \leqslant n,\ j \leqslant n, \\ e^{-\beta\tau_{i,j}^2} & i \neq j, \text{ for } i \leqslant n,\ j \leqslant n, \end{cases} \tag{5.6}$$

As B_n remains to be positive definite, the Oppenheim's inequality can be applied to reach the same conclusion with the approximated exponential model, in which $\xi = 1$.

5.1.2 Benefits of Increased Entropy

While the entropy provides an abstract quantification of the amount of information embedded in the data, it is hard to picture its true impact in real applications. Here one further step is taken to show that asynchronous sampling can indeed help an application improve the regression of the physical process from the asynchronous data.

An important goal of data collection in WSNs could possibly be to reconstruct the physical field under measurement. Instead of reconstruction, the regression of the physical field is implemented when reconstruction is unreachable due to insufficient data. In this section, through an example of linear regression, how asynchronous sampling improves the performance of regression is shown.

A regression model for a physical process is given below:

$$\widetilde{G}(x,y,z,t) = \sum_i w_i J_i(x,y,z,t)$$

where w_i is the ith weight, and J_i is the ith basis function of regression.

Then the distortion of the regression can be calculated from:

$$R_r = E[(G - \widetilde{G})^2]$$

the optimal regression is achieved when $w = (J^T J)^{-1} J^T \widehat{G}$, where $\widehat{G}$ represents sensory data. Thus,

$$R_r = E[(G - J(J^T J)^{-1} J^T \widehat{G})^2]$$

Letting $Q = J(J^T J)^{-1} J^T$, it is obtained that

$$\widetilde{G}_j = \sum_{i=1}^{n} q_{i,j} \widehat{G}_i$$

where $q_{i,j}$ is the covariance coefficient between data samples from nodes i and j.

Therefore,

$$R_r = \sigma_G^2 + \frac{1}{n}\sum_{i=1}^{n}\sum_{j=1}^{n} q_{i,j}^2 \widehat{G}_i^2 + \frac{1}{n}\sum_{k=1}^{n}\sum_{i=1}^{n}\sum_{j=i+1}^{n} q_{i,k} q_{j,k} \rho_{i,j} \widehat{G}_k^2 - \frac{2}{n}\sum_{k=1}^{n}\sum_{i=1}^{n} q_{i,k} \rho_{G,i} G_k^2 \quad (5.7)$$

If sensory data are collected asynchronously, only $\rho_{i,j}$ will decrease due to non-zero $\tau_{i,j}$ introduced in the correlation model. Therefore, it is concluded that asynchronous sampling is capable of reducing the regression distortion.

5.2 Designing Asynchronous Sampling Strategies

While it has been shown that asynchronous sampling can indeed benefit WSNs, different asynchronous sampling strategies can affect the amount of benefits. A key factor here is how each sensor shall determine its sampling time and when an optimal performance (i.e., the maximum entropy) can be achieved. In this section, the optimization problems related to asynchronous sampling is presented firstly. As the optimization problem is shown to be NP-hard, a heuristic algorithm is proposed to design an asynchronous sampling strategy, called O-ASYN, which uses local optimum to approximate the global optimum. Two other asynchronous sampling strategies, called R-ASYN and E-ASYN, are also proposed. R-ASYN is an asynchronous sampling strategy based on randomly assigning sampling shifts, whereas E-ASYN just equally shifts sampling moments of sensor nodes. Bounds on R-ASYN and E-ASYN are derived using inequalities of the Hadamard product. Discussions on the implementation of the strategies are presented at the end of this section.

5.2.1 Optimal Asynchronous Sampling Strategy

Asynchronous sampling strategy increases the entropy of the sensory data by introducing shifts in the sampling time instances among different sensor nodes. Without loss of generality, it is assumed that the sampling time instances of the sensor nodes will be increasing along with their indices. In other words,

$$t_1 \leqslant t_2 \leqslant \cdots \leqslant t_n. \tag{5.8}$$

It is also assumed that

$$\tau_i = \begin{cases} t_{i+1} - t_i, & \text{for } i = 1, \cdots, n-1 \\ T + t_1 - t_i, & \text{for } i = n \end{cases}$$

where T is the sampling interval of the sensor nodes. Thus

$$\sum_{k=1}^{n} \tau_k = T$$

Subsequently, the entry of the correlation matrix A_n has the following form:

$$a_{i,j} = \begin{cases} 1 & i = j, \text{ for } i \leqslant n,\ j \leqslant n, \\ \rho_{i,j} e^{-\beta \tau_{i,j}} & i \neq j, \text{ for } i \leqslant n,\ j \leqslant n, \end{cases}$$

where

$$\tau_{j,i} = \tau_{i,j} = \sum_{k=i}^{j-1} \tau_k \text{ for } i < j$$

To best benefit from the asynchronous sampling strategy, the goal is to determine the best set of $\{\tau_i\}$ so that the entropy of the sensory data can be maximized. Formally, the goal is

$$\begin{aligned} &\max H(S_1, ..., S_n, \tau_1, ..., \tau_n) \\ &\text{subject to} \sum_{k=1}^{n-1} \tau_k \leqslant T,\ \sum_{k=1}^{n} \tau_k = T, \text{ and } \tau_k \geqslant 0 \end{aligned} \tag{5.9}$$

It is argued that the above optimization problem is NP-hard because it is a special case of the Assignment Problem with Extra Constraints (APEC), which is shown to be NP-hard [88].

5.2.2 O-ASYN Strategy

Since the optimal asynchronous sampling is NP-hard, an approximate solution called the O-ASYN strategy is proposed. It is based on finding local optimum of a subproblem by recursively applying Lagrange Multiplier.

First, a subproblem is defined, which optimizes entropy with a given index of the sensor nodes.

$$\begin{aligned} &\max logdet A_n \\ &\text{subject to} \sum_{k=1}^{n-1} \tau_k \leqslant T,\ \sum_{k=1}^{n} \tau_k = T, \text{ and } \tau_k \geqslant 0 \end{aligned} \tag{5.10}$$

Notice that in the formulation (5.10), the problem is under inequality constraints on the time shifts. As equality constraints of an optimization problem may lead to smaller size of feasible solution sets than the inequality constraints, it is desirable to first examine the objective function and the inequality constraints in order to reduce the size of the feasible solution set.

Here, it is proved by contradiction that the optimization problem given in (5.10) is equivalent to the optimization problem shown in (5.11), which has an equality constraint on the sum of time shifts.

$$\begin{aligned} &\max logdet A_n \\ &\text{subject to} \quad \sum_{k=1}^{n-1} \tau_k = T \text{ and } \tau_k \geqslant 0 \end{aligned} \tag{5.11}$$

Proposition 5.2.1 *The optimization problem given in* (5.10) *is equivalent to that in* (5.11).

Proof: Suppose there is an optimal solution $\{\tau_1, ..., \tau_{n-1}\}$ to the problem such that $\sum_{k=1}^{n-1} \tau_k < T$. Then the maximum entropy H_{max} is obtained by applying time

shifts $\{\tau_1, ..., \tau_{n-1}\}$. Let $\delta = T - \sum_{k=1}^{n-1} \tau_k$. A new time shift series $\{\tau_1, ..., (\tau_{n-1} + \delta)\}$ is derived. According to Theorem 5.1.1, the entropy is increased by shifting sampling time points of the nth node from the other nodes. It is obtained that entropy H_δ corresponding to the new time shift series, is greater than or equal to H_{max}. Since it contradicts the assumption that H_{max} is the maximum entropy possible under the constraints $\sum_{k=1}^{n-1} \tau_k \leqslant T$, it is concluded that the entropy is less than the maximum value as long as $\sum_{k=1}^{n-1} \tau_k < T$. Therefore, the optimization problem with the inequality constraints is equivalent to the optimization problem given in (5.11) with an equality constraint on the sum of time shifts.

A recursive algorithm is proposed below, named O-ASYN, to approximate the global optimum using the local optimum. O-ASYN is described in Algorithm 2. Given the indices of sensor nodes, the algorithm starts with three sensor nodes. Since the linearity of the local optimum with k sensor nodes is maintained while searching for the local optimum with $k+1$ sensor nodes, Lagrange Multiplier can be applied recursively to obtain the local optimum for n sensor nodes. The recursion starts from the initial case with three sensor nodes. The optimization problem of three sensor nodes is indeed an optimization problem given by Eq. (5.12).

$$\begin{aligned} &\max detA_3 \\ &\text{subject to} \quad \tau_1 + \tau_2 = T \text{ and } \tau_1, \tau_2 \geqslant 0 \end{aligned} \tag{5.12}$$

where $detA_3 = 1 - \rho_{1,2}^2 e^{-2\beta\tau_1} - \rho_{2,3}^2 e^{-2\beta\tau_2} - \rho_{1,3}^2 e^{-2\beta T} + 2\rho_{1,2}\rho_{2,3}\rho_{1,3} e^{-4\beta T}$.

The solution to this problem can be obtained easily because the maximum value of $detA_3$ is achieved when $\rho_{1,2} e^{-\beta\tau_1} = \rho_{2,3} e^{-\beta\tau_2}$ and $e^{-\beta\tau_1} e^{-\beta\tau_2} = e^{-\beta T}$.

Algorithm 2 O-ASYN algorithm

1. index the sensor nodes
   S: set of sensor nodes
   V: set of sensor nodes with index
   u_i: the ith indexed sensor node
   u: the sensor node without a index
   V=$\emptyset$
   for $i = 1$ to $|S|$
      $u_i = argmax_{u \subset S} Entropy(V \bigcup u)$
      V=$V \bigcup u_i$
      $S = S - u_i$
   end
2. find sampling shifts of the indexed nodes
   $\tau_1 : \frac{T}{2} + \frac{1}{2\beta}(\ln \rho_{1,2} - \ln \rho_{2,3})$
   $\tau_2 : \frac{T}{2} + \frac{1}{2\beta}(\ln \rho_{2,3} - \ln \rho_{1,2})$
   are local optimum of sampling shifts for sensor nodes u_1, u_2 and u_3
   for $k = 1$ to $n - 3$
      for $j = 1$ to $k + 1$
         $\tau_j = \tau_j(T - \tau_{k+2})/(\sum_{i=1}^{k+1} \tau_i)$
      end
      $\tau_{k+2} = argmax Entropy(\tau_1, \cdots, \tau_{k+1}, \tau_{k+2})$
         subject to $\sum_{i=1}^{k+1} \tau_i + \tau_{k+2} = T$ and $\tau_i \geq 0$
   end

5.2.3 R-ASYN and E-ASYN Strategies

In addition to O-ASYN, two other simple strategies are proposed: R-ASYN strategy that randomly assigns the sampling time shifts to sensor nodes with a certain sampling rate, and E-ASYN strategy that assigns equal sampling time shifts to sensor nodes no matter how they are spatially correlated with each other.

Thanks to the inequality of the Hadamard product, several bounds on the performance of R-ASYN and E-ASYN can be derived in terms of the percentage of the increase in the entropy value.

Since R-ASYN and E-ASYN assign time shifts to the sensor nodes without considering the correlation intensity between pairs of sensor nodes, the bounds on their performances indicate their effectiveness regarding different correlation scenarios.

The upper bounds for R-ASYN and E-ASYN are based on the following inequality:

Proposition 5.2.2

$$(det(A \circ B))^2 \leqslant (\frac{1}{2})^n \prod_{i=1}^{n} (\sum_{j=1}^{n} a_{ij}^4 + \sum_{j=1}^{n} b_{ij}^4) \tag{5.13}$$

where a_{ij} (resp. b_{ij}) is the entry of matrix A(resp. B) at ith row and jth column. Equality holds when $a_{ij} = b_{ij}$, for $i \leqslant n$ and $j \leqslant n$ and both A and B are diagonal matrixes.

Proof: According to the inequality of the determinant $(detA)^2 \leqslant \prod_{i=1}^{n} (\sum_{j=1}^{n} a_{ij}^2)$ (Equality holds when A is a diagonal matrix), it has

$$(det(A \circ B))^2 \leqslant \prod_{i=1}^{n} (\sum_{j=1}^{n} (a_{ij} b_{ij})^2),$$

where $\circ$ denotes the Hadamard product. Then

$$\prod_{i=1}^{n} (\sum_{j=1}^{n} (a_{ij} b_{ij})^2) \leqslant (\frac{1}{2})^n \prod_{i=1}^{n} (\sum_{j=1}^{n} (a_{ij}^4 + b_{ij}^4)), \text{ because } (a^2 - b^2)^2 \geqslant 0.$$

Assume A is the correlation matrix given in Eq. (5.3) and B is the sampling shift matrix given in Eq. (5.6). Observe that in Eq. (5.13) the equality holds when $a_{ij} = b_{ij}$. It can be inferred from the spatial correlation model in Eq. (3.6) that it is only possible when the sensor nodes are placed on a straight line.

Next, an upper bound on the performance improvement brought by R-ASYN is derived. Since $\sum_i b_{ij}^4 = nE[b_{ij}^4]$, it has

$$(det(A \circ B))^2 < (\frac{1}{2})^n \prod_{i=1}^{n} (\sum_{j=1}^{n} a_{ij}^4 + nE[b_{ij}^4])$$

Therefore, an upper bound on the performance improvement brought by R-ASYN is

$$E[\frac{logdet(A \circ B)}{logdetA} - 1] < \frac{\frac{1}{2}log[(\frac{1}{2})^n \prod_{i=1}^{n}(\sum_{j=1}^{n} a_{ij}^4 + nE[b_{ij}^4])]}{logdetA} - 1$$

Considering E-ASYN,

$$\max_j \sum_i b_{ij}^4 = \begin{cases} 2\sum_{k=1}^{\frac{j}{2}} e^{-4\beta\frac{kT}{n-1}}, & j \text{ is even} \\ 2\sum_{k=1}^{\frac{j-1}{2}} e^{-4\beta\frac{kT}{n-1}} + e^{-4\beta\frac{j+1}{2}\frac{T}{n-1}}, & j \text{ is odd} \end{cases} \tag{5.14}$$

The upper bound on the performance improvement brought by E-ASYN can be obtained accordingly.

From the inequality of determinant,

$$det(A \circ B) \geqslant detA \times detB$$

The equality holds when A and B are diagonal matrixes, and hence a lower bound on E-ASYN can be derived.

Since $detB = (1 - e^{-\beta\frac{2T}{n-1}})^{n-1}$, when $b_{i,j} = e^{-\beta\frac{|j-i|T}{n-1}}$, thus $logdet(A \circ B) \geqslant logdetA + (n-1)log(1 - e^{-\beta\frac{2T}{n-1}})$. Accordingly, the lower bound on the performance improvement of E-ASYN can be derived.

5.2.4 Implementation Issues

The O-ASYN strategy is different from R-ASYN and E-ASYN in that it requires prior knowledge of correlation between the pairs of sensor nodes. In order to implement the proposed strategy, the key is to compute the temporal correlation parameter, β. Before applying O-ASYN, it is necessary to study the synchronous

samples in order to get the correlation matrix A_n and β. As the correlation between the time shifted samples can be computed, β is estimated using statistical method given the exponential model.

After deriving the optimal sampling time shifts and indices of sensor nodes through approximation, the sink is able to broadcast the sampling time shifts to all the nodes. Then the sensor nodes can adjust their sampling time instances accordingly.

Furthermore, the reconstruction or estimation process does not request the information of the sampling instances from the sensor nodes because the sampling sequences are deterministic given the corresponding time shifts. Thus, the communication load of the system will not increase after introducing the asynchronous sampling strategy.

While the benefits of asynchronous sampling have been discussed mainly in terms of increased entropy and decreased regression distortion, there are other benefits of this strategy.

Incremental Implementation: Notice that the asynchronous sampling can be implemented incrementally over existing designs of communication layers, as it only regulates the sampling time of the sensor nodes. Asynchronous sampling strategies can be easily augmented on top of other methods such as aggregation and compression approaches.

Asymmetry of Operation: Asynchronous sampling also suits well in the highly resource constrained environment and, in particular, the asymmetry between the sink and sensor nodes. By performing asynchronous sampling, a sensor node does not need to perform any additional computation. This is in contrast with other schemes such as compressed sensing [89], where a senor node has to compress sensory data and exchange information with neighboring nodes. In this scheme, the computation

intensive work, such as determining the time shifts as well as the reconstruction, is performed at the sink usually having abundant resources.

Remark: The discussions have been mainly focused on deriving O-ASYN to determine the order and time shifts for asynchronous sampling. However, even simpler strategies as R-ASYN and E-ASYN can benefit the sensor network as well.

5.3 Summary

The asynchronous lossy data gathering strategy is presented in this chapter. According to the exponential correlation model given in the preliminaries of the dissetation, the spatial correlation does not strictly follow the exponential model. However, it does not affect the feasibility of the strategy because the strategy does not require specific pattern of the spatial correlation as shown in the entropy model. Based on the entropy model of the sensory data, the benefits of applying asynchronous sampling for lossy data gathering are discussed. Furthermore, an optimization problem is formulated in the discussion on designing the strategy given the knowledge on the sensory data correlation. Aside from the suboptimal solution, two simple yet effective solutions are presented with the derived bounds on their performances. Finally, the implementation issues are discussed including the benefits and the restrictions of the strategy when implemented.

CHAPTER 6

INFORMATION-DRIVEN MEDIUM ACCESS CONTROL

Motivated by the collision prone traffic generated by the nodes in the event detection scenario, the information-driven medium access control (ID-MAC) is presented in this chapter. The protocol handles the two types of packets differently in order to streamlining the traffic. A method of obtaining the optimal probability for the individual node to choose a transmission slot is adopted. The analysis on the event reports and the estimation accuracy are presented accordingly.

6.1 Motivation

Event detection and monitoring is an important application of wireless sensor networks (WSNs). The sensor nodes observe the detected event and continuously reports to the sink within the duration of the event for further analysis. Examples of event detection and monitoring applications include environment surveillance, fire rescue, border security, and so on.

The biggest challenge of deploying WSNs lies in its limited lifetime due to the small form factor of the devices and the slow progress on boosting the battery capacity. In the detection process, energy consumption can be reduced through scheduling the nodes' duty cycle while guaranteeing the detection performance [90]. Distributed detection of events is also able to conserve energy through eliminating the communication cost for transmitting the raw samples to the central processing node [91]. However, for the monitoring process, when observations on the detected event are collected throughout the event area, the energy consumed by the communications

between the sink and the nodes plays a key role in determining the lifetime of the WSNs. Therefore, energy efficient event reporting is of great importance to the success of WSN applications, especially when the event detection does not contribute significantly to the energy consumption.

The monitoring process exhibits two characteristics that motivate the work presented in this section. They are:

1) The observations on the detected events from different nodes are correlated (or even duplicated) with each other.

2) The data packets traffic from the nodes to the sink has a bursty pattern, in which every node in the event area attempts to send their reports simultaneously.

The correlation among the event reports implies that the performance of the system can be improved by transmitting less correlated data to the sink. In-network data processing [92], compressive sensing [93] and node selection [94] have been proposed to exploit the spatial correlation among the sensory data to achieve energy efficiency.

The bursty traffic generated by the nodes poses additional challenge to the MAC layer by introducing conflicted transmission requests from nodes within a neighborhood. The widely adopted IEEE802.15 protocol is not specifically designed to handle bursty traffic. The delay performance and the packet drop rate are severely impacted by the bursty traffic in the event reporting process. In [95], a MAC protocol was proposed to resolve the problem by selecting a subset of the nodes to transmit their reports to the sink. This approach managed to change the data packets traffic in order to improve the MAC performance without sacrificing the application's performance.

Inspired by the idea of changing the traffic of data packets, a novel information-driven MAC (ID-MAC) protocol is proposed to solve the problems of correlated reports and bursty traffic simultaneously. Instead of choosing a subset of nodes to report

the event, the ID-MAC protocol assigns sampling shifts to nodes in order to change the bursty traffic into a streamlined traffic. Consequently, the MAC performance is improved by essentially replacing the bursty traffic.

The basic idea is that the MAC protocol advises the node on its sampling shift and the transmission slot. For enroute packets to be relayed by the node, the node applies normal CSMA/CA (carrier sense multiple access/collision avoidance) protocol to send the packets in a timely manner. For data packets, ID-MAC suggests node on its sampling moment to reduce correlation with other nodes. At the same time, collisions at the MAC layer are also reduced. As a result, the data packets traffic is no longer bursty after the intervention of the MAC protocol. In addition, the event reports are also less correlated because nodes takes samples at different time moments. An optimal probability model is adopted to select nodes' transmission slots that minimize the transmission collision and in turn reduce the correlation among event reports.

6.2 Protocol Description

The proposed information-driven MAC protocol is described in the following considering two different types of packets: the data packets and the enroute packets.

6.2.1 Overview

Motivated by the conflicts between the bursty traffic of event reporting and the shared medium for transmissions, the ID-MAC protocol changes the bursty traffic through assigning the sampling moments instead of adapting to the bursty traffic. ID-MAC belongs to the class of CSMA/CA protocols. Upon detecting the event, a node senses the channel for a short period of time. After finding out that the channel is idle, the node sends out a message to all the neighboring nodes not to transmit

and then sends its own packets. When the channel is busy, the node will choose a sampling shift from the current detection moment randomly and independently from the other nodes in order to avoid collisions. The whole process will be repeated when the new data packet is ready for transmission. The optimization goal for transmission of data packets is the minimum number of collisions among the neighboring nodes. The probabilities of the slotted non-persistent CSMA/CA protocol are determined by the least collision criteria.

Besides data packets, the node is also responsible for relaying packets from other nodes. Such enroute packets deserve a different scheme, since the goal would be to transmit the packets to the next hop with least delay. Therefore, the node applies the normal CSMA/CA protocol for enroute packets, which aims at the least delay. The protocol details are discussed in the following.

6.2.2 Data Packets

Data packets refer to those generated by the node intending to transmit them to the next node toward the sink. When the event is detected by the node, it begins to carrier sense the channel. Initially, the nodes in the event area A attempts to access the medium simultaneously. the ID-MAC protocol assigns the node a new sampling moment when it detects the channel is busy and a data packet is ready to be transmitted at the same time. The new sampling moment is determined according to the probability distribution p_i. According to [96], the probabilities are given in as a recursive formula, thus leading to minimum collisions for each slot. Different from the usual slots for MAC protocols, the slots for accessing the medium is not continuous. The sampling cycle T is divided by M slots. As shown in Fig. 6.1, the node will only choose K slots (denoted by the black slots) out of all the slots. The probability for one node to choose the $(a \times i)$th slot is p_i, where a is the distance between two

black slots. In contrast, the probability for choosing the rest of the slots (denoted by the white slot) is simply zero. For the sake of convenience, the black slots are called *available* slots, while the white slots as *non-available* slots in the rest of the chapter. The optimal probabilities for the ID-MAC protocol in terms of minimum collisions are given as [96]:

$$p_{a\times i} = \frac{1 - f_{K-i}(N)}{N - f_{K-i}(N)}(1 - p_a - p_{2a} - \cdots - p_{a\times(i-1)}) \tag{6.1}$$

where

$$f_j(N) = (\frac{N-1}{N - f_{j-1}(N)})^{N-1} \tag{6.2}$$

and $f_j(N)$ is a recursive function such that $f_1(N) = 0$. The maximum success probability ζ_{opt} for all the slots being selected without collisions is basically a function of K and N. It is proved in [96] that $\zeta_{opt} = f_K(N)$. Apparently, a larger K and a smaller N lead to higher success probability, although a larger K results in a longer sampling cycle, not favorable to the application in achieving the goal of abundant and timely knowledge about the detected event.

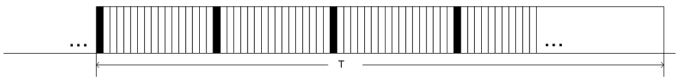

Figure 6.1: Slots allocation of ID-MAC

From the MAC layer's point of view, the proposed protocol increases the collision probability because a smaller number of slots are available for nodes to choose from. However, the length of the sampling cycle is much greater than that of the collision window of CSMA/CA protocols. The number of available slots is still com-

parable to the number of slots in the collision window. Consequently, the collision probability does not increase significantly.

In addition, the chosen slots are the suggested moments for the nodes to take the samples in the next sampling cycle. The collision probability does not represent the severity of the collision problem in the MAC layer; rather it implies how close could the observations be on the same event from different nodes. Since the collision of observations is not desirable in dense networks, ID-MAC adopts the CSMA/CA protocol to find out the sampling moments, that is, the observation moments for the nodes. More discussions on the observations from nodes are presented in Section 6.3.

When there is an incoming data packet from a neighboring node, the node also applies the ID-MAC protocol to find out the sampling moment for itself to avoid collision with relaying the data packets from neighboring nodes.

After the node successfully transmits the packet generated at the suggested sampling moment, it sticks to the sampling moment until the next time the packet collides with others. From a single node's point of view, the samples are taken periodically with the sampling shift suggested by ID-MAC to avoid collisions.

The design parameters of ID-MAC include the sampling cycle T and the distance, a, between two consecutive available slots. With these parameters, the nodes are able to determine the medium access rule by computing the optimal probabilities. Since the parameters are closely related to the quality of event reports, the details on the design parameters are presented in Section 6.3.

6.2.3 Enroute Packets

As long as the data packets arrive at the other nodes on its path to the sink, they become enroute packets, which need to be forwarded to the sink. The goal for the MAC layer is to transmit the enroute packets to the next hop in a timely manner.

Since the enroute packets originate from the data packets, the collisions involving enroute packets are much less than the expected collisions of the bursty traffic.

The ID-MAC protocol applies a different MAC scheme for the enroute packets from the collision minimizing scheme for the data packets. As collisions are already minimized when the traffic is generated, ID-MAC aims at reducing the transmission delay when processing the enroute packets. In ID-MAC, the node tries to access the medium immediately after the arrival of the enroute packets. The state transitions of the protocol, including those involving enroute packets, is shown in Fig. 6.2. The idle state of the protocol is interrupted by the periodically generated data packets (denoted by ①) and the incoming enroute packets (denoted by ②). When there is no contention for the medium, either the data packets or the enroute packets are sent out by exchanging RTS/CTS signals. After that, the protocol returns to the idle state through (denoted by ③) and (denoted by ④). When there are contentions, collisions bring the states back to the ready states waiting for the next trail. The successes of resolving the contention result in returning to the initial idle state.

The focus of ID-MAC is to resolve three contentions: (i) between data packets, (ii) between enroute packets, and (iii) between data packets and enroute packets. The contention between data packets is dealt with the rule of selecting a slot from a limited number of slots within the sampling cycle. The contention between enroute packets is dealt with the normal CSMA/CA protocol, in which nodes uniformly randomly choose a slot from the contention window. Distinctive from these contentions, the contention between data packets and enroute packets in ID-MAC always ends with the success of the enroute packets. The priority of the enroute packets is guaranteed by the condition: $CW < a$, where CW is the length of the collision window. The enroute packets succeed in competing for the medium due to its faster back off than the data packets obeying the rule of choosing a slot at least a slots away.

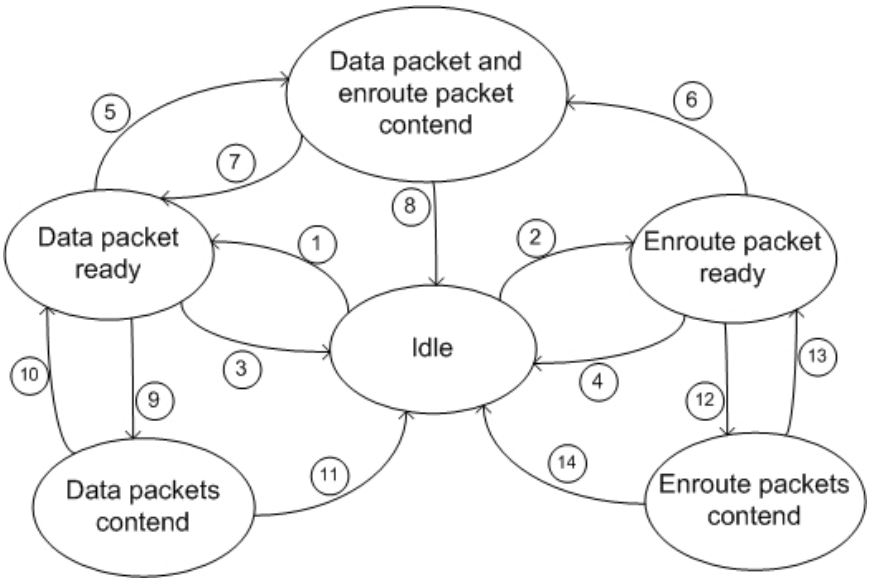

Figure 6.2: State transitions for enroute packets

6.3 Event Reports and Estimation

In this section, the impact of adopting ID-MAC on the application's performance is discussed. The link between the MAC performance and the application's performance is revealed through the analysis on the success probability of the slots and the quality of the event reports in terms of the highest signal frequency to be reconstructed and the lower bound on the estimation accuracy respectively.

6.3.1 Event Reports

It is common that the nodes in area A observes the same event, which is represented by a band-limited signal $f(t)$. Thus, $s_i(t) = f(t)$. The sink collects the data packets from the nodes adopting ID-MAC, according to which the data samples taken by the nodes are not synchronized. In other words, the observations on the same events are taken at different moments to avoid the bursting traffic containing mostly similar observations. Regarding the event in terms of the signal $f(t)$, the goal of collecting the observations is to reconstruct the original signal with the data

packets. Given the suggested sampling moments by ID-MAC, the reconstruction of $f(t)$ relies on a set of irregular samples collected from the data packets.

An adaptive weights method for signal reconstruction with irregular samples is provided by [84]. The method is based on an iterative process, which has the sampling set as shown in Eq.(6.3). The algorithm is described in Eq.(6.4).

$$\mu = \sup_{n \in Z}(x_{n+1} - x_n) < \frac{\pi}{\omega} \tag{6.3}$$

where x_{n+1} and x_n are the sampling moments of two consecutive samples and $\frac{\pi}{\omega}$ is half of the Nyquist rate.

$$\begin{aligned} & f_0 \\ = \quad & \tfrac{\pi^2}{\pi^2+\mu^2\omega^2} \sum f(x_n) \tfrac{x_{n+1}-x_{n-1}}{2} \tfrac{\omega}{\pi} \sin c(\omega x - x_n) \\ & f_{k+1} = fk + S(f - f_k), k \geq 0 \end{aligned} \tag{6.4}$$

Reconstruction error of the algorithm is bounded by the inequality (6.5).

$$\begin{aligned} f &= \lim_{k\to\infty} f_k \\ \|f - f_k\| &\leq \lambda^{k+1}\|f\| \\ \lambda &= \tfrac{2\pi\mu\omega}{\pi^2+\mu^2\omega^2} \end{aligned} \tag{6.5}$$

In order to reconstruct the event signal $f(t)$, the time difference between the sampling moments of two consecutive samples is less than the Nyquist rate of the event signal. Since the samples are taken at the chosen slots in ID-MAC, the difference, d, between two consecutive chosen slots is bounded by the following:[96]

$$d < a[\frac{K^2 - 1}{3K f_K(N)} + (\frac{1}{f_K(N)} - 1)(K + l_{packet})] \tag{6.6}$$

where l_{packet} is the transmission duration of one packet.

Recall that the design parameters of ID-MAC are subject to the requirement on the quality of the event reports. Regarding the sampling cycle T, it is determined by the band-width of the event signal and the least difference between two consecutive samples. Given the bandwidth of the event signal, the least difference between two consecutive available slots is derived with the help of inequaltiy (6.3), thus

$$a[\frac{K^2-1}{3Kf_K(N)} + (\frac{1}{f_K(N)} - 1)(K + l_{packet})] < \frac{\pi}{\omega} \tag{6.7}$$

The left side of the inequality results from ID-MAC, and the right side relates to the highest frequency of the event signal. With fixed N, K, a and l_{packet}, the highest frequency of the event signal that can be reconstructed is bounded. Recall that the maximum success probability ζ_{opt} in the MAC layer is a function of N and K. Then the value of K depends on the desired maximum success probability and N, which depends on the density of the nodes and the size of the event area A. Therefore, the design parameter a can be tuned to achieve a tradeoff between ζ_{opt} and ω, where ω represents the quality of the event reports.

6.3.2 Processing the Reports

Instead of reconstructing the detected event, the sink seeks an alternative goal to estimate certain parameters from the collected reports from the nodes residing in the event area. Even when the collected reports do not contain sufficient information for the reconstruction of the whole event, the sink is still be able to estimate the parameters with certain level of accuracy.

As the nodes observe the same event, their event reports from different nodes are generally correlated. The correlation between two sets of reports from pairs of nodes

is modeled by the exponential model, when the event reports are jointly Gaussian random variables (JGRVs). The covariance matrix of the JGRVs is C, whose element $c_{i,j}$ is given by:

$$c_{i,j} = cov(s_i(t), s_j(t)) = E[s_i s_j]$$

The JGRVs are $\mathbf{x} \sim Normal_N(\mu(\theta), C(\theta))$, where $\boldsymbol{\theta} = [\theta_1, \theta_2, \cdots, \theta_h]$ is the vector of the deterministic parameters to be estimated. Cramer-Rao lower bound (CRLB) is the lower bound on the variance of estimators of the deterministic parameters. It states that the variance of an unbiased estimator could not exceed the inverse of the Fisher information matrix (FIM), whose element is given in the following [97]:

$$I_{i,j} = \frac{\partial \boldsymbol{\mu}^T}{\partial \theta_i} C^{-1} \frac{\partial \boldsymbol{\mu}}{\partial \theta_j} + \frac{1}{2} \mathrm{tr} \left(C^{-1} \frac{\partial C}{\partial \theta_i} C^{-1} \frac{\partial C}{\partial \theta_j} \right)$$

Then the variance of the unbiased estimators U is bounded as follows:

$$Var(\mathbf{U}) \geqslant \frac{1}{I(\boldsymbol{\theta})}$$

Since ID-MAC requests that the nodes generate data packet at particular time slots, the correlation among the event reports is subject to the time shifts of the nodes' sampling moments due to ID-MAC. Specifically, the covariance coefficient $c_{i,j}$ is modeled by $e^{-\alpha t_{i,j}} \rho_{i,j}$, where $t_{i,j}$ is the time difference between the sampling moments of nodes i and j, and $\rho_{i,j}$ is the covariance coefficient of the samples taken at the same time moments. When the nodes take the samples at approximately the same time, then $c_{i,j} \approx \rho_{i,j}$. The result of applying ID-MAC is the time shifts of the nodes, which lead to a lower CRLB.

Consider the estimation of parameters θ from the following signal model:

$$\mathbf{x}(t) = \mathbf{A}(\theta)\mathbf{s}(t) + \mathbf{e}(t)$$

in which, the signals $\mathbf{s}(t)$ are from m sources, $\mathbf{e}(t)$ is the noise signal and $\mathbf{A}(t)$ is the steering function. The received signals $\mathbf{x}(t)$ are Gaussian $\mathbf{N}(\mathbf{A}(\theta)\mathbf{s}(t), C)$, in which C is the variance of noise $\mathbf{e}(t)$.

Let the CRLB for estimating the parameters θ to be denoted by $CRLB_\theta$, thus as shown in [98]

$$CRLB_\theta = \frac{1}{2n}[V \odot P]^{-1}$$

where V is the matrix resulted from manipulating matrix $\mathbf{A}$ and C, and P is the covariance matrix of the source signals $\mathbf{s}(t)$.

Since the source signals are correlated with each other, the covariance matrix of the shifted source signals is P'. According to the temporal correlation model, $P' < P$ because $P - P'$ is positive semi-definite. Therefore, $CRLB_\theta > CRLB'_\theta$, which indicates that the CRLB of parameter estimation is indeed lowered by shifting the sampling moments of the source signals.

Notice that the introduction of the exponential factor in the correlation coefficient model actually helps to improve the achievable CRLB given the correlated event reports. ID-MAC intentionally introduces the non-zero $t_{i,j}$ into the correlation model in its effort to convert the bursting traffic into a streamlining one. The tradeoff between the MAC performance and the estimation accuracy is embodied in tuning the time shifts for the sensor nodes. From ID-MAC's point of view, the time shifts are the result of maximizing the success probability for selecting the slots. On the

other hand, the value of the corresponding CRLB also depends on the set of time shifts.

Through theoretical analysis and simulations, the following results are obtained:

1) The proposed ID-MAC protocol relates the MAC performance with the information quality of the event reports. For scenarios requiring reconstruction of the event signal, the tradeoff between the MAC performance and the highest frequency of the reconstructed signal enables the network to achieve the design goals of both the MAC layer and the application layer through adjusting the number of transmission slots.

2) Energy consumption of the event monitoring process is also related with the MAC performance through the length of sampling cycle of the nodes. High success probability can be achieved at the MAC layer, while nodes consume small amount of energy due to a long sampling cycle.

3) Regarding parameter estimation at the application layer, the Cramer-Rao lower bound is decreased by introducing the ID-MAC protocol to shift the nodes' sampling time instances from each other.

6.4 Summary

Discussion on the event detection and reporting application is presented after the details of the ID-MAC protocol is described. Because of the potentially competitive nature of the event reports, the idea of streamlining the traffic of event reports is revealed through the CSMA-based MAC protocol. In the ID-MAC protocol, there are two types of packets: data packets and enroute packets. The two types of packets are handled differently by the protocol. After applying the ID-MAC protocol, the event reports not only contain more informative sensory data, but also incur less collisions at the MAC layer. Furthermore, the Cramer-Rao lower bound is proposed to quantify

the improvement on the application's performance. It bounds the estimation accuracy that can be achieved by the application through the obtained sensory data. Simulation study reveals the tradeoff between the MAC performance and the application's performance, which can provide guidelines for designing real applications.

CHAPTER 7

SIMULATION STUDY

The simulation study on the proposed asynchronous sampling strategies and the ID-MAC protocol is presented in this chapter. The simulations are conducted on both synthetic and real data set. The results on the reduced energy consumption, the increased entropy, the event reconstruction and the lower bound on estimation accuracy are shown respectively.

7.1 Reduced Energy Consumption

Simulation experiments are conducted on a real data set using the reconstruction method discussed in previous sections. The simulation results show that the reconstruction performance is guaranteed when the sampling interval is adjusted to the clock jitter.

7.1.1 Data Set

In order to show the benefits of asynchronous sampling to the lossless data gathering applications, a real data set is taken as an example. It consists of the soil temperature readings from a WSN deployed at Huntington Gardens in San Marino, CA (http://www.sensorwaresystems.com). The soil temperature readings come from the sensor nodes numbered 3 and 5 located at difference positions. This section will show how the high frequency part signal can be preserved through the asynchronous sampling strategy that shifts the sampling time instances evenly and reduce the sampling rate by half.

The soil temperature readings are collected from 2007-02-19 8:49 to 2007-10-06 16:39 every 5 minutes. The corrupted samples were removed and the average of every 100 samples were taken in order to reduce the impact of noises. Furthermore, the mean of the soil temperatures was subtracted from the two data sequences, respectively. The spectrum of the obtained data sequences are shown in Figs. 7.1 and 7.2. Observing that the spectra resemble those of the signal models discussed in Section 4, the asynchronous sampling strategy was applied to reduce the number of samples needed for the reconstruction of the signals. Due to the remaining noises in the data, neither the low frequency nor the high frequency part of the signals from the two nodes is equal to each other. However, as shown in the figures, the high frequency part of the signals do approximate to each other. In order to illustrate the benefit of the asynchronous sampling strategy, the high frequency part of the signals is regarded as the common part signal in the following. Given the sampling rate of the obtained data series at 1 sample per 500 minutes, the high frequency part of the signal, centered at 36% of the sampling frequency, represents the changes of the soil temperature at a daily basis, whereas, the low frequency part represents the other long term changes.

7.1.2 Reconstruction Performance

In the asynchronous sampling scheme, the data with odd sequence numbers are chosen from the first sequence and those with even sequence numbers from the second sequence. The spectrum of the resulting asynchronous data is presented in Figs. 7.3 and 7.4, respectively. Notice that the high frequency part of the signals are attenuated in terms of both its power and frequency.

Following the steps described in Fig. 4.2, the data are recovered accordingly. The results are shown in Figs. 7.5 and 7.7, respectively. In comparison, the results

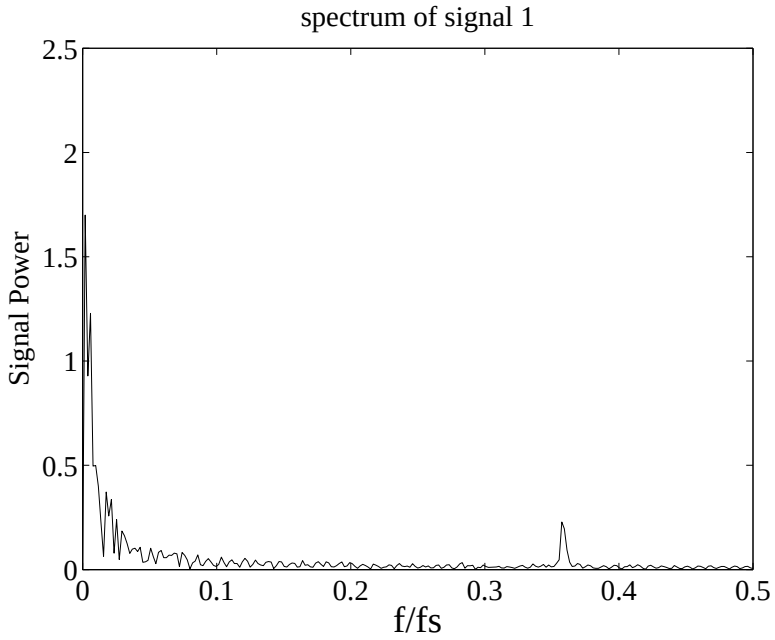

Figure 7.1: Spectrum of the data from node 3

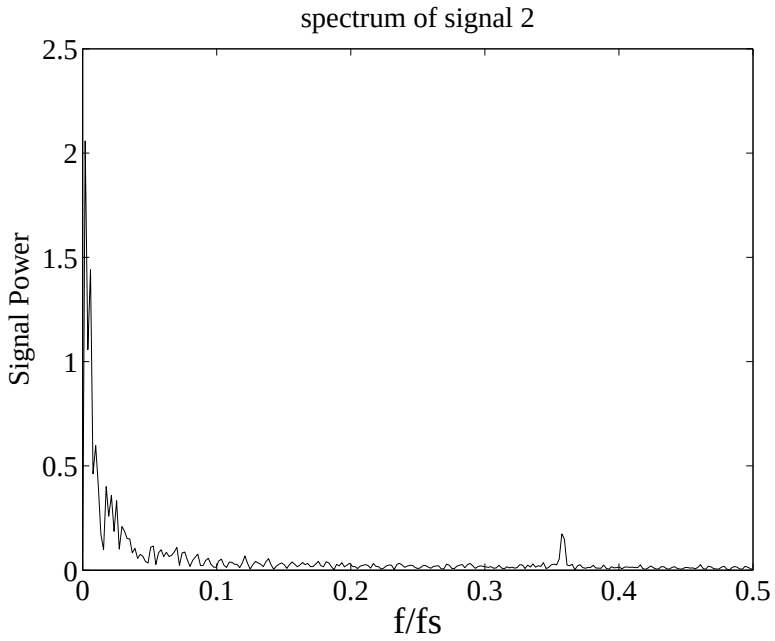

Figure 7.2: Spectrum of the data from node 5

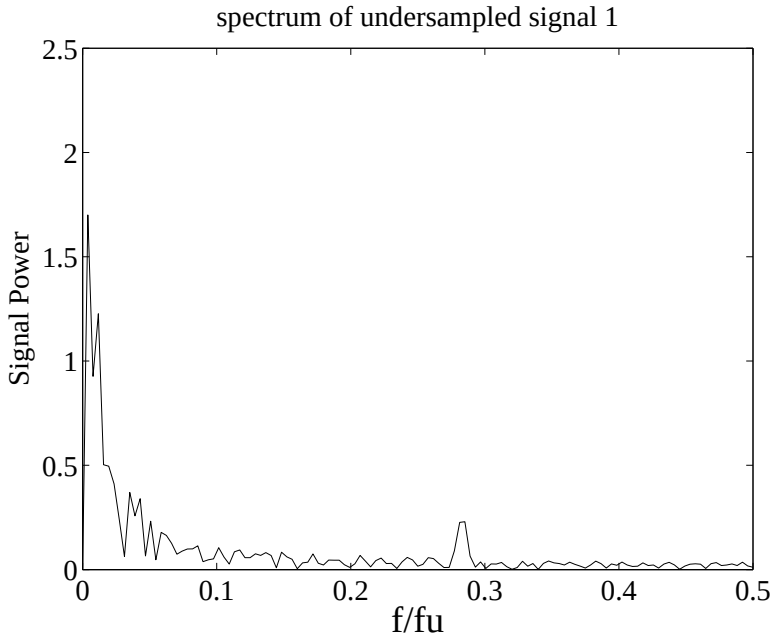

Figure 7.3: Spectrum of the undersampled data from node 3

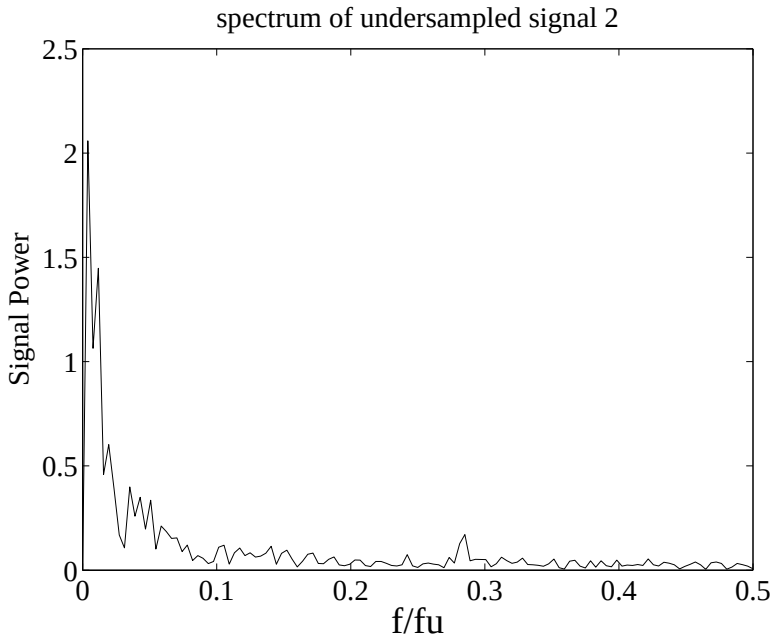

Figure 7.4: Spectrum of the undersampled data from node 5

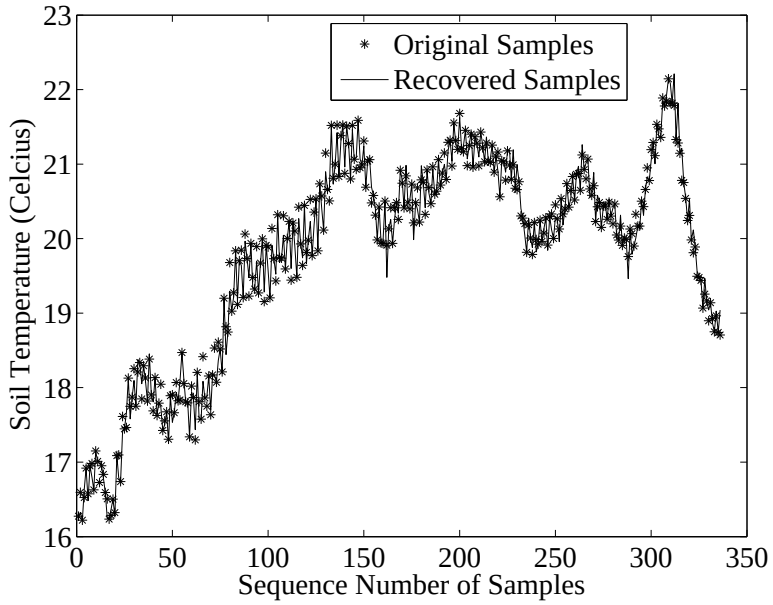

Figure 7.5: Data from node 3 recovered with asynchronous sampling

from the synchronous data are shown in Figs. 7.6 and 7.8. It is worth noticing that the results from the asynchronous data contain more high frequency component than those from the synchronous data. The observation is validated through the spectrum analysis on the recovered data sequences. As shown in Fig. 7.9, the results from the asynchronous data do preserve the high frequency component with a sampling rate that is half of its synchronous counterpart. Similar observations can also be found in Fig. 7.10.

7.1.3 Impact of Local Clocks

The impact of local clocks on the performance of the reconstruction method is also simulated in the experiments. The simulation is implemented using two correlated sample sequences. The clock jitter is defined according to its ratio to the sampling interval. In Fig. 7.11, the clock jitter ratio varies from 0 to 0.1, while the reconstruction error of the common part signal remains around 1% for sampling in-

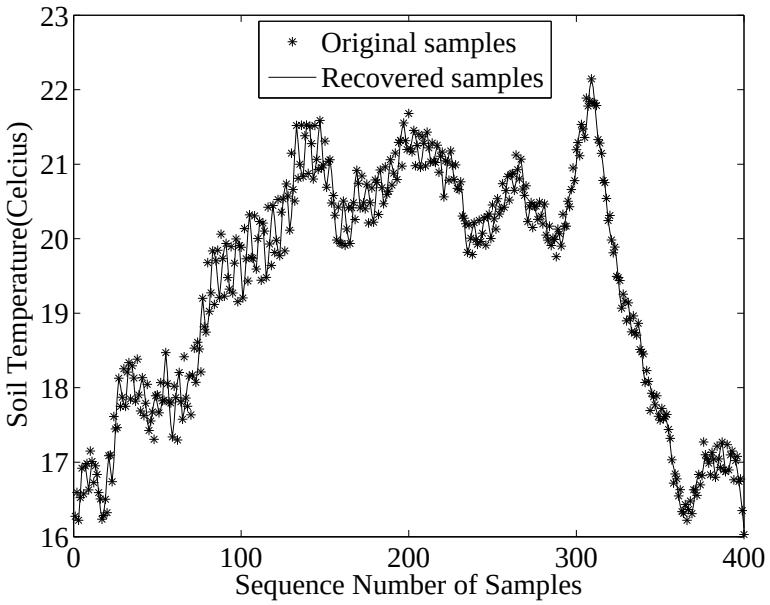

Figure 7.6: Data from node 3 recovered with synchronous sampling

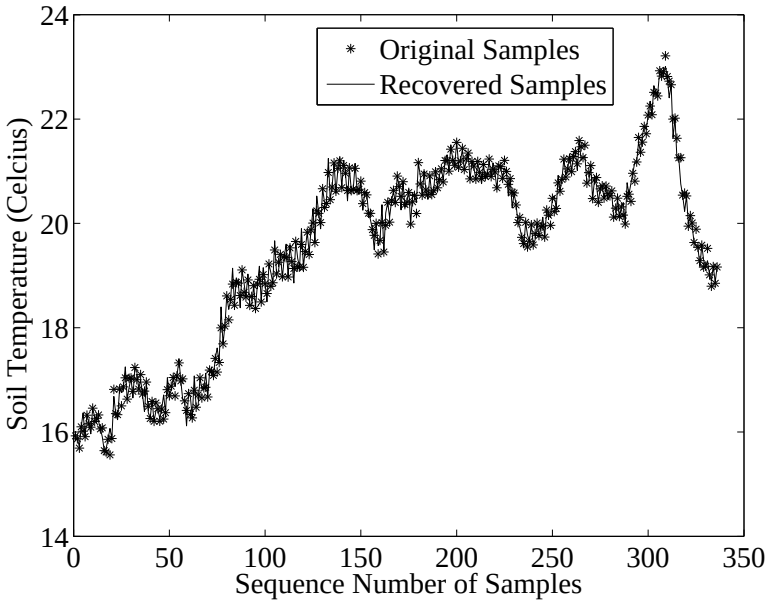

Figure 7.7: Data from node 5 recovered with asynchronous sampling

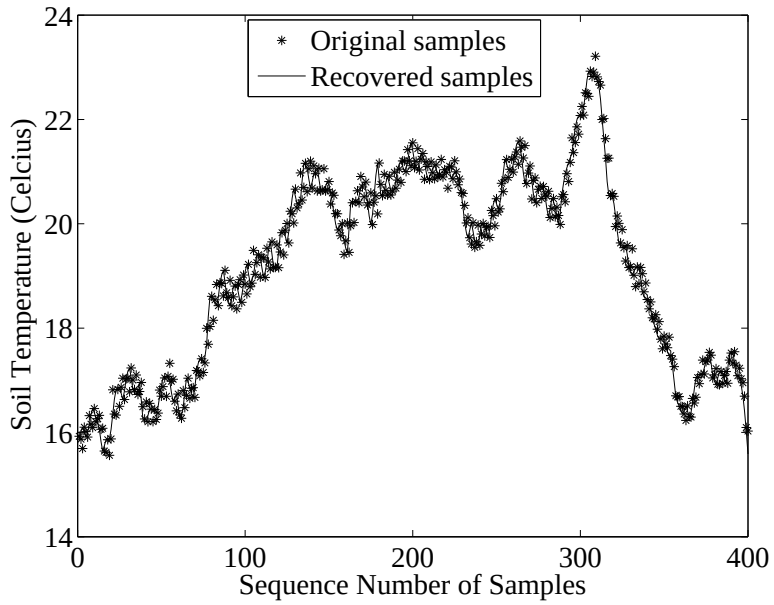

Figure 7.8: Data from node 5 recovered with synchronous sampling

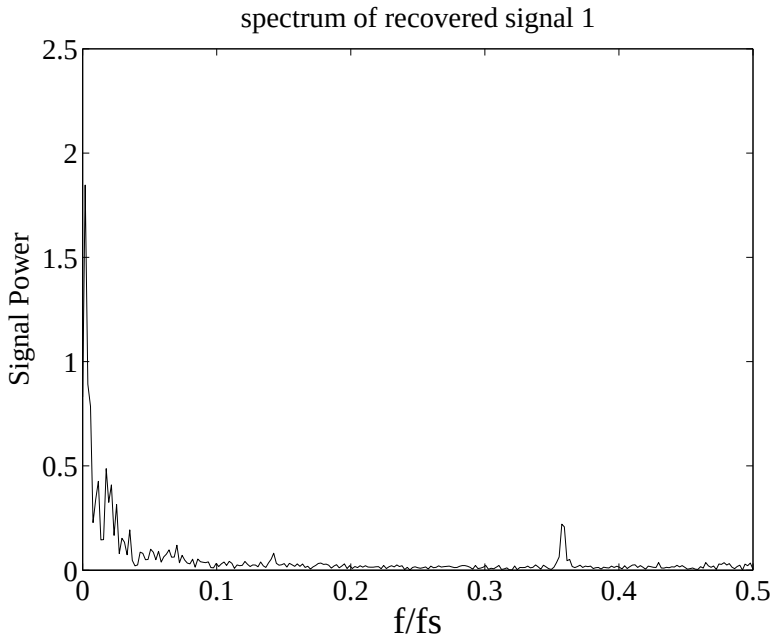

Figure 7.9: Spectrum of data from node 3 with asynchronous sampling

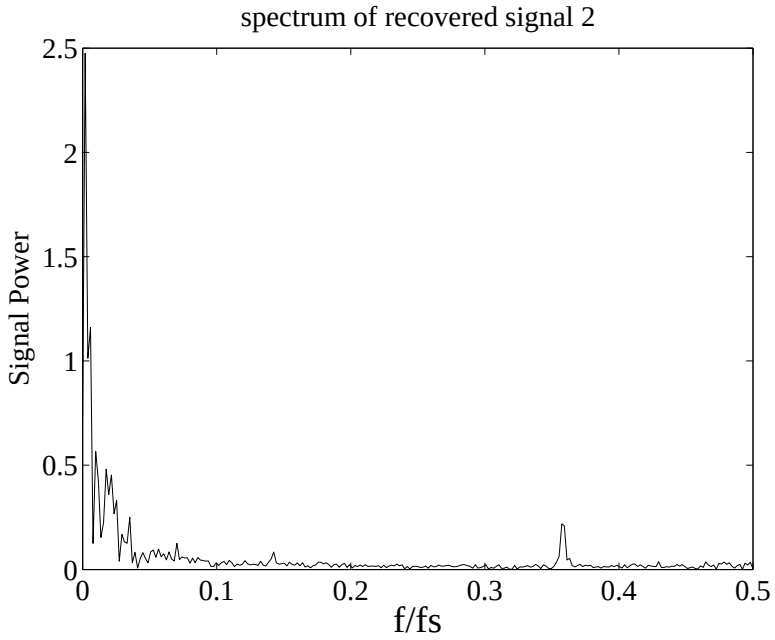

Figure 7.10: Spectrum of data from node 5 with asynchronous sampling

terval 1.5 times the Nyquist interval; and the reconstruction error increases to more than 9% for sampling interval 1.8 times the Nyquist interval.

7.2 Increased Entropy

Similarly, the simulation of the increased entropy also has been conducted on both synthetic and real data sets, which are illustrated respectively.

7.2.1 Synthetic Data Set

Before presenting the simulation results, the correlation model for 10 sensor nodes is set up. It is assumed that the sensor nodes are located in three-dimensional space, and the spatial correlation between two sensor nodes is determined by their distance from each other. Locations of the sensor nodes are randomly distributed in a $10m \times 10m \times 10m$ space as shown in Fig. 7.12.

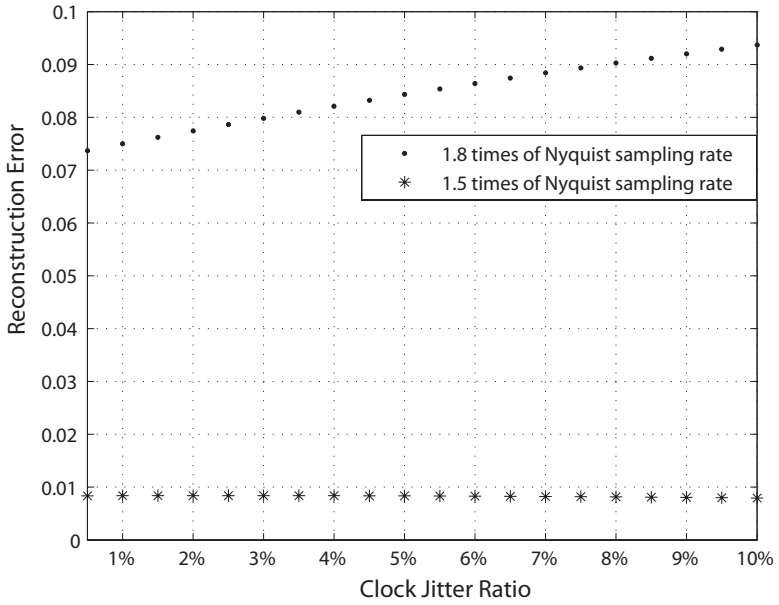

Figure 7.11: Reconstruction performance of the common part signal

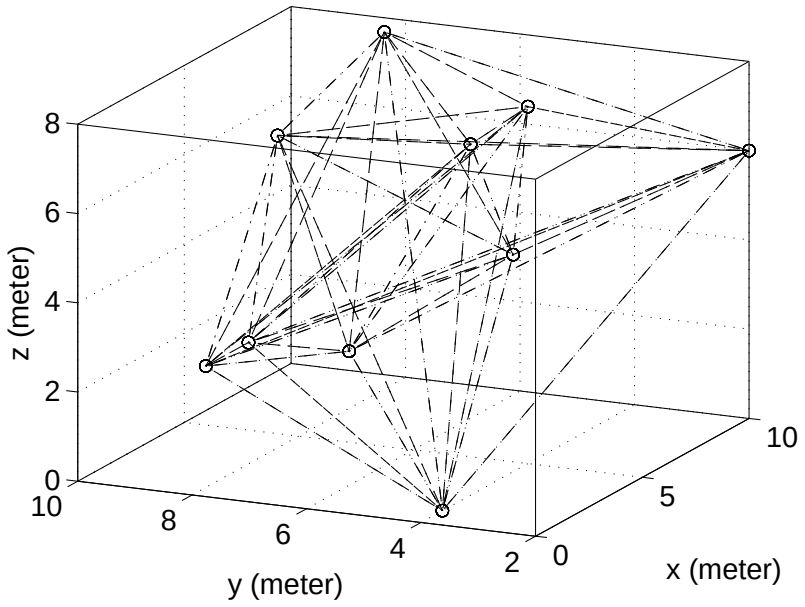

Figure 7.12: Locations of the sensor nodes

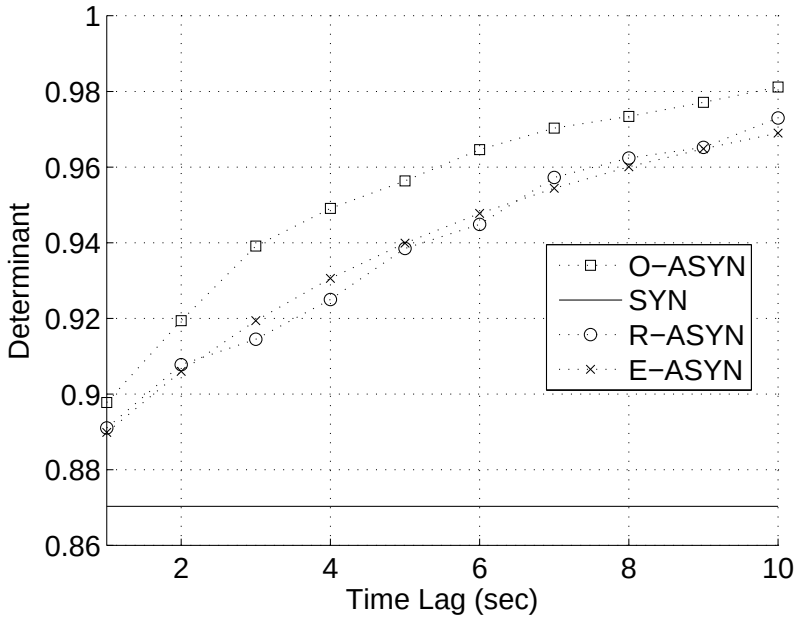

Figure 7.13: Asynchronous strategies on synthetic data

Given the locations of the sensor nodes, the correlation between sensory data generated by different sensor nodes can be obtained accordingly through applying the exponential correlation model with spatial correlation constant α.

7.2.2 Real Data Set

Firstly, it is shown how to find the correlation parameter β from the synchronous samples by using a data set containing temperature measurements in a room. Through the simulated correlation model and experimental data, it is shown that the O-ASYN strategy produces satisfying results for a group of randomly correlated sample sequences. Besides, it is shown that R-ASYN and E-ASYN strategies can increase the entropy or decrease the distortion without searching for the optimal assignment of the time shifts.

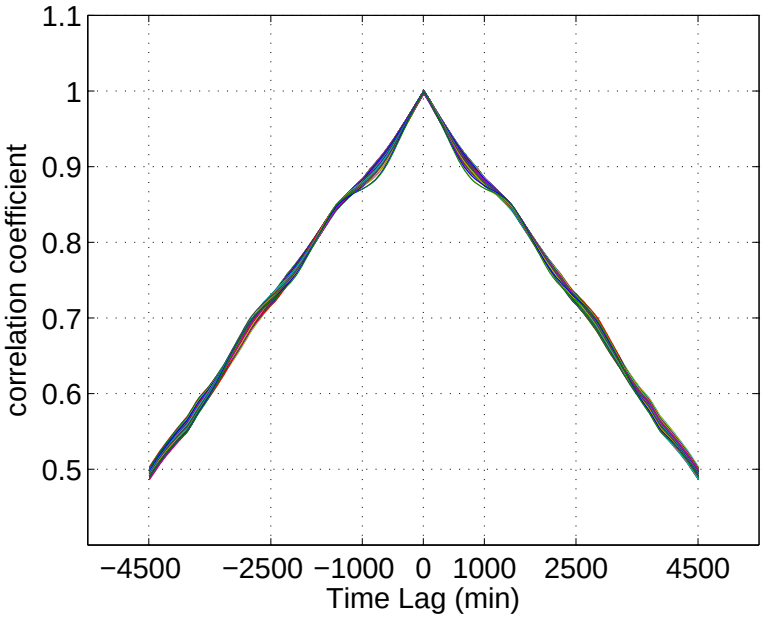

Figure 7.14: Fitting the temporal correlation model

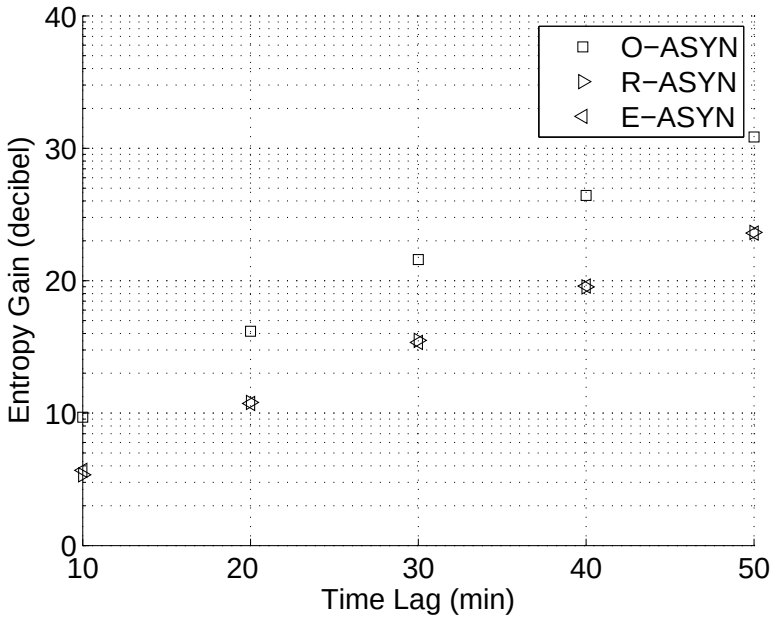

Figure 7.15: Asynchronous strategies on real data

The correlation matrix given in Eq. (5.3) is obtained accordingly with $\alpha = 0.5$ and $\beta = 0.2$. First, the entropy is simulated using the correlation matrix without asynchronous sampling. Then R-ASYN and E-ASYN strategies are simulated, and finally O-ASYN is applied to the same correlation matrix.

The simulation experiment is repeated with respect to T ranging from $1s$ to $50s$. The results are shown in Fig. 7.13. O-ASYN produces a partition of T, implying that the entropy converges to the maximum value. Whereas, R-ASYN and E-ASYN outperform the synchronous sampling and get closer to the approximation algorithm when T increases.

As the implementation of asynchronous sampling strategy relies on the prior knowledge of temporal correlation model, it is shown that the correlation parameter β is obtained through statistical study on the synchronous samples. The data set from the Intel Berkeley Lab. [83] is adopted. It contains temperature measurements in a room for about one month. Among the 54 sensor nodes deployed, there are 50 nodes which transmitted valid sample series to the sink. They take samples of temperature and other environment parameters at the same time. Due to uncertainties of multi-hop communication, samples taken at some epoch time are missing and some of the measurements are beyond the normal range. Before computing correlation of the time shifted samples, the corrupted data are excluded from the samples. In order to deal with missing samples, an average of samples during a time period of several epochs is computed as the value for the epoches with no samples that successfully received by the sink.

As shown in Fig. 7.14, the correlation parameter $\beta = 0.0012$, which fits in the statistical model of temporal correlation.

7.2.3 Regression Performance

Based on the value of β, the simulation is conducted on the asynchronous sampling strategy with the data set from the 50 sensor nodes. The simulation experiment is conducted in two stages. First, the indices of the sensor nodes are obtained through recursion. Then the optimal sampling shifts are determined using numerical method. The maximum time shift varies from 10 minutes to 50 minutes. The simulation result on the entropy gain is shown in Fig. 7.15. It is shown that when the sampling rate has to be traded off for longer lifetime of WSNs, asynchronous sampling produces more informative samples. Simulation results on entropy of samples from sensor nodes provide quantified improvement on the information of the physical process retrieved from sensor nodes.

More specifically, the regression distortion of the temperature values is computed given the sensory data sampled at reduced sampling rate. The regression results corresponding to synchronous samples and asynchronous samples are shown in Figs. 7.16 and 7.17, respectively, while the sensory data sampled at the original sampling rate are shown in Fig. 7.18. Regression distortion of synchronous sampling and asynchronous sampling are compared in Fig. 7.19. Observe that the overall regression distortion of asynchronous sampling is lower than that of synchronous sampling.

7.3 Event Reconstruction

Simulation results for the MAC performance and the reconstruction performance are presented first to show the tradeoff between them under ID-MAC. Then the simulation result on the MAC performance and the lower bound on the estimation accuracy is shown to demonstrate the ID-MAC's improvements on MAC performance and the estimation performance.

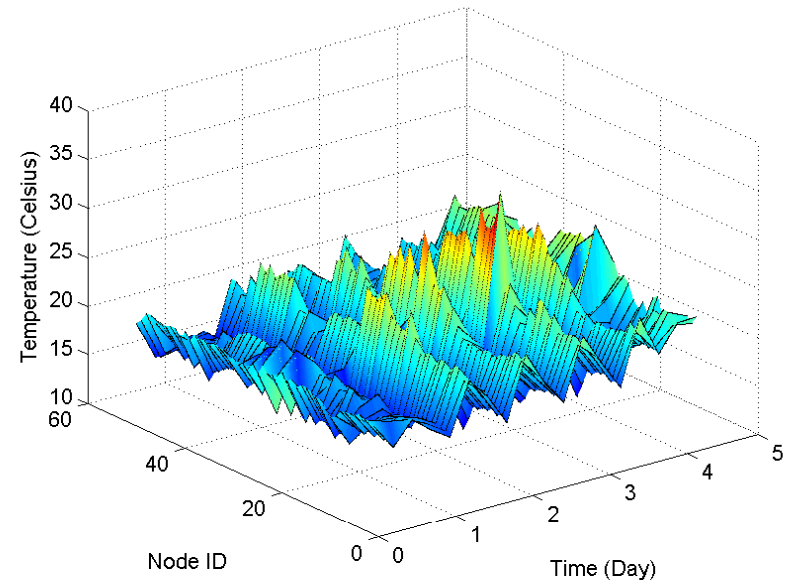

Figure 7.16: Synchronous sampling at reduced rate

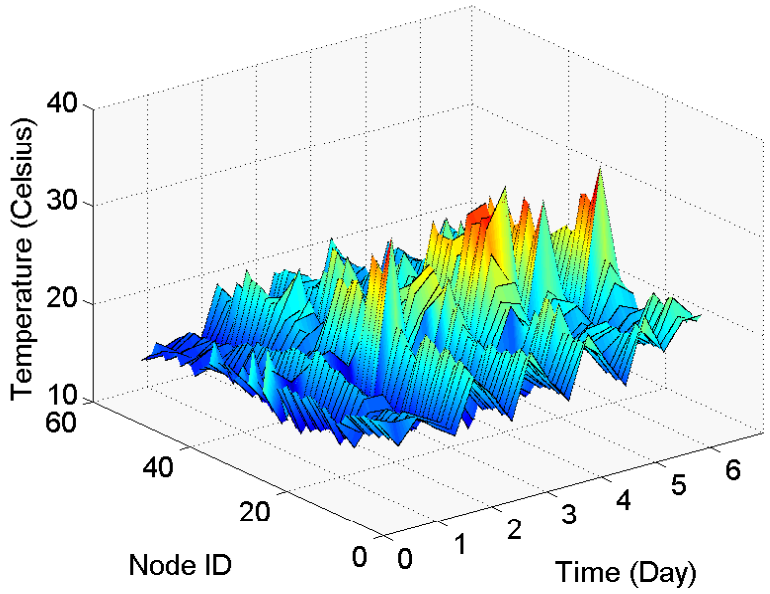

Figure 7.17: Asynchronous sampling at reduced rate

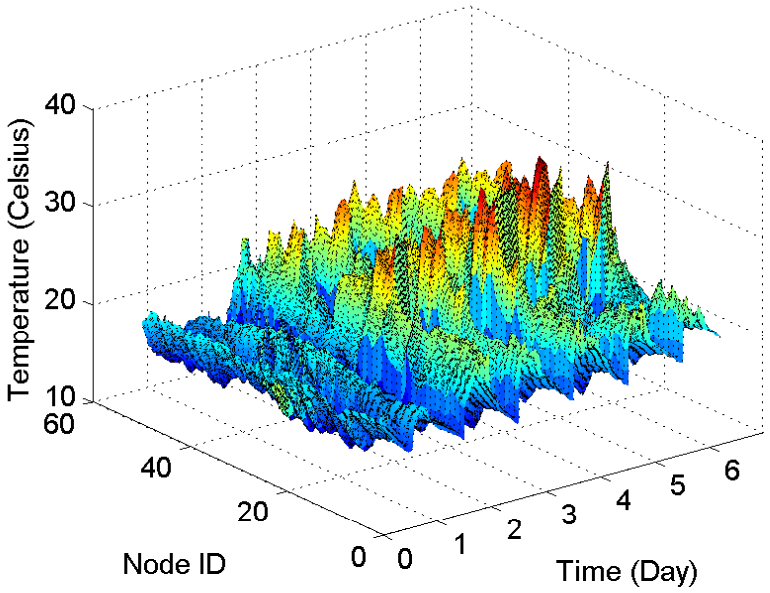

Figure 7.18: Synchronous sampling at original rate

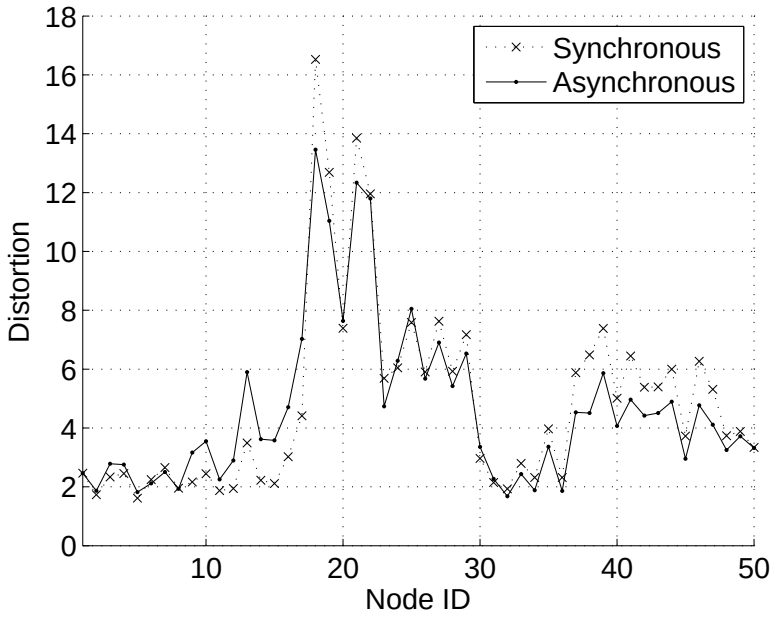

Figure 7.19: Comparison of regression performance

Given ID-MAC and its design parameters, such as the number of slots, it shows the tradeoff between the MAC performance and the quality of event reports. Since the goal is to reconstruct the event with the reports from the nodes, the sampling shifts suggested by ID-MAC should be able to meet the reconstruction algorithm's requirement on the largest difference between two consecutive sampling moments. The tradeoff between MAC performance and the quality of event reports also relies on the condition stated in the inequality (6.7). Although the event reports are sufficient for the reconstruction, the higher the frequency of the event signal, the more reports are required during certain period of time. The challenge of collecting more reports is also true at the MAC layer. The more the reports transmitted from nodes to the sink, the busier is the medium for the nodes. ID-MAC aims at changing the bursty traffic by selecting sampling shifts for nodes, which in turn introduces the interaction between the MAC layer and the application's task. Specifically, the frequency of the event signal that can be reconstructed decreases when ID-MAC increases the number of available slots for better success probability.

As mentioned, in ID-MAC, the success probability is determined by K and N. Since the number of nodes in the event area is normally a constant after the nodes are deployed, the protocol can choose to have more available slots in order to improve the success probability. In the simulated example, $N = 5, 10, 15$ and K starts from 16 to 86, 24 to 74 and 32 to 82, respectively. The difference between ID-MAC and the optimal CSMA/CA protocol is the non-available slots in between two available slots. Here, the number of non-available slots is $a = l_{packet} + 5$, which guarantees that the node would be able to send the packet before the next available slot. According to the inequality (6.7), the highest frequency of the recoverable event signal is computed given K, N, a and l_{packet}. Since the result is with respect to a unit length of the slot, a reasonable value was assigned to the length of the slot in order to get the exact

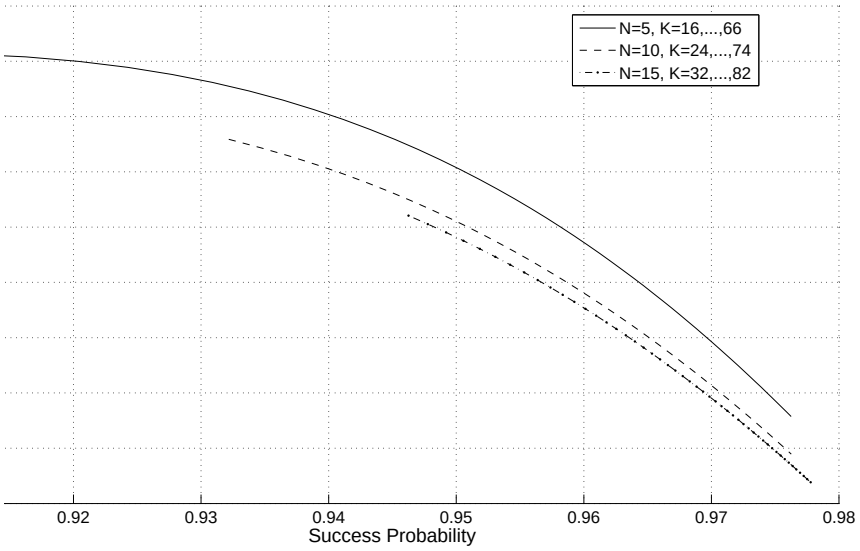

Figure 7.20: Tradeoff between MAC performance and the quality of event reports

frequency. On the other hand, the success probability is also computed according to Eq. (6.2). Therefore, the tradeoff is obtained as shown in Fig. 7.20. The success probability is above 80%, however the highest frequency decreases sharply when the success probability exceeds 90%. The simulation results show that the design of ID-MAC involves the tradeoff between MAC performance and the quality of the event reports. The key parameter is K, which determines not only the success probability but also the highest frequency that can be recovered.

Additionally, the number, K, of available slots in ID-MAC, also plays an important role in achieving energy efficiency. Because the reconstruction of the event signal is accomplished through the cooperation among nodes observing the same event, the sampling cycle of each node equals to $a \times K$. Apparently, the communication cost in terms of energy consumption is positively proportional to the amount of reports sent to the sink, which is directly related to the sampling cycle of each node. The larger the number of reports to be sent to the sink, the more energy has to be consumed to

accomplish the transmission. The goals of energy efficiency and better MAC performance are met by adjusting K. The simulation on the energy efficiency is conducted using the same set of parameters and the results are shown in Fig. 7.21. As the success probability increases, the length of the sampling cycle increases sharply, which leads to much fewer number of reports generated by each node.

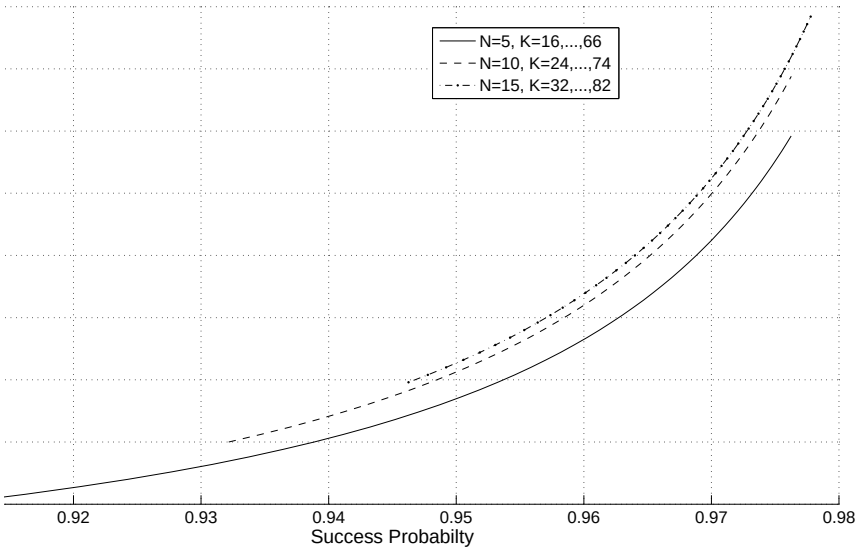

Figure 7.21: Sampling cycle and the MAC performance

The two simulations on the quality of event reports and energy efficiency reveal that ID-MAC links the MAC performance with the application's performance. The existing literature shows that energy efficiency can be achieved separately at the MAC layer and the application layer. In ID-MAC, the goal is cooperatively achieved at both layers.

7.4 Lower Bound of Estimation Accuracy

Regarding the estimation of parameters from the event reports, the MAC performance and the estimation accuracy are both improved with the help of the ID-MAC protocol. The estimation accuracy is represented by CRLB of the event reports. The simulation is based on the example case discussed in Section 6.3.2. The event reports are correlated random variables with Normal distribution. The parameter to be estimated is the average of the samples. The covariance matrix of the reports is computed through the exponential model of correlation. The event is detected by five nodes, whose reports are correlated. Thus $N = 5$. The sampling shifts for the five nodes are randomly chosen. And K increases from 26 to 520. For the example case, the lowest CRLB is $\sigma^2/5$ when the collected event reports do not have correlation with each other.

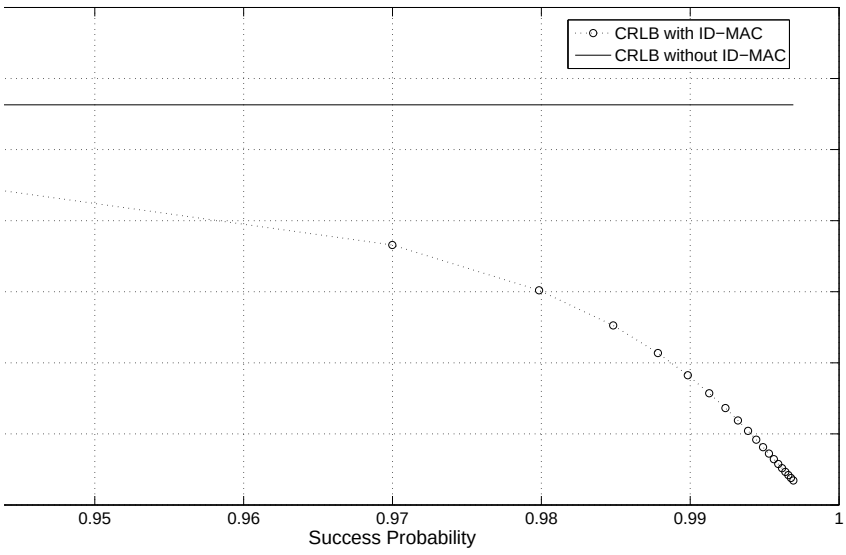

Figure 7.22: Lower bound of the estimation accuracy and the MAC performance

The simulation results are shown in Fig. 7.22. As the success probability increases, the CRLB decreases sharply, which is also the result of a greater K. The CRLB value is in terms of its percentage to the variance of the event reports. The CRLB ratio of the original event reports without ID-MAC is shown in the figure to provide the comparison with the CRLB under ID-MAC. Notice that the CRLB ratio approaches the lowest value at 0.2. However, ID-MAC can not obtain the lowest CRLB ratio since the correlation among the event reports can not be reduced to zero through ID-MAC.

7.5 Summary

Asynchronous sampling strategies are applied not only to the synthesized data but also to real data to show their benefits. On one hand, an under-sampled signal can be reconstructed with the help of shifted sampling instances. On the other hand, the entropy of sensory data is increased by shifting the sampling instances. Simulation experiments show that data regression performance is improved as a result. The simulation study on the asynchronous strategies include two aspects of the tradeoff between the energy consumption and the quality of the information, which is the center of the asynchronous strategies. One is the to reduce the energy consumption while guaranteeing the recovering of the original signal, the other is to increase the entropy of the sensory data without additional communication cost. Both synthetic and real data sets are presented to demonstrate the performance of the asynchronous sampling strategies. Since lossless data gathering applications always assume the fully recovering of the original signal, the simulation study on the reduced energy consumption is conducted regarding lossless data gathering. Whereas, the simulation study of lossy data gathering lies on increase the entropy of the sensory data. The impact of clock jitters on the lossless data gathering strategy is also studied. Simulation

results show that the asynchronous strategies are able to improve the performance of the application for both lossless data gathering and lossy data gathering.

The simulation results on the ID-MAC protocol are based on the analysis of the event reconstruction and the lower bound on estimation accuracy. The tradeoff between the sampling rate and the energy consumption is verified by the simulation of the event reconstruction scenario, while the tradeoff between the lower bound on estimation accuracy and the collision probability demonstrates the benefit of applying ID-MAC protocol.

CHAPTER 8

CONCLUSIONS AND FUTURE WORK

Three scenarios for data gathering are studied in this dissertation: lossless data gathering, lossy data gathering and event reporting. Asynchronous sampling strategies have been proposed for the data gathering applications, while the ID-MAC protocol is proposed to address the problem of collision prone traffic generated by the correlated sensor nodes detecting the same event.

According to the theoretical analysis and simulation results on the asynchronous sampling strategy for lossless data gathering applications, the following conclusions are reached:

1. For correlated signals, the asynchronous sampling strategy is able to reduce energy consumption through extending the sampling cycle of sensor nodes. The energy saving ratio depends on the degree of correlation.
2. The asynchronous sampling strategy does not introduce additional computation load to individual sensor node.

Similarly, the study of asynchronous sampling strategies for lossy data gathering applications can be concluded as follows:

1. For temporal-spatial correlated data sources, the quality of information obtained from the sensory data is improved in terms of increased entropy of the sensory data. Consequently, the application's regression performance is improved in terms of decreased regression distortion.
2. The sampling time shifts of sensor nodes can be scheduled to maximize the entropy of sensory data collected through the asynchronous sampling strategy.

However, assigning equal time shifts or random time shifts to sensor nodes are simple yet effective alternatives to the sub-optimal asynchronous sampling strategy.

Introducing the idea of sampling time shifts to MAC layer, the information-driven MAC protocol accomplishes the following:

1. The collision prone traffic generated by sensor nodes observing the same event can be streamlined by assigning sampling shifts to sensor nodes according to the feedbacks from MAC layer.
2. The quality of information is improved in terms of the decreased lower bound on estimation accuracy. Thus a better tradeoff between MAC layer performance and application performance is obtained by applying the proposed MAC protocol.

Simulation experiments have been conducted on both synthetic and real data set. The advantages of asynchronous sampling strategies and the information-driven MAC protocol are verified respectively. Comparison with the other information-driven data gathering approaches shows that asynchronous sampling strategies along with the proposed MAC protocol are able to further reduce the energy consumption without requiring additional resources.

Inspired by the information-driven data gathering strategies, future work includes information-driven cluster formation for the asynchronous sampling strategies and the ID-MAC protocol. As the proposed strategies assume that the problem is within one cluster of sensors that are spatially correlated with each other, the size of the cluster and the nodes in the clusters play important roles in the performance of the information-driven strategies that are applied within each cluster.

REFERENCES

[1] Texas Instrument, "A true system-on-chip solution for 2.4 ghz IEEE 802.15.4", 2007.

[2] Sun Labs, "Sun SPOT theory of operation red release 5.0", 2009.

[3] A. Mainwaring, D. Culler, J. Polastre, R. Szewczyk, and J. Anderson, "Wireless sensor networks for habitat monitoring," in *WSNA '02: Proceedings of the 1st ACM International Workshop on Wireless Sensor Networks and Applications*, New York, NY, USA: ACM, pp. 88–97, 2002.

[4] J. K. Hart and K. Martinez, "Environmental sensor networks: A revolution in the earth system science?" in *Earth-Science Reviews*, vol. 78, pp. 177–191, 2006.

[5] Crossbows, "Wireless Systems for environmental monitoring", 2009.

[6] T. He, P. Vicaire, T. Yan, L. Luo, L. Gu, G. Zhou, R. Stoleru, Q. Cao, J. A. Stankovic, and T. Abdelzaher, "Achieving real-time target tracking usingwireless sensor networks," in *RTAS '06: Proceedings of the 12th IEEE Real-Time and Embedded Technology and Applications Symposium*, Washington, DC, USA: IEEE Computer Society, pp. 37–48, 2006.

[7] L. Hu and D. Evans, "Localization for mobile sensor networks," in *MobiCom '04: Proceedings of the 10th Annual International Conference on Mobile Computing and Networking*, New York, NY, USA: ACM, pp. 45–57, 2004.

[8] S. R. Madden, M. J. Franklin, J. M. Hellerstein, and W. Hong, "TinyDB: An acquisitional query processing system for sensor networks," *ACM Transactions on Database Systems*, vol. 30, no. 1, pp. 122–173, 2005.

[9] S. Madden, R. Szewczyk, M. J. Franklin, and D. Culler, "Supporting aggregate queries over ad-hoc wireless sensor networks," in *WMCSA '02: Proceedings of the Fourth IEEE Workshop on Mobile Computing Systems and Applications*, Washington, DC, USA: IEEE Computer Society, p. 49, 2002.

[10] C. Intanagonwiwat, D. Estrin, R. Govindan, and J. Heidemann, "Impact of network density on data aggregation in wireless sensor networks," in *ICDCS '02: Proceedings of the 22 nd International Conference on Distributed Computing Systems*, Washington, DC, USA: IEEE Computer Society, p. 457, 2002.

[11] C. Schurgers, V. Tsiatsis, S. Ganeriwal, and M. Srivastava, "Topology management for sensor networks: Exploiting latency and density," in *MobiHoc'02: International Symposium on Mobile Ad Hoc Networking and Computing*, vol. 1, no. 1, pp. 135–145, 2002.

[12] X. Wang, G. Xing, Y. Zhang, C. Lu, R. Pless, and C. Gill, "Integrated coverage and connectivity configuration in wireless sensor networks," in *SenSys '03: Proceedings of the 1st International Conference on Embedded Networked Sensor Systems*, New York, NY, USA: ACM, pp. 28–39, 2003.

[13] R. C. Shah, S. Roy, S. Jain, and W. Brunette, "Data mules: Modeling a three-tier architecture for sparse sensor networks," in *IEEE SNPA Workshop*, pp. 30–41, 2003.

[14] S. Meguerdichian, F. Koushanfar, M. Potkonjak, and M. B. Srivastava, "Coverage problems in wireless ad-hoc sensor networks," in *INFOCOM '01: the 20th IEEE International Conference on Computer Communications*, pp. 1380–1387, 2001.

[15] Y. Wu, J. A. Stankovic, T. He, and S. Lin, "Realistic and efficient multi-channel communications in wireless sensor networks," in *INFOCOM '08: the 27th IEEE International Conference on Computer Communications*, pp. 1193–1201, 2008.

[16] J. Chou, D. Petrovic, and K. Ramchandran, "Tracking and exploiting correlations in dense sensor networks," in *Conference Record of the Thirty-Sixth Asilomar Conference on Signals, Systems and Computers*, pp. 39–43, 2002.

[17] V. Shnayder, M. Hempstead, B. rong Chen, G. W. Allen, and M. Welsh, "Simulating the power consumption of large-scale sensor network applications," in *SenSys '04: Proceedings of the 2nd International Conference on Embedded Networked Sensor Systems*, New York, NY, USA: ACM, pp. 188–200, 2004.

[18] V. Raghunathan, A. Kansal, J. Hsu, J. Friedman, and M. Srivastava, "Design considerations for solar energy harvesting wireless embedded systems," in *IPSN 05: Proceedings of the 4th International Symposium on Information Processing in Sensor Networks*, IEEE Press, pp. 457–462, 2005.

[19] S. Soro and W. Heinzelman, "A survey of visual sensor networks," *Advances in Multimedia*, vol. 2009, pp. 1–22, 2009.

[20] K. A. Delin and E. Small, "The sensor web: Advanced technology for situational awareness," *Wiley Handbook of Science and Technology for Homeland Security*, 2009.

[21] J. A. Parasiso and T. Starner, "Energy scavenging for mobile and wireless electronics," *IEEE Pervasive Computing*, vol. 4, no. 1, pp. 18–27, 2005.

[22] Vernier, "User Manual for the Soil Moisture Sensor".

[23] B. Gedik, L. Liu, and P. S. Yu, "ASAP: An adaptive sampling approach to data collection in sensor networks," *IEEE Transactions on Parallel and Distributed Systems*, vol. 18, no. 12, pp. 1766–1783, 2007.

[24] G. Anastasi, M. Conti, and M. D. Francesco, "Extending the lifetime of wireless sensor networks through adaptive sleep," *IEEE Transactions on Industrial Informatics*, vol. 5, no. 3, pp. 351–365, 2009.

[25] Winbond, "16M-bit Serial flash memory with dual and quad SPI".

[26] FTDI Chip, "FT2232c dual USB UART/FIFO I.C".

[27] B. Krishnamachari, D. Estrin, and S. B. Wicker, "The impact of data aggregation in wireless sensor networks," in *ICDCSW '02: Proceedings of the 22nd International Conference on Distributed Computing Systems*, Washington, DC, USA: IEEE Computer Society, pp. 575–578, 2002.

[28] B. Przydatek, D. Song, and A. Perrig, "SIA: Secure information aggregation in sensor networks," in *SenSys '03: Proceedings of the 1st International Conference on Embedded Networked Sensor Systems*, New York, NY, USA: ACM, pp. 255–265, 2003.

[29] S. Nath, P. B. Gibbons, S. Seshan, and Z. R. Anderson, "Synopsis diffusion for robust aggregation in sensor networks," in *SenSys '04: Proceedings of the 2nd International Conference on Embedded Networked Sensor Systems*, New York, NY, USA: ACM, pp. 250–262, 2004.

[30] W. Ye, J. S. Heidemann, and D. Estrin, "An energy-efficient MAC protocol for wireless sensor networks," in *INFOCOM '02: 21th IEEE International Conference on Computer Communications*, 2002.

[31] X. Wang, G. Xing, Y. Zhang, C. Lu, R. Pless, and C. Gill, "Integrated coverage and connectivity configuration in wireless sensor networks," in *SenSys '03: Proceedings of the 1st International Conference on Embedded Networked Sensor Systems*, New York, NY, USA: ACM, pp. 28–39, 2003.

[32] Y. Gu, T. He, M. Lin, and J. Xu, "Spatiotemporal delay control for low-duty-cycle sensor networks," in *RTSS '09: Proceedings of the 2009 30th IEEE Real-Time Systems Symposium*, Washington, DC, USA: IEEE Computer Society, pp. 127–137, 2009.

[33] R. Mangharam, A. Rowe, and R. Rajkumar, "Firefly: a cross-layer platform for real-time embedded wireless networks," *Real-Time Systems*, vol. 37, no. 3, pp. 183–231, 2007.

[34] B. Hohlt, L. Doherty, and E. Brewer, "Flexible power scheduling for sensor networks," in *IPSN '04: Proceedings of the 3rd International Symposium on Information Processing in Sensor Networks*, New York, NY, USA: ACM, pp. 205–214, 2004.

[35] A. Keshavarzian, H. Lee, and L. Venkatraman, "Wakeup scheduling in wireless sensor networks," in *MobiHoc '06: Proceedings of the 7th ACM International Symposium on Mobile Ad Hoc Networking and Computing*, New York, NY, USA: ACM, pp. 322–333, 2006.

[36] G. L. B. Krishnamachari, "Minimum latency joint scheduling and routing in wireless sensor networks," *Ad Hoc Networks*, vol. 5, no. 6, pp. 832–843, 2007.

[37] J. Luo and J.-P. Hubaux, "Joint mobility and routing for lifetime elongation in wireless sensor networks," in *INFOCOM '05: the 24th IEEE International Conference on Computer Communications*, pp. 1735–1746, 2005.

[38] G. Wang, G. Cao, and T. F. L. Porta, "Movement-assisted sensor deployment," *IEEE Transactions on Mobile Computing*, vol. 5, no. 6, pp. 640–652, 2006.

[39] W. Wang, V. Srinivasan, and K.-C. Chua, "Extending the lifetime of wireless sensor networks through mobile relays," *IEEE/ACM Transactions on Networking*, vol. 16, no. 5, pp. 1108–1120, 2008.

[40] R. G. Baraniuk, "Compressive sensing," *Lecture Notes in IEEE Signal Processing Magazine*, vol. 24, no. 4, pp. 118–120, 2007.

[41] V. Cevher and R. G. Baraniuk, "Compressive sensing for sensor calibration," in *SAM 2008 Workshop*, Darmstadt/Germany, 2008.

[42] D. Baron, S. Sarvotham, and R. G. Baraniuk, "Bayesian compressive sensing via belief propagation," *IEEE Transactions on Signal Processing*, vol. 58, no. 1, pp. 269–280, July 2009.

[43] S. Pattem, B. Krishnamachari, and R. Govindan, "The impact of spatial correlation on routing with compression in wireless sensor networks," in *IPSN '04: Proceedings of the 3rd International Symposium on Information Processing in Sensor Networks*, New York, NY, USA: ACM, pp. 28–35, 2004.

[44] C. Luo, F. Wu, J. Sun, and C. W. Chen, "Compressive data gathering for large-scale wireless sensor networks," in *MobiCom '09: Proceedings of the 15th Annual International Conference on Mobile Computing and Networking*, New York, NY, USA: ACM, pp. 145–156, 2009.

[45] C. Tang and C. S. Raghavendra, "Compression techniques for wireless sensor networks," *Wireless Sensor Networks*, pp. 207–231, 2004.

[46] J.-J. Xiao, A. Ribeiro, Z.-Q. Luo, and G. Giannakis, "Distributed compression-estimation using wireless sensor networks," *IEEE Signal Processing Magzine*, vol. 23, no. 4, pp. 27–41, 2006.

[47] H. Gupta, V. Navda, S. R. Das, and V. Chowdhary, "Efficient gathering of correlated data in sensor networks," in *MobiHoc '05: Proceedings of the 6th ACM International Symposium on Mobile Ad Hoc Networking and Computing*, New York, NY, USA: ACM, pp. 402–413, 2005.

[48] I. F. Akyildiz, T. Melodia, and K. R. Chowdhury, "A survey on wireless multimedia sensor networks," *Computer Networks*, vol. 51, no. 4, pp. 921–960, 2007.

[49] D. Slepian and J. Wolf, "Noiseless coding of correlated information sources," *IEEE Transactions on Information Theory*. vol. 19, no. 4, pp. 471–480, 1973.

[50] A. Wyner and J. Ziv, "The rate-distortion function for source coding with side information at the decoder," *IEEE Transactions on Information Theory*, vol. 22, no. 1, pp. 1–10, 1976.

[51] P. Tan and T. J. Li, "A general and optimal framework to achieve the entire rate region for slepian-wolf coding," *Signal Processing*, vol. 86, no. 11, pp. 3102–3114, 2006.

[52] M. F. Duarte, M. B. Wakin, D. Baron, and R. G. Baraniuk, "Universal distributed sensing via random projections," in *IPSN 06: Proceedings of the 5th International Symposium on Information Processing in Sensor Networks*, pp. 177–185, 2006.

[53] S. Lee, S. Pattem, M. Sathiamoorthy, B. Krishnamachari, and A. Ortega, "Spatially-localized compressed sensing and routing in multi-hop sensor networks," in *GSN '09: Proceedings of the 3rd International Conference on GeoSensor Networks*, Berlin, Heidelberg: Springer-Verlag, pp. 11–20, 2009.

[54] S. R. Schnelle, J. N. Laska, C. Hegde, M. F. Duarte, M. A. Davenport, and R. G. Baraniuk, "Texas hold 'em algorithms for distributed compressive sensing," in *ICASSP'10: IEEE International Conference on Acoustics, Speech, and Signal Processing*, Dallas, TX, Mar. 2010.

[55] M. C. Vuran, Özgr B. Akan, and I. F. Akyildiz, "Spatio-temporal correlation: theory and applications for wireless sensor networks," *Computer Networks*, vol. 45, no. 3, pp. 245–259, 2004.

[56] A. Jindal and K. Psounis, "Modeling spatially correlated data in sensor networks," *ACM Trans. Sen. Netw.*, vol. 2, no. 4, pp. 466–499, 2006.

[57] M. F. Duarte, S. Sarvotham, M. B. Wakin, D. Baron, and R. G. Baraniuk, "Joint sparsity models for distributed compressed sensing," in *Proceedings of*

the Workshop on Signal Processing with Adaptative Sparse Structured Representations, Rennes, France, 2005.

[58] R. Cristescu, B. Beferull-lozano, and M. Vetterli, "Networked slepian-wolf: Theory, algorithms and scaling laws," *IEEE Transactions on Information Theory*, vol. 51, pp. 4057–4073, 2003.

[59] D. Marco and D. L. Neuhoff, "Reliability vs. efficiency in distributed source coding for field-gathering sensor networks," in *IPSN '04: Proceedings of the 3rd International Symposium on Information Processing in Sensor Networks*, New York, NY, USA: ACM, pp. 161–168, 2004.

[60] J. Barros and S. D. Servetto, "Network information flow with correlated sources," *IEEE Transactions on Information Theory*, vol. 52, pp. 155–170, 2006.

[61] R. Dai and I. F. Akyildiz, "A spatial correlation model for visual information in wireless multimedia sensor networks," *IEEE Transactions on Multimedia*, vol. 11, no. 6, pp. 1148–1159, 2009.

[62] S. S. Pradhan, E. Pradhan, and K. Ramchandran, "Distributed source coding using syndromes (DISCUS): Design and construction," *IEEE Transactions on Information Theory*, vol. 49, pp. 626–643, 1999.

[63] M. Marcellin and T. Fischer, "Trellis coded quantization of memoryless and gauss-markov sources," *IEEE Transactions on Communications*, vol. 38, no. 1, pp. 82–93, 1990.

[64] Z. Xiong, A. D. Liveris, and S. Cheng, "Distributed source coding for sensor networks," *IEEE Signal Processing Magazine*, vol. 21, no. 5, pp. 80–94, 2004.

[65] D. J. C. Mackay, *Information Theory, Inference & Learning Algorithms*, Cambridge University Press, 2002.

[66] B. Girod, A. M. Aaron, S. Rane, and D. Rebollo-Monedero, "Distributed video coding," *Proceedings of the IEEE*, vol. 93, no. 1, pp. 71–83, 2005.

[67] P. Jung and J. Plechinger, "Performance of rate compatible punctured turbo-codes for mobile radio applications," *Electronics Letters*, vol. 33, no. 25, pp. 2102–2103, 1997.

[68] K. R. Rao and P. Yip, *Discrete cosine transform: algorithms, advantages, applications*, San Diego, CA, USA: Academic Press Professional, Inc., 1990.

[69] A. Krause, C. Guestrin, A. Gupta, and J. Kleinberg, "Near-optimal sensor placements: maximizing information while minimizing communication cost," in *IPSN '06: Proceedings of the 5th International Conference on Information Processing in Sensor Networks*, pp. 2–10, 2006.

[70] C. E. Rasmussen, *Gaussian processes for machine learning*, MIT Press, 2006.

[71] M. A. Osborne, S. J. Roberts, A. Rogers, S. D. Ramchurn, and N. R. Jennings, "Towards real-time information processing of sensor network data using computationally efficient multi-output gaussian processes," in *IPSN '08: Proceedings of the 7th International Conference on Information Processing in Sensor Networks*, Washington, DC, USA: IEEE Computer Society, pp. 109–120, 2008.

[72] Texas Instrument, "High-Accuracy, Low-Power, Digital Temperature Sensor", 2009.

[73] Texas Instrument, "CC1100 Low-Power Sub- 1 GHz RF Transceiver".

[74] IEEE Computer Society, "IEEE standard 802.15.4d," 2009.

[75] ANALOG DEVICES, "16-Bit Low Power Sigma-Delta ADC," 2009.

[76] F. Zhao, J. Liu, J. Liu, L. Guibas, and J. Reich, "Collaborative signal and information processing: an information-directed approach," *Proceedings of the IEEE*, vol. 91, no. 8, pp. 1199–1209, 2003.

[77] L. Krishnamachari, D. Estrin, and S. Wicker, "The impact of data aggregation in wireless sensor networks," *ICDCSW '02: Proceedings of the 22nd Interna-*

tional Conference on Distributed Computing Systems Workshops, pp. 575–578, 2002.

[78] Y. Yu, B. Krishnamachari, and V. Prasanna, "Data gathering with tunable compression in sensor networks," *IEEE Transactions on Parallel and Distributed Systems*, vol. 19, no. 2, pp. 276–287, Feb. 2008.

[79] H. Luo, Y. Liu, and S. K. Das, "Distributed algorithm for en route aggregation decision in wireless sensor networks," *IEEE Transactions on Mobile Computing*, vol. 8, no. 1, pp. 1–13, 2009.

[80] M. F. Duarte, S. Sarvotham, D. Baron, M. B. Wakin, and R. G. Baraniuk, "Distributed compressed sensing of jointly sparse signals," *Proceedings of the 39th Asilomar Conference on Signals, Systems, and Computers*, Nov. 2005.

[81] P. J. Diggle, J. A. Tawn, and R. A. Moyeed, "Model-based geostatistics," *Applied Statistics*, vol. 47, no. 3, pp. 299–350, 1998.

[82] D. Mackay, "Gaussian processes - a replacement for supervised neural networks?" *Lecture notes for a tutorial at Neural Information Processing Systems Conference*, 1997.

[83] Intel Berkeley Lab, in *http://db.lcs.mit.edu/labdata/labdata.html*, 2004.

[84] H. G. Feichtinger and K. Gröchenig, "Theory and practice of irregular sampling," in *Wavelets: Mathematics and Applications*, J. J. Benedetto and M. W. Frazier, Eds. Boca Raton, FL: CRC Press, pp. 305–363, 1994.

[85] B. A. Shenoi, *Introduction to Digital Signal Processing and Filter Design*. Wiley-Interscience, 2005.

[86] F. Sivrikaya and B. Yener, "Time synchronization in sensor networks: a survey," *IEEE Network*, vol. 18, no. 4, pp. 45–50, 2004.

[87] K. Sun, P. Ning, and C. Wang, "Fault-tolerant cluster-wise clock synchronization for wireless sensor networks," *IEEE Transactions on Dependable and Secure Computing*, vol. 2, no. 3, pp. 177–189, 2005.

[88] S. Arora and A. Frieze, "A new rounding procedure for the assignment problem with applications to dense graph arrangement problems," *Proceedings of the 37th IEEE Symposium on Foundations of Computer Science*, pp. 21–30, 1996.

[89] D. Donoho, "Compressed sensing," *IEEE Transactions on Information Theory*, vol. 52, no. 4, pp. 1289–1306, 2006.

[90] Q. Cao, T. Abdelzaher, T. He, and J. Stankovic, "Towards optimal sleep scheduling in sensor networks for rare-event detection," in *IPSN '05: Proceedings of the 4th International Symposium on Information Processing in Sensor Networks*, Piscataway, NJ, USA: IEEE Press, p. 4, 2005.

[91] R. Niu, P. K. Varshney, and Q. Cheng, "Distributed detection in a large wireless sensor network," *Information Fusion*, vol. 7, no. 4, pp. 380–394, 2006.

[92] N. Rabbat and R. Nowak, "Distributed optimization in sensor networks," in *IPSN '04: Proceedings of the 3rd International Symposium on Information Processing in Sensor Networks*, New York, NY, USA: ACM, pp. 20–27, 2004.

[93] E. J. Candes and M. B. Wakin, "An introduction to compressive sampling," *IEEE Signal Processing Magazine*, vol. 25, no. 2, pp. 21–30, 2008.

[94] C. Guestrin, A. Krause, and A. P. Singh, "Near-optimal sensor placements in gaussian processes," in *ICML '05: Proceedings of the 22nd International Conference on Machine Learning*, New York, NY, USA: ACM Press, pp. 265–272, 2005.

[95] M. C. Vuran and I. F. Akyildiz, "Spatial correlation-based collaborative medium access control in wireless sensor networks," *IEEE/ACM Transactions on Networking*, vol. 14, no. 2, pp. 316–329, 2006.

[96] Y. Tay, K. Jamieson, and H. Balakrishnan, "Collision-Minimizing CSMA and its Applications to Wireless Sensor Networks," *IEEE Journal on Selected Areas in Communications*, 2004.

[97] M. J. Schervish, *Theory of Statistics*, Springer, 1995.

[98] F. Haddadi, M. M. Nayebi, and M. R. Aref, "Direction-of-arrival estimation for temporally correlated narrowband signals," *IEEE Transactions on Signal Processing*, vol. 57, no. 2, pp. 600–609, 2009.

BIOGRAPHICAL STATEMENT

Jing Wang received a Bachelor of Electrical Engineering Degree from Xi'an Jiaotong University in 1998. She received a Master of Electrical Engineering Degree from Xi'an Jiaotong University in 2001. Jing Wang joined the Department of Computer Science and Engineering at the University of Texas at Arlington in Spring 2006 for her Ph. D. study.